Click Chemistry as Efficient Ligation Strategy for Complex Macromolecular Architecture and Surface Engineering

DISSERTATION

zur Erlangung des akademischen Grades eines Doktors der Naturwissenschaften (Dr. rer. nat.) in der Fakultät für Biologie, Chemie und Geowissenschaften der Universität Bayreuth

vorgelegt von

Anja Sabrina Goldmann

geboren in Deggendorf

Bayreuth, 2009

Die vorliegende Arbeit wurde in der Zeit von Januar 2006 bis Dezember 2009 in Bayreuth am Lehrstuhl Makromolekulare Chemie II unter Betreuung von Herrn Prof. Dr. Axel H. E. Müller angefertigt.

Vollständiger Abdruck der von Fakultät für Biologie, Chemie und Geowissenschaften der Universität Bayreuth genehmigten Dissertation zur Erlangung des akademischen Grades eines Doktors der Naturwissenschaften (Dr. rer. nat.).

Dissertation eingereicht am: 18.12.2009

Zulassung durch die Promotionskommission: 10.01.2010

Wissenschaftliches Kolloquium: 23.02.2010

Amtierender Dekan: Prof. Dr. Clemens Stephan

Prüfungsausschuß:

Prof. Dr. A. H. E. Müller (Erstgutachter)

Prof. Dr. M. Thelakkat (Zweitgutachter)

Prof. Dr. H. G. Alt (Vorsitzender)

Prof. Dr. A. Fery

Meiner Familie

„The sky is the limit!“

Miguel de Cervantes in Don Quijote

Table of Contents

Table of Contents

1. Click Chemistry

The "click" concept, proposed by Sharpless[1] in 2001, is undeniably one of the most noticeable synthetic trends in the research area of chemistry and material science of this new century.[1-3] The catchy term "click" refers to energetically favored, specific and versatile chemical transformations, which lead to a single reaction product. In other words, the essence of click chemistry is simplicity and efficiency.

Click chemistry is therefore not a new type of chemistry, but rather a term used for a class of reactions that can create complex molecules in a very efficient manner.

This exciting concept seems to perfectly answer the needs of modern scientists working in research areas as diverse as molecular biology, drug design, biotechnology, macromolecular chemistry or materials science.[4-10] It is indeed noteworthy that over recent years, complicated reactions requiring either complex apparatus or harsh experimental conditions, have been less frequently studied than in the last century and gradually replaced by simpler tools. In this context, the straightforward click reactions have become tremendously popular in both academic and industrial research.[3]

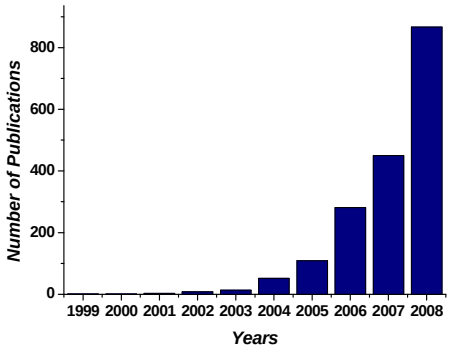

Figure 1.1. Number of scientific publications on click chemistry (search performed by SciFinder with the following keyword: click chemistry)

The overwhelming success of click chemistry over the past years becomes apparent when looking at the numbers of papers published over the last nine years (Figure 1.1). The number of publications increases exponentially and shows the importance of these efficient reactions in different fields of chemistry.

Click chemistry describes chemistry tailored to generate substances quickly and reliably by joining small units together as nature does. It is defined as a fast, modular, process-driven approach to irreversible connections of the substrates involved in click reactions. Click

chemistry uses only the most reliable reactions to build complex molecules from olefins, electrophiles, and heteroatom linkers.[9]

The criteria for being classified as click chemistry contain a yield close to 100% as well as a preferential and rapidly occurring irreversible, highly selective and orthogonal reaction. The reaction conditions should be mild, insensitive to oxygen and water and use either no solvents or benign solvents like water. Click reactions in organic solvents have also a high significance in polymer and material science. The bonds generated in the product should be chemically stable under a range of physiological conditions. Additionally, for click reactions involved in polymerizations, the counter functionalities of the reagents should be unreactive under free radical polymerization conditions or be easily protected during the polymerization stage and functionalized afterwards.

1.1. Huisgen 1,3–dipolar cycloaddition of azides and alkynes

Of all currently identified click reactions, the heteroatom cycloaddition class of reactions is the most reliable and versatile category. Within this category, the Huisgen 1,3-dipolar cycloaddition of azides and alkynes is known for being closest to an “ideal” click reaction. Cu(I)-catalyzed Huisgen 1,3-dipolar cycloaddition of azides and alkynes yields 1,2,3-triazole products. Traditionally, uncatalyzed cycloadditions of azides and alkynes require long reaction times, high temperatures and result in the formation of two products, 1,4- and 1,5-regioisomers as shown in Figure 1.2.

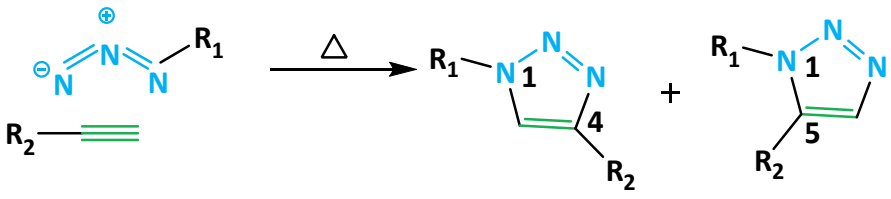

approx. 1:1 mixture

Figure 1.2. Uncatalyzed 1,3-dipolar cycloaddition of azides and alkynes yields 1,4- and 1,5 triazole products

The synthesis of 1,2,3-triazoles by 1,3-dipolar cycloaddition was discovered by Michael[11] at the end of the 19th century and significantly advanced by Huisgen in the 1960s.[12,13]

The groups of Sharpless and Meldal[14] separately discovered the Cu(I)-catalyzed variation of this reaction, which allows very fast and efficient formation of exclusively 1,4-triazoles at mild reaction conditions.[1]

This breakthrough led to a remarkable renaissance of Huisgen cycloadditions in synthetic chemistry. Hence, research in this direction has led to its widespread application in all fields of polymer chemistry and biochemistry over the last few years.[15-20] Moreoever, since azide and alkyne functions are widely absent in the biological world, azide–alkyne chemistry constitutes a very interesting chemoselective platform for the functionalization or ligation of biomaterials, such as stationary phases for bioseparation, site-specific modified proteins or viruses, drug- or gene-delivery carriers, protein or oligonucleotide microarrays, and functionalized cell surfaces.[21-25]

The high kinetic stability of azide and alkyne groups that was disadvantageous in uncatalyzed cycloadditions is an advantage in the Cu(I)-catalyzed process, meaning the two functional groups are inert under a wide range of conditions and do not interact with water, oxygen, biological molecules or other functionalities present in the reaction. Both the azide and alkyne groups can also be added easily to different molecules, requiring minimal initial functionalization stages or protective chemistry. The Cu(I)-acetylide facilitates the cycloaddition of the azide group as shown in the proposed reaction scheme of Figure 1.3.[6] of Bock and coworkers.

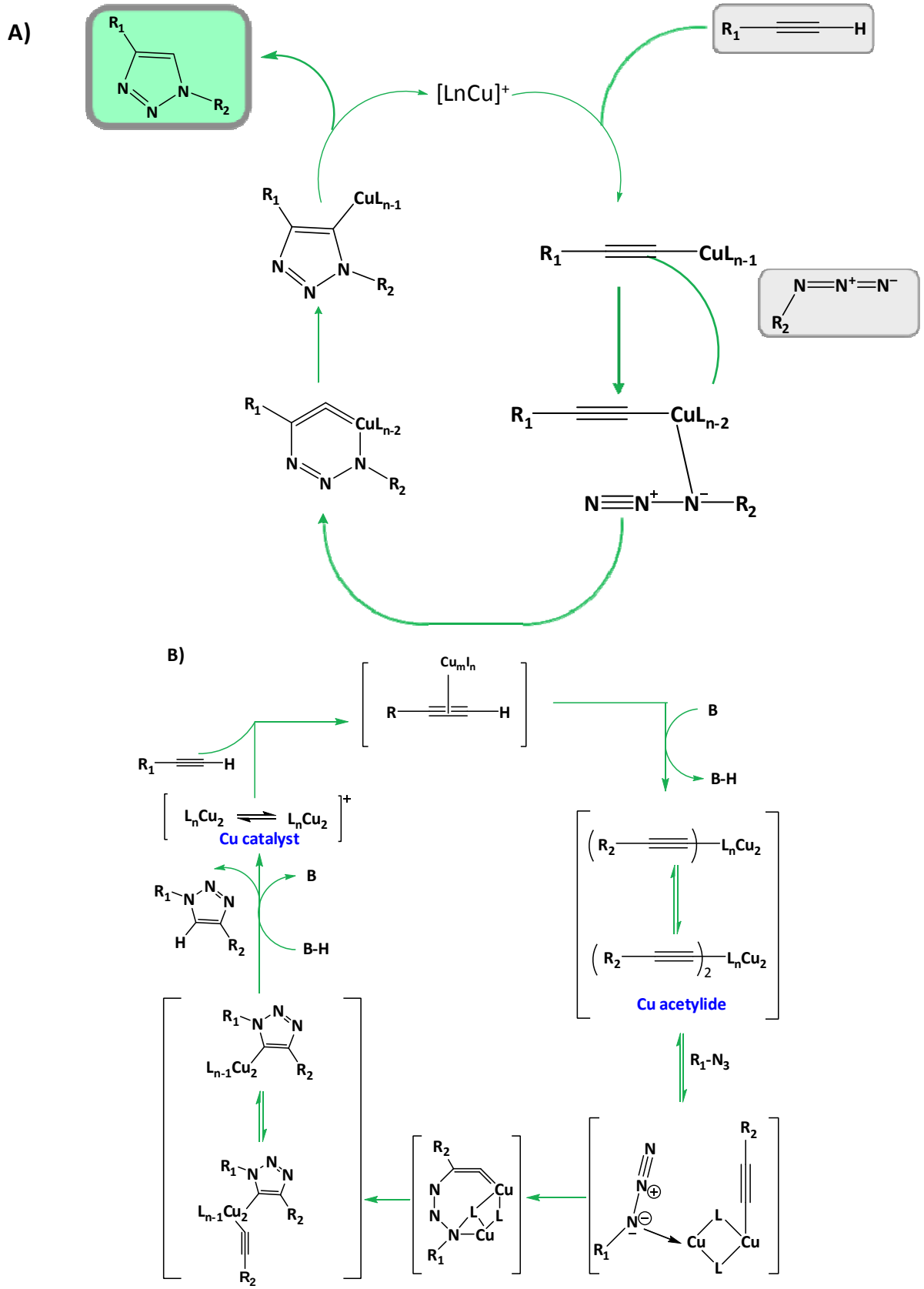

Figure 1.3. Proposed catalytic cycle of stepwise Cu(I)-catalyzed Azide-Alkyne Cycloaddition; A) First order with respect to copper; and B) second order with respect to copper[6]

In both mechanisms the first copper group initiates the formation of copper acetylide. In the first order mechanism the acetylide formed is thought to be capable of immediately forming an acetylide-azide complex, while in the second order mechanism a second copper component in the acetylide group is required to activate the azide molecule and form a copper acetylide-azide complex. The copper acetylide-azide complex then undergoes cyclization and formation of a metallocycle due to the nucleophilic attack of an acetylide carbon by the azide group. Finally, ring contraction occurs and the catalyst dissociates and is regenerated via protonation of the triazole-copper molecule.

1.2. Metal-Free Click Strategies

However, in some particular cases, the presence of transition metal catalysts may be a problem. Some examples of in vitro copper-induced degradation of viruses or oligonucleotide strands have been reported.[26,27] Additionally, the use of copper(I)-catalyzed azide–alkyne cycloaddition (CuAAC) for in vivo applications is limited by the fact that, if present in more than trace quantities, copper ions are potentially toxic for living organisms. In this context, the development of metal-free click strategies is particularly relevant. In recent years, metal-free [3+2] cycloaddition reactions, Diels–Alder reactions, and thiol-alkene radical addition reactions have come to the fore as click reactions because of their simple synthetic procedures and high yields. Figure 1.4. represents alternative click-reactions to expand the range of opportunities for new applications.[28]

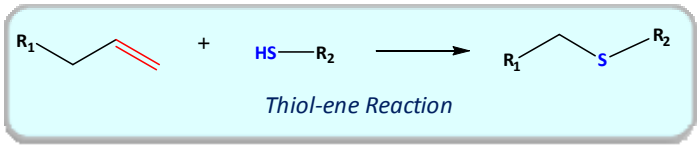

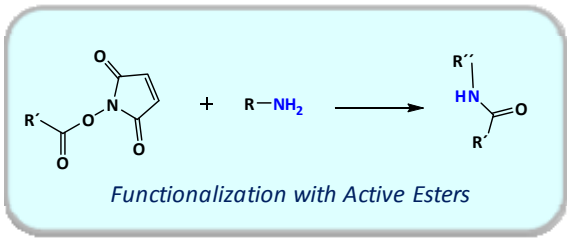

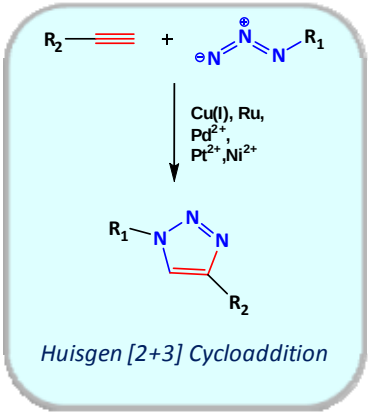

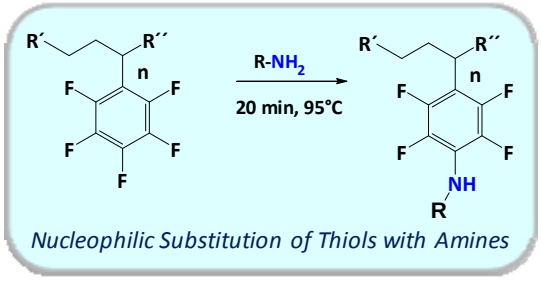

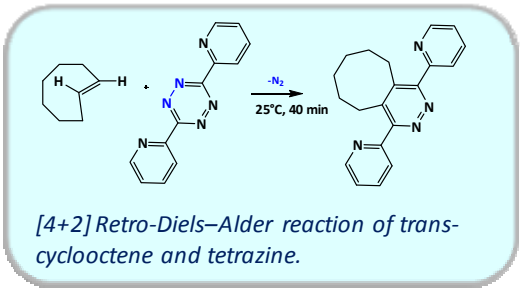

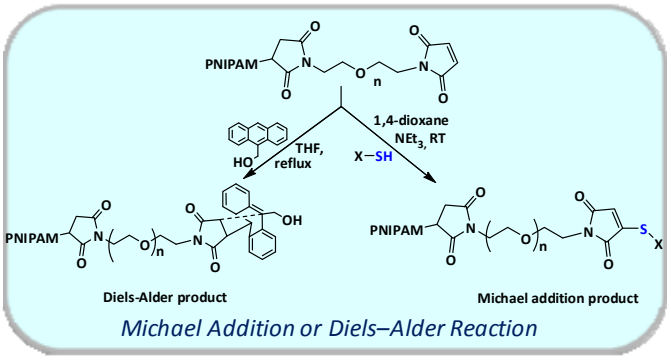

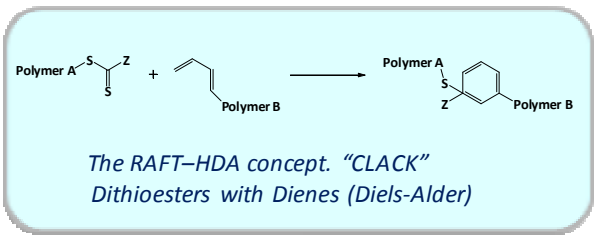

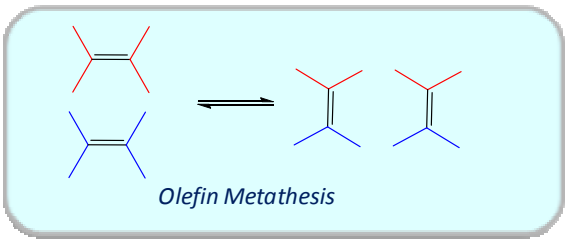

Figure 1.4. Overview of click chemistry strategies

1.3. Thiol-Ene Reaction

Among the various click chemistry methods shown above, special emphasis is placed on the thiol-ene reaction due to its relevance within the framework of this thesis. The radical addition of thiols to double bonds is – under certain conditions – a highly efficient method used for polymerizations, curing reactions, grafting reactions and for the modification of polymers (see Figure 1.5).

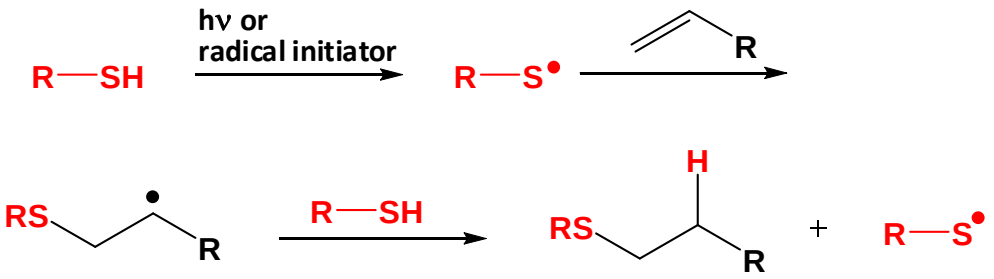

Figure 1.5. The thiol-ene radical reaction[29,30]

Schlaad and co-workers demonstrated a post-polymerization modification of a well-defined poly[2-(3-butenyl)-2-oxazoline].[31] The reactions were performed by exposure to UV light, as well as under irradiation with direct sunlight. Earlier they demonstrated the free-radical addition of ω-functional mercaptans onto 1,2-polybutadienes.[32] The great potential of thiol–ene chemistry was exploited by Hawker and co-workers in the synthesis of poly(thioether) dendrimers (Figure 1.6.).[33] The thiol-ene reaction between the polyalkene substrate and monofunctionalized thiols enabled functionalization of the periphery of the dendrimer in a complete manner up to the fourth generation.

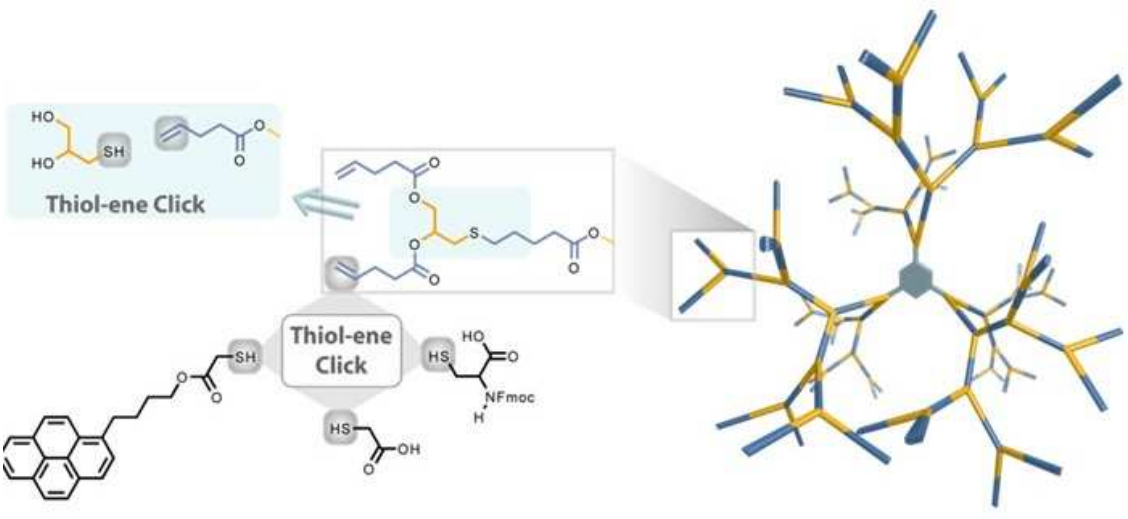

Figure 1.6. Dendrimers up to the fourth generation using thiol-ene reaction[33]

2. Tailor-Made Polymer Architectures

Due to the various architectures and functionalities of nanostructures, soft materials like polymers have been playing extremely important roles in the templated synthesis, surface protection and surface functionalization.[34] Recent progress in "living"/controlled polymerization techniques has enabled the precise preparation of polymers with various well-defined topologies. Figure 2.1. summarizes the general polymer architectures.

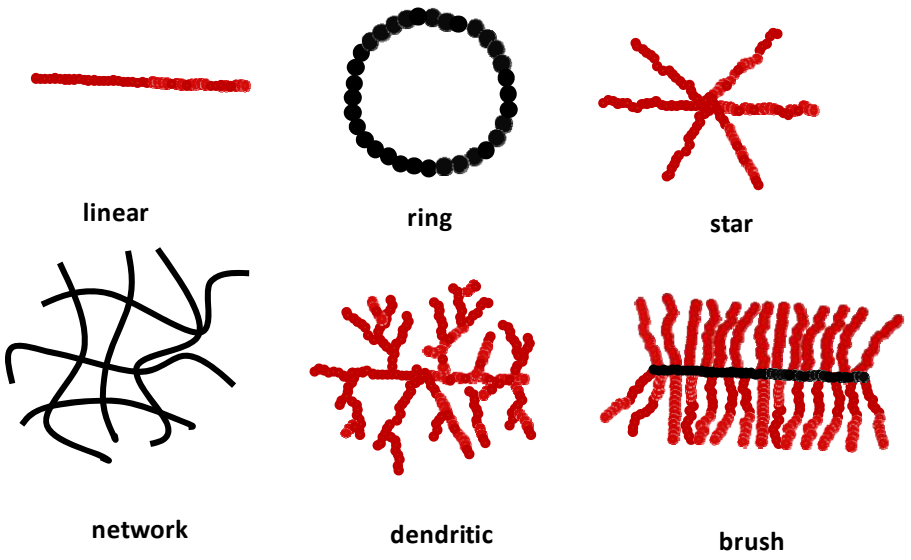

Figure 2.1. General topologies of polymers

2.1. Cyclic Polymers

Ring-shaped polymers have gained increasing attention in polymer science not only because they are found in the natural products such as circular DNA molecules, cyclic peptides, and cyclic polysaccharides,[35] but they can also be used in polymer recycling based on chain-ring equilibria.[36] Furthermore, the difficulties associated with their preparation as well as their unknown solution/bulk properties have stirred significant interest of polymer scientists. Cyclization reactions represent an inherent, unavoidable component of step-growth polymerization and may be dominant factor for limitation of chain growth. Therefore, many researchers and theoreticians tried to study and elucidate the role of cyclizations, the factors affecting the degree of cyclization and the relation between the conversion and the extent of cyclization.[37-44] The concurrent formation of linear and cyclic molecules is a general

characteristic of polymer systems containing reactive functions at the ends of main backbone chain. Cyclic polymers formed in linear-ring step and chain polymerizations are often undesirable side-products. These side-products are present in linear high molecular mass polymers and may hamper the physical and mechanical properties of polymeric materials.

However, cyclic polymers remain fascinating curiosities for theoreticians and chemists. The preparation of well-defined cyclic polymers and the study of their intrinsic properties are still a challenge in polymer science. The absence of chain ends and consequently the topological restriction imposed by the cyclic architecture result in a variety of molecular characteristics and physical properties that significantly distinguish them from their linear counterparts.[45]

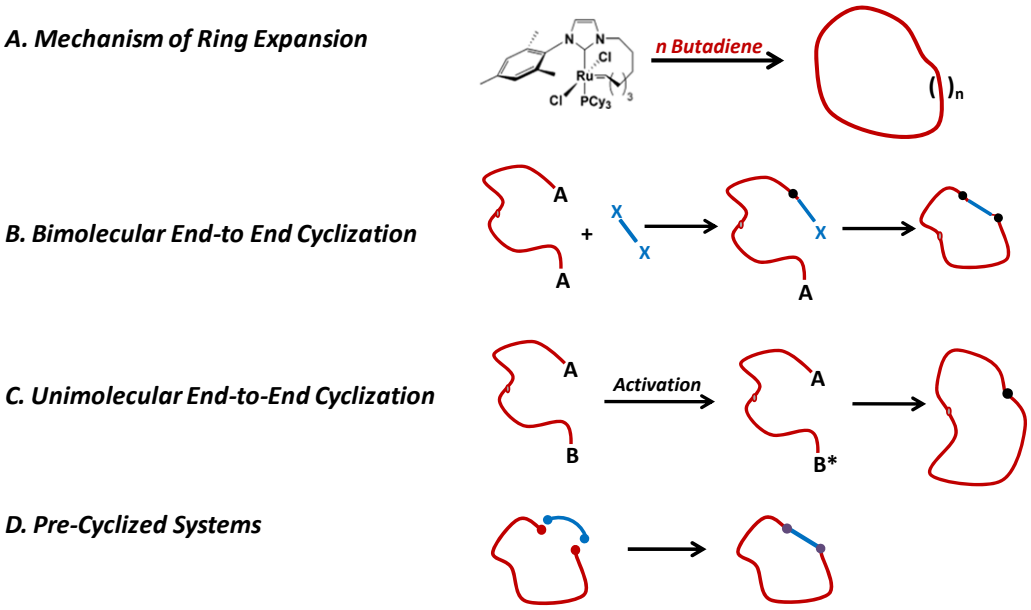

Figure 2.2. General Methods of Synthesis of Cyclic Polymers

In the following section different preparation strategies of macrocylic polymers are pointed out. One of the most remarkable example concerns the cyclic carbene-ruthenium complex used in ring opening metathesis polymerization (Figure 2.2., A).[46,47] In this coordinated polymerization the cyclic alkene coordinates onto the ruthenium center before insertion into the cyclic carbene ring which grows of one monomer unit. This unique strategy leads to near 100% cyclic polymers, yet it is limited in terms of the polymer functionality interfering with the metal center.

The most appropriate methods for the synthesis of cyclic polymers of controlled size and narrow polydispersity are based on the end-to-end chain coupling of α,ω-difunctional linear

chains in highly dilute reaction conditions (Figure 2.2, C). The use of living polymerization techniques (e.g. anionic or RAFT polymerization) for the preparation of the linear precursors allows control over the molar mass and a narrow molar mass distribution. Different approaches exist for the end-to-end closure: Cassasa[48] proposed the direct coupling of α,ω-polymer dianions, where the polymer has two identical end-functionalized groups and the ring-closure requires the use of a bifunctional coupling agent (Figure 2.2, B). Several groups used this strategy for the access to macrocycles.[49]

The unimolecular ring closure corresponds to the reaction between the α– and ω-polymer ends. The high dilution, required to favour the cyclization versus chain extension, is unfavorable to the quantitative formation of the hetero-difunctional polymer intermediate. To overcome this difficulty another approach involves the direct synthesis of an α,ω-heterodifunctional linear precursor. The cyclization is then performed in a separate step under high dilution. The concept of unimolecular end-to-end closure was used in the click-approach for the synthesis of cyclic polystyrene, which will be discussed in detail in Chapter IV. Pre-organization of macromolecular precursors bearing specific ionic end-functions via electrostatic non-covalent interactions is an interesting and original strategy that was recently applied to the preparation of various types of chain architectures. This approach was thoroughly investigated by Tezuka and coworkers for a broad diversity of cyclic polymers (Figure 2.2, D).[50]

The concept of cyclic polymers was extended to the synthesis of ring-shaped polymer brushes by Deffieux et al. Macrocyclic polymer brushes can be considered as a special case of cylindrical polymer brushes, in which the two ends of the brushes meet each other by a coupling reaction. Although macrocyclic polymers were first obtained 40 years ago,[51] the preparation of large macrocyclic (co)polymer brushes is limited by the difficulty to get pure α,ω-difunctional high molar mass precursors, the drastic decrease of the end-to-end ring closing efficiency when increasing the distance between the chain ends and the separation from linear contaminants of comparable molar mass.

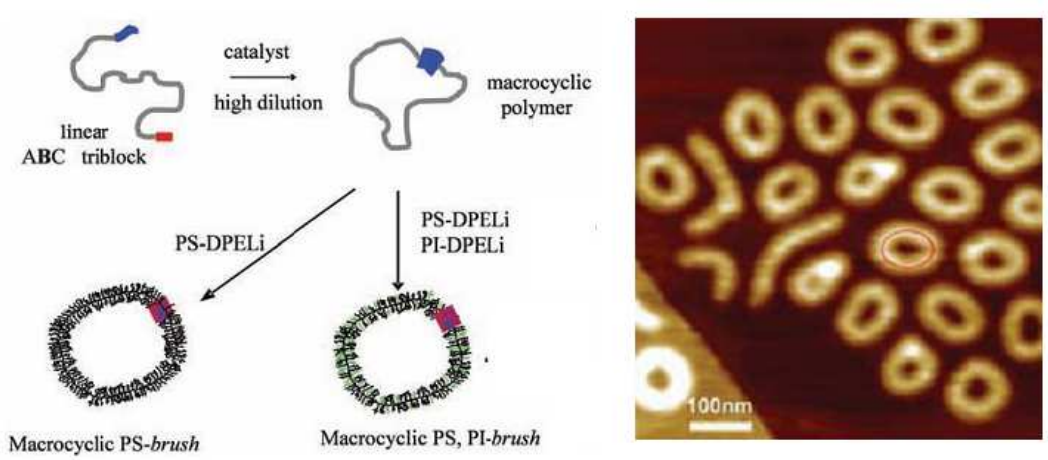

Figure 2.3. Left: strategy for the synthesis of macrocyclic copolymer brushes. PS-DPELi, (1,1-diphenylethylene) end-capped polystyryllithium; PI-DPELi, (1,1-diphenylethylene) end-capped polyisoprenyllithium. Right: AFM image of macrocyclic PS brushes with PS branch after fractionation by precipitation.

Deffieux et al.[52] developed an impressive new strategy to synthesize large polymer macrocycles based on an ABC block terpolymer by sequential living cationic polymerization of three different vinyl ethers. In the triblock terpolymer, the long central B block is extended by two short A and C sequences bearing monomer units with reactive antagonist functions. The external blocks are then selectively activated under dilute conditions to allow intramolecular coupling between the A and C blocks to form the macrocyclic polymers, with further functionalization to form the corresponding brush polymers with PS or randomly distributed PS and polyisoprene (PS/PI) branches. These macrocylic polymer brushes were readily visualized by AFM.

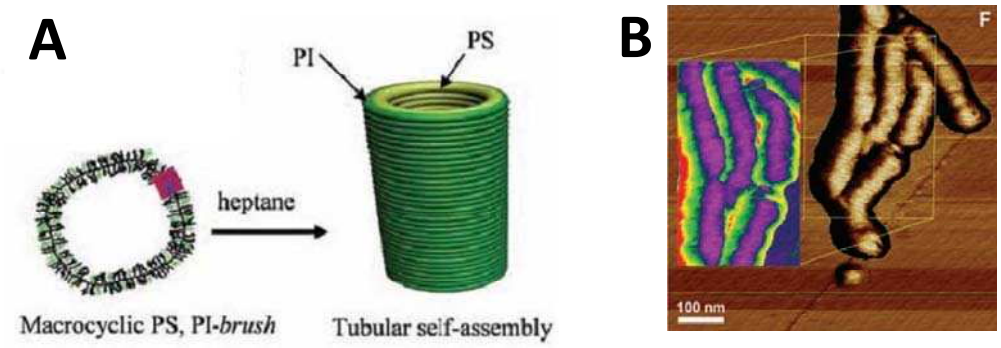

Figure 2.4. A. Self-assembly of macrocyclic brushes into cylindrical tubes in heptane. B. Series of tubes interconnected by their polyisoprene shell (black) and image in reverse mode showing the internal PS (purple) and external PI (green) parts. The stripes corresponding to the elementary macrocyclic copolymer brushes are also visible.

In a selective solvent for the PI branches (heptanes), macrocyclic PS/PI brushes self-assembled into submicron-sized cylindrical tubes (Figure 2.4), indicated by dynamic light scattering (DLS) and AFM on solid substrates.

As for applications, the development of new and more reliable techniques toward cyclic polymers has opened up a significant variety of areas in which such polymer topologies can show superior performance. For instance, Fréchet and coworkers[53] studied the circulation time of linear and cyclic polymers for the delivery of drugs to solid tumors in mice. Long circulation times of water-soluble polymers are essential for the successful delivery of drugs to solid tumors. The circulation time of such a polymer depends upon molecular weight and polymer architecture.[54] Linear polymers traverse a nanopore by the end-on motion of the polymer chain, and since only one polymer segment needs to enter the pore for a linear polymer to traverse it, linear polymers cross nanopores more easily than star polymers.[55] Cyclic polymers lack chain ends, so two chain segments would need to enter the pore for the cyclic polymer to transit. Therefore, they predicted that cyclic polymers would behave differently in vivo than linear polymers of the same molecular weight (M_W). The longer elimination half-life of the cyclic polymer compared with the linear polymer of the same M_W may provide a window of opportunity for cyclic polymers as drug carriers or imaging agents: In the cyclized state, the polymer would circulate, releasing the drug; when the chain was broken on demand, the polymer would be more rapidly eliminated.

3. Reversible Addition Fragmentation Chain Transfer Polymerization (RAFT)

Currently, there are three main types of "living"/controlled radical polymerization (CRP): atom transfer radical polymerization (ATRP), stable free radical polymerization (SFRP) including nitroxide mediated polymerization (NMP), and reversible addition fragmentation chain transfer (RAFT) polymerization. ATRP involves a reversible chain termination using the exchange of an organic halide via a reversible redox reaction in the presence of a transition metal catalyst. SFRP also uses reversible chain termination by means of exchange of a stable radical group. In the case of NMP, the stable radical is a nitroxide group. NMP benefits from the absence of copper and sulfur compounds, yet it is limited by low reaction rates, limited monomer compatibility and requires high reaction temperatures. With the discovery of CRP techniques at the end of the twentieth century, a great variety of complex macromolecular architectures became available under non-demanding reaction conditions. Polymers with well-defined structure and different functionality can be created.[2,56,57] RAFT polymerization in particular has proven to be a versatile tool, as RAFT reactions are less oxygen sensitive, proceed at lower temperatures than ATRP and NMP and are compatible with a wider range of monomers, including acrylate, methacrylate and styrenic monomers.

RAFT polymerization was pioneered in Australia[58-61] and the mechanism as proposed by the CSIRO group is shown in Figure 3.1.

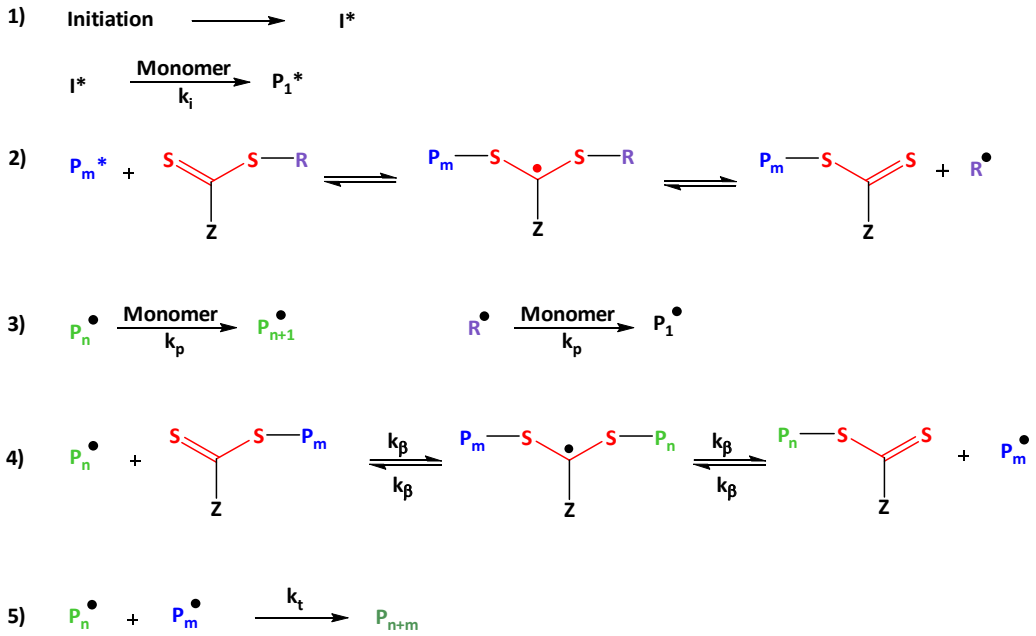

Figure 3.1. Proposed general mechanism of RAFT polymerizations showing the steps of initiation (1), propagation (2), pre-equilibrium (3), reinitiation, main-equilibrium (4) and termination (5).

In RAFT polymerization a thiocarbonylthio group containing compound, with a general structure of Z-C(=S)S-R (Figure 3.1., step 2), is added to an otherwise conventional free radical polymerization in order to obtain a controlled radical polymerization. These controlling agents are reversible chain transfer agents (CTAs) or RAFT agents. First, a radical initiator decomposes, creating radicals that initiate the polymerization. A propagating radical then adds to the thiocarbonyl group of the CTA molecule and forms an intermediate radical (also called "dormant" species). Eventually the intermediate radical undergoes a β-scission reaction, either re-forming the original radical or creating a new propagating radical from the leaving group (R group). Additionally, the CTA molecule is recovered in this reaction step. After the initial phase an equilibrium is established between the propagating radicals and the intermediate radical species. Only when a certain chain length is exceeded, the rate coefficients become independent of the chain length. Therefore, one has to distinguish between a so-called "pre-equilibrium", where low molecular weight CTAs are still present, and the "main-equilibrium" with polymeric RAFT agents. With the polymerization being of a radical nature, side reactions like transfer, recombination and disproportionation cannot fully be suppressed. Still, RAFT polymerizations show a linear growth of the molecular weight

with respect to conversion and yield polymers with narrow molecular weight distributions when the equilibrium reactions are fast compared to propagation.

4. Click Chemistry in Combination with RAFT Polymerizations

Living free radical polymerization and click pericyclic reactions are independently known for having many similar advantages, including reaction under mild conditions and tolerance of a range of functionalities. Recently, research groups have begun combining these click reactions with different polymerization techniques to synthesize new polymeric materials previously inaccessible via traditional polymerization methods. For example block copolymers, which are currently difficult to synthesize because of different polymerization mechanisms, have been successfully prepared via RAFT polymerization of homopolymer chains with the requisite azide and alkyne endfunctionalities and subsequent post-polymerization click additions.[62]

Combining RAFT polymerization and click pericyclic reactions is a relatively novel concept, which provides many useful opportunities and benefits. The ability to synthesize well-defined amphiphilic block copolymers and other complex polymer architectures from highly reactive monomers, will allow for the potential development of many new materials with wide industrial and biomedical applications.[63-68]

Sinnwell et al.[69] synthesized three-arm star block copolymers from linear polystyrene (PS) and poly(ε-caprolactone) (PCL) building blocks. Through the use of an α-diene-ω-alkyne functionalized PCL, the PS-*b*-PCL stars were synthesized via either forming the PS-*b*-PCL arms first with the hetero Diels–Alder (HDA) cycloaddition and their subsequent coupling to a triazide coupling agent through CuAAC (arm-first) or vice versa, the core-first method (Figure 4.1.).

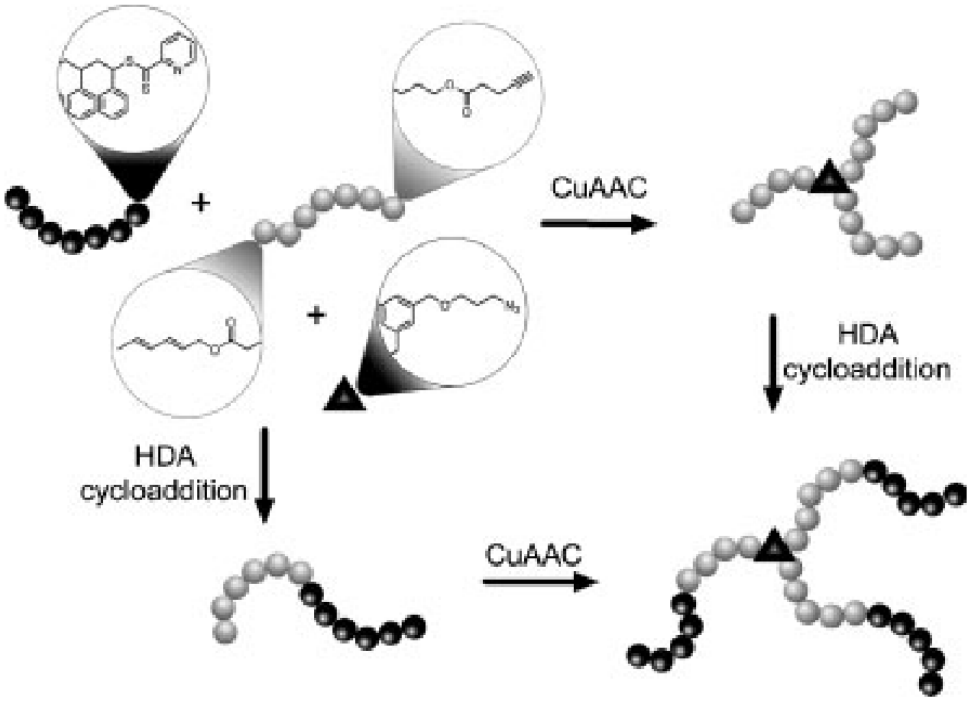

Figure 4.1. Combination of RAFT polymerization, click chemistry and HDA cycloaddition to create three-arm star polymers[69]

Another example for the combination of RAFT polymerization and click chemistry is given by Sumerlin and coworkers to synthesize responsive polymer-protein conjugates.[70] A model protein, bovine serum albumin (BSA), was functionalized with an alkyne moiety. Then azido-terminated poly(N-isopropylacrylamide) (PNIPAAm-N_3) was prepared via RAFT, and the polymer-protein coupling was accomplished by CuAAC (Figure 4.2.).

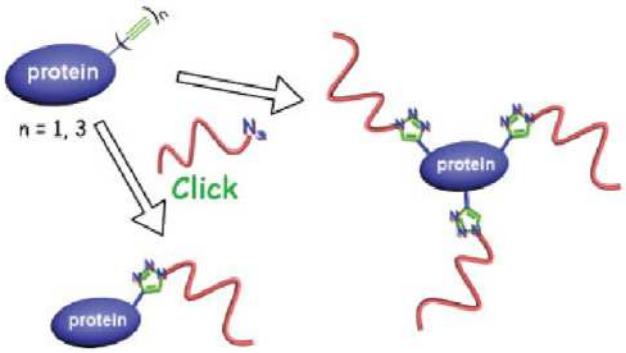

Figure 4.2. Bovine serum albumin (BSA) functionalized via a combination of RAFT polymerization and click chemistry

Perrier and coworkers[71] investigated the limitations of click chemistry in combination with living radical polymerization. They found that in special cases unwanted side reactions can occur. For example the azide undergoes 1,3-cycloaddition with the double bond of monomers (*N*-isopropylacrylamide, dimethylacrylamide, methyl acrylate, methyl methacrylate), in the absence of catalyst, at high temperatures (60 °C) and for long reaction times. Short polymerization time and low temperatures should be targeted to limit these side reactions.

5. Nano- and Microparticles [72]

A nanoparticle is a colloidal particle ranging in the size from 1 to 1000 nm. The fact that nanoparticles exist in the same size domain as proteins makes them suitable for bio tagging or labeling. A large scope of the application of nanoparticles are fluorescent biological labels,[73-75] drug and gene delivery,[76,77] bio detection of pathogens,[78] detection of proteins,[79] Probing of DNA structure,[80] tissue engineering,[81,82] tumour destruction via heating (hyperthermia),[83] separation and purification of biological molecules and cells,[84] MRI contrast enhancement,[85] phagokinetic studies,[86] optical probes for biological interactions or rheological measurements in confined space,[87] as purpose for reduction of the oil–water interfacial tension (surface activity)[88] or use as transfection agents.[89-94]

Figure 5.1. shows the classes of nano- and microparticles which are all very general and multifunctional, but have applications in a very broad field as described above.

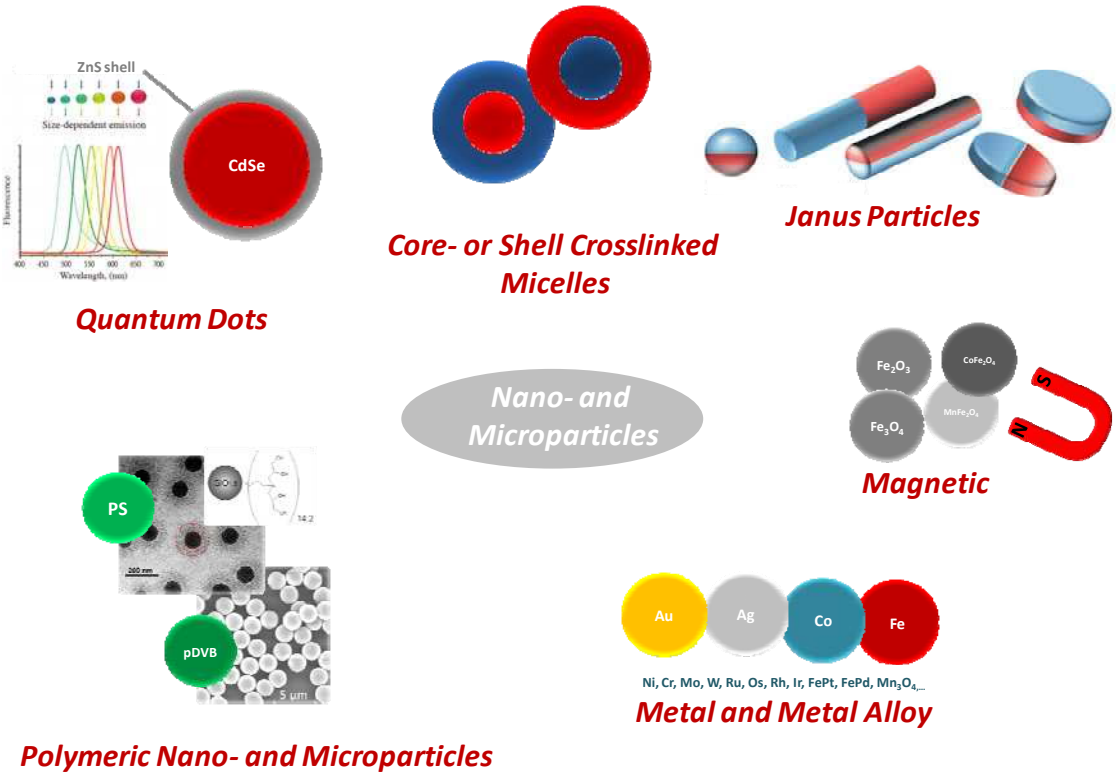

Figure 5.1. Different Classes of Nano- and Microparticles

A high motivation exists for the modification of these materials and surfaces to render these outstanding materials viable for future applications in materials and bioscience. Nowadays, investigating the methodologies that can be employed to modify surfaces in a selective and efficient fashion is a main goal as well as surface engineering to control the chemical composition at the material interface. The particle surface can be modified with a secondary metal or polymer to create core–shell structures. The outer shells function as protective layers for the inner metal/metal oxide cores and alter the surface chemistry to enable post-synthetic modification of the surfactant chemistry.

5.1. Magnetic Nanoparticles

Particularly magnetic nanoparticles (MNPs) based on iron oxides have attracted much attention because of their diverse applications in biotechnology and medicine (magnetic resonance imaging contrast agents,[95] heating mediators for cancer thermotherapy, magnetic force-based gene delivery, and selective separation and detection of biomolecules).

The postsynthetic surface modification of magnetic nanoparticles is important to render chemical functionalities and control their solubility. For biomedical applications and

bioanalysis, the ability to solubilize the nanoparticles in water and to modify their surfaces with molecules, proteins, oligonucleotides, or other targeting agents, is a crucial step toward their widespread application.

Ligand place exchange reactions have been shown quite successful for exchanging silanes, acids, thiols, and dopamine ligands onto the surfaces of some magnetic particles.

The research of the group of Schmidt involves the design, fabrication and investigation of organic-inorganic nanostructured materials, especially the functionalization of magnetic nanoparticles (e.g., Fe_3O_4, Fe/Pt, Co, Fe_2O_3) with a polymeric shell.[96-100] The biofunctional nanosystems are achieved by the attachment of an ATRP initiator to the surface and adjacent "grafting-from" method of responsive polymers. The role of the polymer in these systems is manifold: Covalently attached to the particles surface, it serves as a steric stabilizer and compatibilizer with the environment and may be used for a reversible phase separation in response to different stimuli. In addition, the polymer arms provide the option to introduce functional groups that serve as biomarkers or (bio)catalytically active groups.

The "grafting-from" technique in combination with Nitroxide Mediated Polymerization (NMP) or Atom Transfer Radical Polymerization (ATRP) was pioneered by Jeffrey Pyun.[101-103] For instance, they describe the synthesis and characterization of polymer-coated ferromagnetic cobalt nanoparticles (CoNPs).[101] The versatile synthetic method enabled the production of multigram quantities of these polymeric surfactants that stabilized ferromagnetic CoNPs when dispersed in organic media. Moreover, the application of a dual-stage thermolysis with $Co_2(CO)_8$ allowed the preparation of large samples per batch of well-defined and dispersable ferromagnetic nanoparticles.

Zhang et al.[104] developed amphiphilic polymer brushes with poly(acrylic acid) as core and poly(*n*-butyl acrylate) as shell. These amphiphilic brushes are unimolecular cylindrical micelles and can be used as single-molecular templates for the synthesis of inorganic nanoparticles because of the carboxylic acid groups (or carboxylate groups after neutralization) in the polymer core can coordinate with various metal ions such as Fe^{3+} and Fe^{2+}. Ultrafine magnetic nanoparticles were synthesized within the core of these polymer brushes, as confirmed by various characterization techniques.

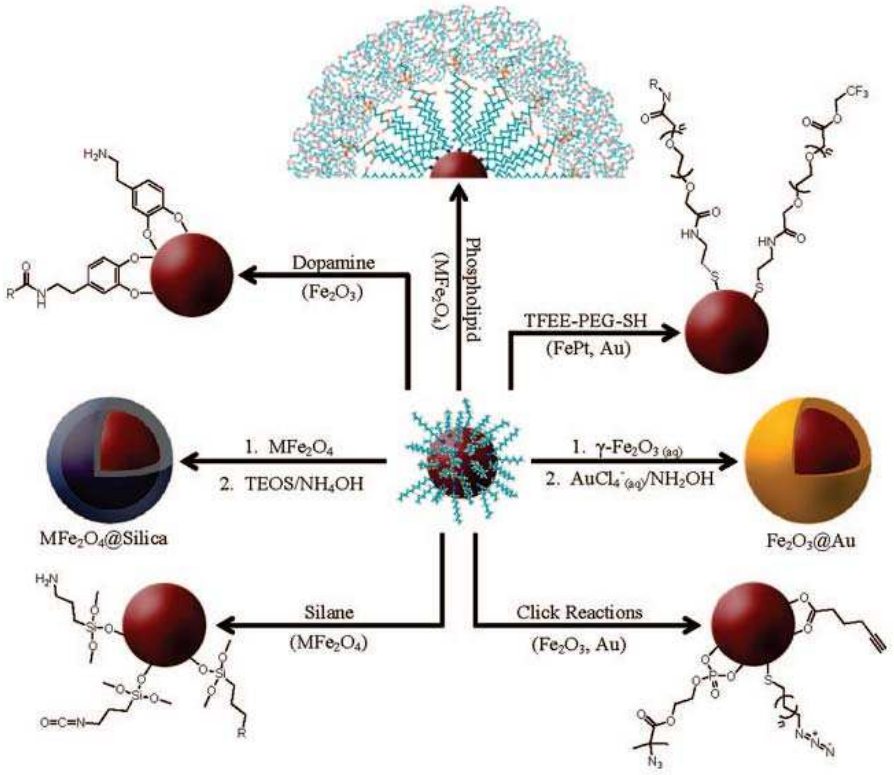

Figure 5.2. Selected Functionalization Routes for Magnetic Nanoparticles[95]

Ligand-place-exchange reactions on the surface of Au nanoparticles were pioneered by Murray et al. and provide a way to append chemically functional species.[105] To an extent, these reactions should be applicable to magnetic nanoparticles, but different affinity of ligands with metal and metal oxide is a key factor controlling the efficacy of place exchange. A relatively new functionalization route that holds great promise as a general method for materials applications is the use of click chemistry, which was initially reported for nanoparticles by Williams and coworkers[106] and further studied by others.[107] The Turro group further elaborated on this method to functionalize Fe_2O_3 nanoparticles. Alkyne-containing organophosphates and carboxylates were exchanged onto the surface of oleic acid stabilized Fe_2O_3 nanoparticles.[107] Taken together, these papers point toward a potentially broad adaptability of click chemistry for nanoparticle functionalization.

Not only the click-functionalization of magnetic particles is an interesting tool for researchers. As pointed out, particles have characteristic free groups at the outer layer, therefore accessible for functionalization. PS grafted silica nanoparticles have been prepared by a tandem process that simultaneously employs RAFT polymerization and click chemistry by the group of Brittain.[108] In a single pot procedure, azide-modified silica, an alkyne

functionalized RAFT agent and styrene were combined to produce the desired product. Li et al.[64] demonstrated the surface initiated RAFT polymerization and click reactions to modify the surface of nanoparticles. A functional monomer with a pendant azide moiety, was polymerized on the surface of silica nanoparticles via surface-initiated RAFT polymerization with considerable control over the molecular weight and molecular weight distribution.

Fleming et al.[109] illustrated the use of 1,3-dipolar cycloadditions as a facile route toward the functionalization of monolayer-protected gold nanoparticles. They used alkyne derivatives of ferrocene, other aromatic molecules and poly(ethylene glycol) (PEG) for the post-functionalization, yielding redox-active, fluoerescent or highly soluble Au nanoparticles.

5.2. Functionalization of Poly(divinylbenzene) Microspheres

Tightly crosslinked spherical polymeric microspheres based on poly(divinylbenzene) (pDVB) microspheres are highly attractive materials for a wide range of applications due to their mechanical, chemical, and thermal stability, as well as their tolerance to a wide pH regime.[110] For instance, functionalized microspheres can be used as tailor-made column materials for chromatography applications.[111] Besides, molecularly imprinted microspheres[112,113] have been successfully tested as devices for the detection of degradation products of chemical warfare agents[114] and towards their chiral selectivity.[115] In addition, they exhibit a large specific surface area and are easy to recover from suspensions. They can be synthesized via the precipitation polymerization technique as mono- or narrowdisperse particles with diameters between 1 and 5 μm and possess residual vinyl bonds on their surfaces.[110] These groups facilitate the attachment of polymer strands to the surface of the particles via a wide range of polymerization protocols or chemical transformations[116-128] The modification of pDVB microspheres via grafted polymers enables them to convert them into functional particles.

Barner et al. applied the RAFT technique to graft polystyrene from cross-linked pDVB microspheres. An advantage of this technique is that the residual vinyl groups on the surface can be used directly to graft polymers from the surface without prior functionalization of the core microspheres.[129] The RAFT process was used to synthesize pDVB microspheres that contain residual RAFT end groups on the surface and within the particle. In addition, Joso et al.[130] reported the successful grafting of poly(N,N-dimethyl acrylamide) and poly(n-butyl

acrylate) from p(DVB) microspheres via the mediation of the RAFT agent cumyl dithiobenzoate (CDB).

Although there is a general need for simple and convenient methods to covalently conjugate a molecule of interest to a surface, nano- or microparticle, no single coupling strategy has been broadly adopted. Instead, numerous coupling strategies have been reported in the literature. Clearly, the reason corroborating this observation is that most of the coupling methods suffer from one or more problems including: incomplete surface functionality transformation, requirement of harsh conditions, the need of highly reactive coupling partners, side reactions, and extensive organic synthesis.

Contrasting all these methods, click chemistry can provide an alternative and moreover universal synthetic methodology for modifying surfaces.

In Chapter V the surface-modification of microspheres is described via the Huisgen and thiol-ene click chemistry to demonstrate a very high versatility toward attaching all kinds of polymers based on various functions.

(1) Kolb, H. C.; Finn, M. G.; Sharpless, K. B. *Angewandte Chemie International Edition* **2001**, *40*, 2004.

(2) Hawker, C. J.; Wooley, K. L. *Science* **2005**, *309*, 1200.

(3) Lutz, J.-F. *Angewandte Chemie International Edition* **2008**, *47*, 2182.

(4) Angell, Y. L.; Burgess, K. *Chemical Society Reviews* **2007**, *36*, 1674.

(5) Binder, H.; Kluger, C. *Curr. Org. Chem.* **2006**, *10*, 1791.

(6) Bock, V. D.; Hiemstra, H.; Maarseveen, J. H. v. *European Journal of Organic Chemistry* **2006**, *2006*, 51.

(7) Dondoni, A. *Chemistry - An Asian Journal* **2007**, *2*, 700.

(8) Lutz, J.-F. *Angewandte Chemie International Edition* **2007**, *46*, 1018.

(9) Sharpless, W. D.; Wu, P.; Hansen; Vidar;, T.; Lindberg, J. G. *J. Chem. Educ.* **2005**, *82*, 1833.

(10) Wu, P.; Fokin, V. V. *Aldrichchimica Acta* **2007**, *40*, 7.

(11) Michael, A. *J. Prakt. Chem.* **1893**, *48*, 94.

(12) Huisgen, R. *Angewandte Chemie International Edition* **1963**, *2*, 565.

(13) Huisgen, R. *Angewandte Chemie International Edition* **1963**, *2*, 633.

(14) Tornoe, C. W.; Christensen, C.; Meldal, M. *The Journal of Organic Chemistry* **2002**, *67*, 3057.

(15) Collman, J. P.; Devaraj, N. K.; Chidsey, C. E. D. *Langmuir* **2004**, *20*, 1051.

(16) Díaz, D. D.; Punna, S.; Holzer, P.; McPherson, A. K.; Sharpless, K. B.; Fokin, V. V.; Finn, M. G. *Journal of Polymer Science Part A: Polymer Chemistry* **2004**, *42*, 4392.

(17) Helms, B.; Mynar, J. L.; Hawker, C. J.; Fréchet, J. M. J. *Journal of the American Chemical Society* **2004**, *126*, 15020.

(18) Lutz, J.-F.; Börner, H. G.; Weichenhan, K. *Macromolecular Rapid Communications* **2005**, *26*, 514.

(19) Wu, P.; Feldman, A. K.; Nugent, A. K.; Hawker, C. J.; Scheel, A.; Voit, B.; Pyun, J.; Fréchet, J. M. J.; Sharpless, K. B.; Fokin, V. V. *Angewandte Chemie* **2004**, *116*, 4018.

(20) Wu, P.; Feldman, A. K.; Nugent, A. K.; Hawker, C. J.; Scheel, A.; Voit, B.; Pyun, J.; Fréchet, J. M. J.; Sharpless, K. B.; Fokin, V. V. *Angewandte Chemie International Edition* **2004**, *43*, 3928.

(21) Deiters, A.; Cropp, T. A.; Summerer, D.; Mukherji, M.; Schultz, P. G. *Bioorganic & Medicinal Chemistry Letters* **2004**, *14*, 5743.

(22) Lin, P.-C.; Ueng, S.-H.; Tseng, M.-C.; Ko, J.-L.; Huang, K.-T.; Yu, S.-C.; Adak, A. K.; Chen, Y.-J.; Lin, C.-C. *Angewandte Chemie International Edition* **2006**, *45*, 4286.

(23) Link, A. J.; Vink, M. K. S.; Tirrell, D. A. *Journal of the American Chemical Society* **2004**, *126*, 10598.

(24) Punna, S.; Kaltgrad, E.; Finn, M. G. *Bioconjugate Chemistry* **2005**, *16*, 1536.

(25) Seo, T. S.; Li, Z.; Ruparel, H.; Ju, J. *The Journal of Organic Chemistry* **2002**, *68*, 609.

(26) Gierlich, J.; Burley, G. A.; Gramlich, P. M. E.; Hammond, D. M.; Carell, T. *Organic Letters* **2006**, *8*, 3639.

(27) Wang, Q.; Chan, T. R.; Hilgraf, R.; Fokin, V. V.; Sharpless, K. B.; Finn, M. G. *Journal of the American Chemical Society* **2003**, *125*, 3192.

(28) Becer, C. R.; Hoogenboom, R.; Schubert, Ulrich S. *Angewandte Chemie International Edition* **2009**, *48*, 4900.

(29) Dondoni, A. *Angewandte Chemie International Edition* **2008**, *47*, 8995.

(30) Boutevin, B.; Hervaud, Y.; Mouledous, G. *Polym. Bull.* **1998**, *41*, 145.

(31) Gress, A.; Volkel, A.; Schlaad, H. *Macromolecules* **2007**, *40*, 7928.

(32) Justynska, J.; Hordyjewicz, Z.; Schlaad, H. *Polymer* **2005**, *46*, 12057.

(33) Killops, K. L.; Campos, L. M.; Hawker, C. J. *Journal of the American Chemical Society* **2008**, *130*, 5062.

(34) Hamley, I. W. *Angewandte Chemie International Edition* **2003**, *42*, 1692.

(35) Semlyen, J. A. *Large Ring Molecules*; John Wiley & Sons: New York, 1996.

(36) Colquhoun, H. M.; Lewis, D. F.; Ben-Haida, A.; Hodge, P. *Macromolecules* **2003**, *36*, 3775.

(37) Flory, P. J. *Principles of Polymer Chemistry* Ithaca, 1953; Vol. Chapters III and IV.

(38) Gordon, M.; Temple, W. B. *Die Makromolekulare Chemie* **1972**, *152*, 277.

(39) Gordon, M.; Temple, W. B. *Die Makromolekulare Chemie* **1972**, *160*, 263.

(40) Jacobson, H.; Beckmann, C. O.; Stockmayer, W. H. *The Journal of Chemical Physics* **1950**, *18*, 1607.

(41) Jacobson, H.; Stockmayer, W. H. *The Journal of Chemical Physics* **1950**, *18*, 1600.

(42) Stanford, J. L.; Stepto, R. F. T.; Waywell, D. R. *J. Chem. Soc.* **1975**, *71*, 1308.

(43) Stepto, R. F. T.; Waywell, D. R. *Die Makromolekulare Chemie* **1972**, *152*, 263.

(44) Ziegler, K. *Ber. Dtsch. Chem. Ges* **1943**, *67A*, 139.

(45) Deffieux, A.; Borsali, R. *Controlled Synthesis and Properties of Cyclic Polymers in Macromolecular Engineering*; Wiley VCH, 2007.

(46) Bielawski, C. W.; Benitez, D.; Grubbs, R. H. *Science* **2002**, *297*, 2041.

(47) Bielawski, C. W.; Grubbs, R. H. *Angewandte Chemie International Edition* **2000**, *39*, 2903.

(48) Casassa, E. F. *Journal of Polymer Science Part A: General Papers* **1965**, *3*, 605.

(49) Deffieux, A.; Borsali, R. *Macromolecular Engineering*; Wiley VCH: Weinheim, 2007; Vol. 2.

(50) Tezuka, Y.; Oike, H. *Journal of the American Chemical Society* **2001**, *123*, 11570.

(51) Semlyen, J. A.; Walker, G. R. *Polymer* **1969**, *10*, 597.

(52) Schappacher, M.; Deffieux, A. *Science* **2008**, *319*, 1512.

(53) Nasongkla, N.; Chen, B.; Macaraeg, N.; Fox, M. E.; Fréchet, J. M. J.; Szoka, F. C. *Journal of the American Chemical Society* **2009**, *131*, 3842.

(54) Gillies, E. R.; Dy, E.; Fréchet, J. M. J.; Szoka, F. *Mol. Pharm.* **2005**, *2*, 129.

(55) Uzgiris, E. *In est. Radiol.* **2004**, *39*, 131.

(56) Barner, L.; Davis, T. P.; Stenzel, M. H.; Barner-Kowollik, C. *Macromolecular Rapid Communications* **2007**, *28*, 539.

(57) Matyjaszewski, K. *Progress in Polymer Science*, *30*, 858.

(58) Barner-Kowollik, C.; Davis, T. P.; Heuts, J. P. A.; Stenzel, M. H.; Vana, P.; Whittaker, M. *Journal of Polymer Science Part A: Polymer Chemistry* **2003**, *41*, 365.

(59) Cacioli, P.; Hawthorne, D. G.; Laslett, R. L.; Rizzardo, E.; H., S. D. *J. Macromol. Sci. Chem* . **1986**, *23*, 839.

(60) Delduc, P.; Tailhan, C.; Zard, S. Z. *J. Chem. Soc. Chem. Commun.* **1988**, 308.

(61) Hutson, L.; Krstina, J.; Moad, C. L.; Moad, G.; Morrow, G. R.; Postma, A.; Rizzardo, E.; Thang, S. H. *Macromolecules* **2004**, *37*, 4441.

(62) Quémener, D.; Hellaye, M. L.; Bissett, C.; Davis, T. P.; Barner-Kowollik, C.; Stenzel, M. H. *Journal of Polymer Science Part A: Polymer Chemistry* **2008**, *46*, 155.

(63) An, Z.; Tang, W.; Wu, M.; Jiao, Z.; Stucky, G. D. *Chemical Communications* **2008**, 6501.

(64) Li, Y.; Benicewicz, B. C. *Macromolecules* **2008**, *41*, 7986.

(65) Ranjan, R.; Brittain, W. J. *Macromolecular Rapid Communications* **2008**, *29*, 1104.

(66) Shi, G.-Y.; Tang, X.-Z.; Pan, C.-Y. *Journal of Polymer Science Part A: Polymer Chemistry* **2008**, *46*, 2390.

(67) Yang, L.; Zhou, H.; Shi, G.; Wang, Y.; Pan, C.-Y. *Journal of Polymer Science Part A: Polymer Chemistry* **2008**, *46*, 6641.

(68) Zhang, T.; Zheng, Z.; Ding, X.; Peng, Y. *Macromolecular Rapid Communications* **2008**, *29*, 1716.

(69) Sinnwell, S.; Inglis, A. J.; Stenzel, M. H.; Barner-Kowollik, C. *Macromolecular Rapid Communications* **2008**, *29*, 1090.

(70) Li, M.; De, P.; Gondi, S. R.; Sumerlin, B. S. *Macromolecular Rapid Communications* **2008**, *29*, 1172.

(71) Ladmiral, V.; Legge, T. M.; Zhao, Y.; Perrier, S. b. *Macromolecules* **2008**, *41*, 6728.

(72) Nebhani, L.; Barner-Kowollik, C. *Advanced Materials* **2009**, *21*, 3442.

(73) Bruchez, M., Jr.; Moronne, M.; Gin, P.; Weiss, S.; Alivisatos, A. P. *Science* **1998**, *281*, 2013.

(74) Chan, W. C. W.; Nie, S. *Science* **1998**, *281*, 2016.

(75) Wang, S.; Mamedova, N.; Kotov, N. A.; Chen, W.; Studer, J. *Nano Letters* **2002**, *2*, 817.

(76) Mah, C.; Zolotukhin, I.; Fraites, T. J.; Dobson, J.; Batich, C. *B. J. Byrne* **2000**, *1*, 239.

(77) Pantarotto, D.; Partidos, C. D.; Hoebeke, J.; Brown, F.; Kramer, E.; Briand, J.-P.; Muller, S.; Prato, M.; Bianco, A. *Chemistry & Biology* **2003**, *10*, 961.

(78) Edelstein, R. L.; Tamanaha, C. R.; Sheehan, P. E.; Miller, M. M.; Baselt, D. R.; Whitman, L. J.; Colton, R. J. *Colton Biosensors Bioelectron*, *14*, 805.

(79) Nam, J.-M.; Thaxton, C. S.; Mirkin, C. A. *Science* **2003**, *301*, 1884.

(80) Mahtab, R.; Rogers, J. P.; Murphy, C. J. *Journal of the American Chemical Society* **2002**, *117*, 9099.

(81) de la Isla, A.; Brostow, W.; Bujard, B.; Estevez, M.; Rodriguez, J. R.; Vargas, S.; Castano, V. M. *Mat. Resr. Innovat.*, *7*, 110.

(82) Ma, J.; Wong, H.; Kong, L. B.; Peng, K. W. *Nanotechnology* **2003**, 619.

(83) Yoshida, J.; Kobayashi, T. J. *Magn. Magn. Mater.* **1999**, *194*, 176.

(84) Molday, R. S.; MacKenzie, D. J. *Immunol. Methods*, *52*, 353.

(85) Weissleder, R.; Elizondo, G.; Wittenburg, J.; Rabito, C. A.; Bengele, H. H.; Josephson, L. *Radiology* **1990**, *175*, 489.

(86) Parak, W. J.; Boudreau, R.; Gros, M. L.; Gerion, D.; Zanchet, D.; Micheel, C. M.; Williams, S. C.; Alivisatos, A. P.; Larabell, C. *Advanced Materials* **2002**, *14*, 882.

(87) Walther, A.; Müller, A. H. E. *Soft Matter* **2008**, *4*, 663.

(88) Glaser, N.; Adams, D. J.; Boker, A.; Krausch, G. *Langmuir* **2006**, *22*, 5227.

(89) Fang, H.; Zhang, K.; Shen, G.; Wooley, K. L.; Taylor, J.-S. A. *Molecular Pharmaceutics* **2009**, *6*, 615.

(90) Nyström, A. M.; Bartels, J. W.; Du, W.; Wooley, K. L. *J. Polym. Sci., Part A: Polym. Chem.* **2009**, *47*, 1023.

(91) Zhang, K.; Fang, H.; Wang, Z.; Taylor, J.-S. A.; Wooley, K. L. *Biomaterials* **2009**, *30*, 968.

(92) Nyström, A. M.; Wooley, K. L. *Tetrahedron* **2008**, *64*, 8543.

(93) Remsen, E. E.; Thurmond, K. B.; Wooley, K. L. *32* **1999**, *11*.

(94) Huang, H.; Kowalewski, T.; Remsen, E. E.; Gertzmann, R.; Wooley, K. L. *JACS* **1997**, *119*, 11653.

(95) Latham, A. H.; Williams, M. E. *Accounts of Chemical Research* **2008**, *41*, 411.

(96) Gelbrich, T.; Feyen, M.; Schmidt, A. M. *Phys. Chem.* **2006**, *220*, 1.

(97) Gelbrich, T.; Feyen, M.; Schmidt, A. M. *Macromolecules* **2006**, *39*, 3469.

(98) Gürler, C.; Feyen, M.; Behrens, S.; Mattoussevitch, N.; Schmidt, A. M. *Polymer* **2008**, *49*, 2211.

(99) Kaiser, A.; Gelbrich, T.; Schmidt, A. M. *J. Phys. Cond. Matter* **2006**, *18*, 2563.

(100) Schmidt, A. *Colloid & Polymer Science* **2007**, *285*, 953.

(101) Keng, P. Y.; Shim, I.; Korth, B. D.; Douglas, J. F.; Pyun, J. *ACS Nano* **2007**, *1*, 279.

(102) Korth Bryan, D.; Keng Pei, Y.; Shim, I.; Tang, C.; Kowalewski, T.; Pyun, J. In *Nanoparticles: Synthesis, Stabilization, Passivation, and Functionalization*; American Chemical Society: Washington, DC, 2009, p 272.

(103) Pyun, J.; Matyjaszewski, K. *Chemistry of Materials* **2001**, *13*, 3436.

(104) Zhang, M.; Estournès, C.; Bietsch, W.; Müller, A. H. E. *Advanced Functional Materials* **2004**, *14*, 871.

(105) Templeton, A. C.; Wülfing, W. P.; Murray, R. W. *Acc. Chem. Res.* **2000**, *33*, 27.

(106) Fleming, D. A.; Thode, C. J.; Williams, M. E. *Chem. Mater.* **2006**, *18*, 2327.

(107) White, M. A.; Johnson, J. A.; Koberstein, J. T.; Turro, N. J. *Journal of the American Chemical Society* **2006**, *128*, 11356.

(108) Ranjan, R.; Brittain, W. J. *Macromolecular Rapid Communications* **2007**, *28*, 2084.

(109) Fleming, D. A.; Thode, C. J.; Williams, M. E. *Chemistry of Materials* **2006**, *18*, 2327.

(110) Barner, L. *Advanced Materials* **2009**, *21*, 2547.

(111) Perrier-Cornet, R.; Heroguez, V.; Thienpont, A.; Babot, O.; Toupance, T. *J. Chromatography A* **2008**, *1179*, 2.

(112) Wang, J. F.; Cormack, p. A. G.; Sherrington, D. C.; Khoshdel, E. *Pure Appl. Chem.* **2007**, *79*, 1505.

(113) Ye, L.; Cormack, P. A. G.; Mosbach, K. *Anal. Comm.* **1999**, *36*, 35.

(114) Malosse, L.; Buvat, P.; Ades, D.; Siove, A. *Analyst* **2008**, *133*, 588.

(115) Yoshimatsu, K.; Reimhult, K.; Krozer, A.; Mosbach, K.; Sode, K.; Ye, L. *Anal. Chim. Acta* **2007**, *584*, 112.

(116) Kawaguchi, H. *Prog. Polym. Sci.* **2000**, *25*, 1171.

(117) Granville, A. M.; Brittain, W. J. *Polymer Brushes*; Wiley-VHC: Weinheim, 2004.

(118) Parvole, J.; Montfort, J.-P.; Reiter, G.; Borisov, O.; Billon, L. *Polymer* **2006**, *47*, 972.

(119) Voccia, S.; Jerome, C.; Detrembleur, C.; Leclere, P.; Gouttebaron, R.; Hecq, M.; Gilbert, B.; Lazzaroni, R.; Jerome, R. *Chemistry of Materials* **2003**, *15*, 923.

(120) Garcia, F. G.; Pinto, M. R.; Soares, B. G. *European Polymer Journal* **2002**, *38*, 759.

(121) Joso, R.; Reinicke, S.; Walther, A.; Schmalz, H.; Müller, A. H. E.; Barner, L. *Macromolecular Rapid Communications* **2009**, *30*, 1009.

(122) Li, Y.; Schadler, L. S.; Benicewicz, B. C. *Handbook of RAFT Polymerization*; Wiley-VCH: Weinheim, 2008.

(123) Nebhani, L.; Sinnwell, S.; Inglis, A. J.; Stenzel, M. H.; Barner-Kowollik, C.; Barner, L. *Macromolecular Rapid Communications* **2008**, *29*, 1431.

(124) Nordborg, A.; Limé, F.; Shchukarev, A.; Irgum, K. *J. Separation Sci.* **2008**, *31*, 2143.

(125) Vivek, A. V.; Dhamodharan, R. *Journal of Polymer Science Part A: Polymer Chemistry* **2007**, *45*, 3818.

(126) Zheng, G.; Stover, H. D. H. *Macromolecules* **2002**, *35*, 6828.

(127) Zheng, G.; Stover, H. D. H. *Macromolecules* **2002**, *35*, 7612.

(128) Zheng, G.; Stover, H. D. H. *Macromolecules* **2003**, *36*, 7439.

(129) Barner, L.; Li, C. E.; Hao, X.; Stenzel, M. H.; Barner-Kowollik, C.; Davis, T. P. *Journal of Polymer Science Part A: Polymer Chemistry* **2004**, *42*, 5067.

(130) Joso, R.; Stenzel, M. H.; Davis, T. P.; Barner-Kowollik, C.; Barner, L. *Aust. J. Chem.* **2005**, *58*, 468.

Summary

Click chemistry was utilized as ligation strategy for the synthesis of cyclic polymers, surface modification of large microspheres and iron oxide particles. The broad spectra of this universal and powerful tool in complex macromolecular architecture and surface-functionalization is presented.

Cyclic polystyrene was synthesized by the combination of Reversible Addition Fragmentation Chain Transfer (RAFT) Polymerization and the copper-catalyzed Huisgen [2+3] cycloaddition click reaction. Therefore, an azido dithiobenzoate click RAFT agent was employed as chain transfer agent in the RAFT polymerization of styrene resulting in low molecular weight azido-terminated polymers. The exchange of the dithio moiety of the polymeric chains was carried out by using an alkyne-modified initiator, leading to a heterotelechelic linear polymer precursor for the click cyclization. The properties of the macrocyclic polymer, as compared to the linear counterpart were investigated. The combination of several analytic methods proved the cyclic structure. From the viscosity measurements in the good solvent THF a contraction factor of $g' = [\eta]_{cyc}/[\eta]_{lin}$ =0.70-0.74 was calculated. This value is consistent with the theoretically calculated value g´=0.67 for θ-conditions.

Surface modification of large poly(divinylbenzene) microspheres (pDVB, 1.3 μm) was undertaken with two different strategies, on the one hand with Huisgen [2+3] cycloaddition reaction and on the other hand with thiol-ene click chemistry. The pDVB microspheres have a thin surface layer consisting of partially crosslinked and swellable poly(divinylbenzene) and contain vinyl groups on their surfaces which are accessible for modification, i.e. direct surface modification via *"grafting to"* techniques. The RAFT technique was used to synthesize SH-functionalized poly(*N*-isopropylacrylamide) (pNIPAAm-SH) polymers to generate surface-modified microspheres via thiol-ene reaction. Surface-sensitive characterization methods were used to identify the characteristic polymer shell on the outer layer. The visualization of the particles was carried out with Scanning Electron Microscopy (SEM). Suspension studies of the microspheres demonstrate an appealing gain of hydrophilicity when grafted with $pNIPAAm_{45}$ and therefore could be suspended in water after surface modification. This observation was supported by a turbidimetric study. In an alternative approach, multifunctional azido-functionalized microspheres were prepared via the thiol-ene reaction of 1-azido-undecan-11-thiol with residual double bonds on the surface

and subsequent 1,3 Huisgen dipolar cycloaddition reaction. These surface-modified particles are grafted with poly(hydroxyethyl methacrylic)acid (pHEMA). Grafting of hydrophilic polymers to hydrophobic particles can truly enhance the suspension properties of the particles in aqueous environment.

Finally, magnetite Fe_3O_4 nanoparticles were surface-modified by the Huisgen [2+3] cycloaddition reaction. A versatile biomimetic anchor, dopamine, was used to stabilize and concomitantly functionalize the particles. An alkyne-functionalized dopamine derivative was synthesized leading to multifunctionalized stable Fe_3O_4 nanoparticles. Surface modification was carried out with azide-endgroup modified polyethylene glycol (PEG). Furthermore, visualization of the surface-modified particles was accomplished by reaction with an azido-modified Rhodamine derivative and investigated with confocal fluorescence microscopy. With this approach, hydrophobic Fe_3O_4 nanoparticles can be converted into watersoluble particles. Furthermore the hydrophilic PEG-coating leads to a biocompatible shell.

In general, all these new applications show the versatility of click chemistry and broaden the scope of alternative and easy approaches for surface modification strategies and for the access towards complex macromolecular architecture.

Zusammenfassung

Click-Chemie wurde als Ligations-Strategie für die Synthese von cyclischen Polymeren und zur Oberflächenmodifizierung von großen Mikrokugeln und magnetischen Eisenoxidpartikeln verwendet. Das breite Spektrum dieses universellen und leistungsstarken Instruments im Bereich der komplexen makromolekularen Architektur und Oberflächenmodifizierung ist hier dargelegt.

Cyclisches Polystyrol wurde mittels der Kombination der „Reversiblen Additions-Fragmentierungs-Kettenübertragungs-Polymerisation" (RAFT) und der kupferkatalysierten Huisgen [2+3] Cycloadditons Click-Reaktion synthetisiert. Ein Azido-funktionalisiertes Dithiobenzoat Click-RAFT-Agens wurde als Kettenüberträger in der RAFT Polymerisation von Styrol verwendet, die in niedermolekularen azido-terminierten Polymeren resultierte. Der Austausch der Dithio-Gruppe der Polymerkette wurde mit einem Alkin-modifizierten Initiator durchgeführt und führte zu einem heterotelechelischen linearen Polymerprecursor für die Click-Cyclisierung. Die Eigenschaften des makrocyclischen Polymers im Vergleich zum linearen Gegenstück wurden untersucht. Die Kombination aus mehreren Analytikmethoden konnte die cyclische Struktur beweisen. Aus den Viskositätsmessungen im guten Lösungsmittel THF wurde ein Kontraktionsfaktor $g' = [\eta]_{cyc}/[\eta]_{lin}$ = 0.70-0.74 bestimmt. Dieser Wert stimmt mit dem theoretisch bestimmten Wert g´=0.67 für θ-Bedingungen überein.

Die Oberflächenmodifizierung von großen Poly(divinylbenzol) Mikrokugeln (pDVB, 1,3 μm) wurde mit zwei verschiedenen Strategien durchgeführt, zum einen der Huisgen [2+3] Cycloadditionsreaktion und zum anderen mit der Thiol-en Click-Chemie. Die pDVB Mikrokugeln besitzen eine dünne Oberflächenschicht die aus teilweise vernetztem und quellfähigem Poly(divinylbenzol) besteht und darüber hinaus über Vinylgruppen auf ihren Oberflächen verfügen die für eine Modifizierung zugänglich sind, beispielsweise einer direkter Oberflächenmodifizierung durch Pfropfungstechniken („grafting-to“). Die RAFT-Technik wurde benutzt um SH-funktionalisierte Poly(N-Isopropylacrylamid)-Polymere (pNIPAAm-SH) zu synthetisieren und oberflächenmodifizierte Mikrokugeln über Thiol-en-Reaktion zu generieren. Oberflächensensitive Charakterisierungsmethoden wurden zur Identifizierung der charakteristischen Polymerhülle auf der Außenschale verwendet. Die Visualisierung der Partikel wurde mit der Rasterelektronenmikroskopie (REM) durchgeführt. Suspensionsstudien der Mikrokugeln zeigen einen ansprechenden Gewinn der Hydrophilie

nachdem sie mit $pNIPAAm_{45}$ gepfropft wurden und somit nach der Oberflächenmodifizierung in Wasser suspendiert werden können. Diese Beobachtung wurde durch eine Trübungsstudie unterstützt. In einer alternativen Vorgehensweise wurden multifunktionelle Azido-funktionalisierte Mikrokugeln über die Thiol-En-Reaktion von 1-Azido-undecan-11-thiol mit den verbleibenden Doppelbindungen auf der Oberfläche und anschließender 1,3 Huisgen dipolarer Cycloadditionsreaktion hergestellt. Diese oberflächenmodifizierten Partikel wurden mit Poly(hydroxyethylmethacrylat) (pHEMA) gepfropft. Das Aufpfropfen von hydrophilen Polymeren auf hydrophobe Partikel kann die Suspendierungseigenschaften der Partikel im wässrigen Medium deutlich erhöhen.

Schließlich wurden Magnetit-Nanopartikel (Fe_3O_4) mit der Huisgen [2+3] Cycloadditionsreaktion oberflächenmodifiziert. Dabei wurde ein vielseitiger biomimetischer Anker, Dopamin, verwendet um die Partikel zu stabilisieren und gleichzeitig zu funktionalisieren. Die Synthese eines Alkin-Dopamin-Derivats führt zu multifunktionellen stabilen Fe_3O_4-Nanopartikeln. Die Oberflächenmodifizierung wurde mit einem Azid-funktionalisierten Polyethylenglykol (PEG) und desweiteren mit einem Azid-modifizierten Rhodamin-Derivat durchgeführt. Diese Eisenoxid-Partikel wurden mit konfokaler Fluoreszenzmikroskopie untersucht. Mit diesem Ansatz können hydrophobe Fe_3O_4-Nanopartikel in wasserlösliche Partikel umgewandelt und in Wasser redispergiert werden. Außerdem führt die hydrophile PEG-Schicht zu einer biokompatiblen Hülle.

Im Allgemeinen zeigen all diese neuen Anwendungen die Vielseitigkeit der Click-Chemie und erweitern die Bandbreite alternativer und einfacher Ansätze für Oberflächenmodifizierungsstrategien und den Zugang zu komplexer makromolekularer Architektur.

Overview of the thesis

The research presented in this thesis deals with the application of click chemistry in the synthesis of cyclic polymers, surface functionalization of magnetic nanoparticles and polymeric microspheres. This thesis consists of three chapters including three publications.

Chapter IV presents the synthesis of macrocyclic polystyrene via a combination of Reversible Addition Fragmentation Chain Transfer (RAFT) polymerization and click chemistry. A heterotelechelic linear backbone was synthesized via RAFT polymerization followed by endgroup modification to facilitate click chemistry for the formation of ring shaped polystyrene.

Chapter V focuses on the synthesis and surface-functionalization of polydivinylbenzene microspheres (pDVB). The grafting of polymer chains via two separate approaches is highlighted. Therefore, thiol-ene chemistry and azide-alkyne click reactions of pDVB are used to directly graft polymers from the residual accessible double bonds of pDVB microspheres in a one-step process.

In Chapter VI the synthesis of magnetic Fe_3O_4 nanoparticles is described along with the functionalization to obtain clickable nanoparticles. Click-functionalized dopamine, a mussel adhesive inspired biomimetic material, is utilized as an anchor to the surface of the Fe_3O_4 nanoparticles. Fluorescent markers and N_3-poly(ethylene glycol) were attached via click chemistry.

In the following, a brief summary of the main results is presented.

3.1. Cyclic Polystyrenes *via* a Combination of Reversible Addition Fragmentation Chain Transfer (RAFT) Polymerization and Click Chemistry

The coupling of the reversible addition-fragmentation chain transfer (RAFT) polymerization technique with the copper catalyzed Huisgen 1,3-dipolar cycloaddition (click chemistry) as a simple and effective way to generate polystyrene (PS) macrocycles is presented (Figure 2.1.).

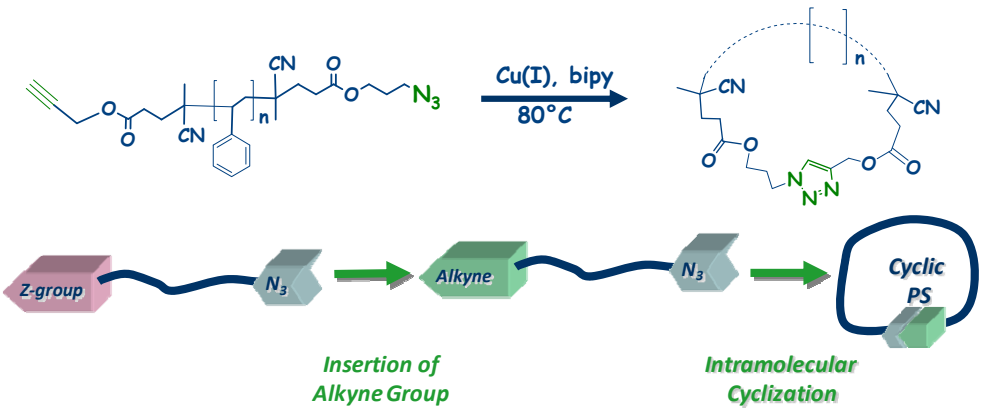

Figure 2.1. General pathway towards cyclic polymers via click chemistry

The synthesis entails linear PS backbones followed by endgroup modification to allow click chemistry for the formation of ring shaped polymers. An azido group modified 4-cyanopentanoic acid dithiobenzoate is employed as the chain transfer agent in the RAFT mediated polymerization.

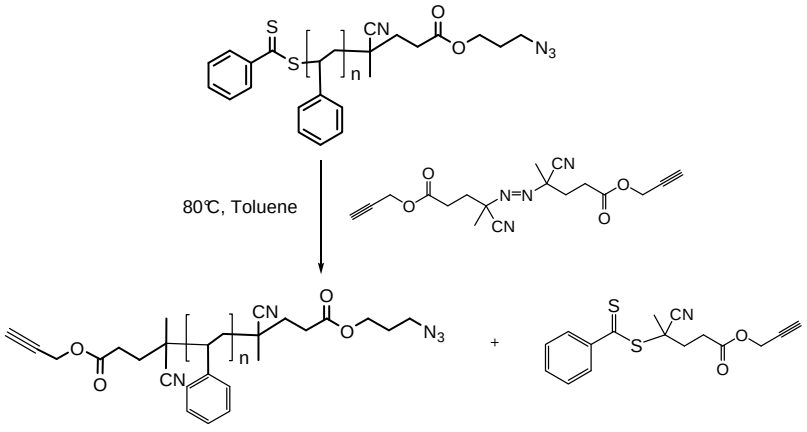

Scheme 2.1. Endgroup modification of the PS chain via removal of the thiocarbonyl-thio functionality to obtain α,ω-heterotelechelic homopolymers

The cyclization of the polystyrene chains by click coupling, is conducted by removal of the thiocarbonyl thio endgroup and concomitantly replacing by an alkyne bearing function (Figure 2.1.).

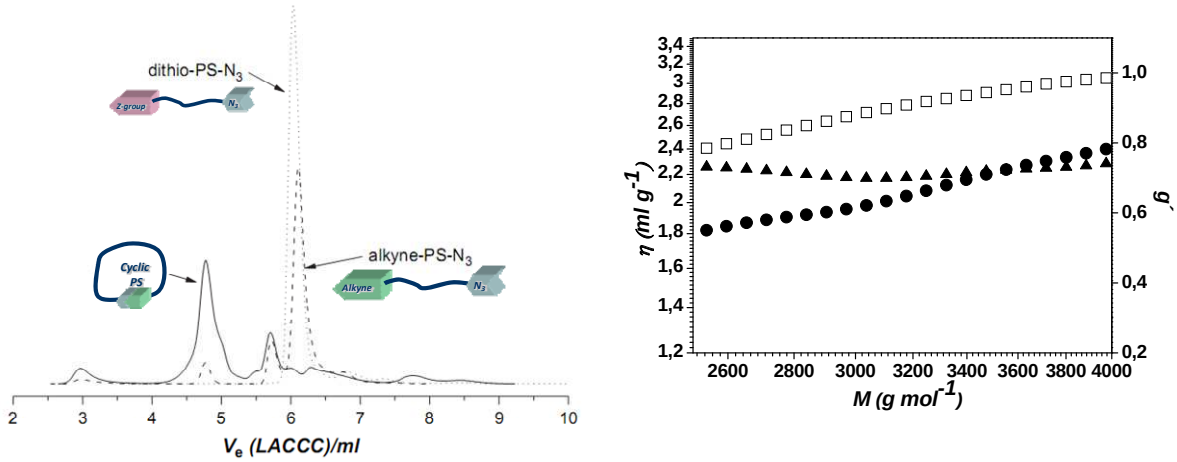

Figure 2.2. Left: LACCC chromatograms (normalized by area) at critical conditions of alkyne-PS-N_3 for linear dithio-PS-N_3 precursor linear alkyne-PS-N_3 and cyclic polystyrenes. Right: Mark-Houwink plots of intrinsic viscosity versus molecular weight, for linear (□) and cyclic (●) polystyrenes (7): contraction factors, g'.

The LACCC traces (Liquid Adsorption Chromatography at critical conditions) of the dithio-PS-N_3 precursor, linear alkyne-PS-N_3 and cyclic polystyrenes at critical conditions of alkyne-PS-N_3 are given in Figure 2.2. (left). The linear precursors, dithio-PS-N_3 precursor and alkyne-PS-N_3 elute nearly at the same elution volume. As expected, the cyclic PS elutes significantly earlier than the linear counterparts. Furthermore the intrinsic viscosities of cyclic and linear precursor resulted in parallel lines. Mark-Houwink exponents were found to be in the range predicted and are consistent with the previous results obtained for polymers in solution.

3.2. Surface Modification of Poly(Divinylbenzene) Microspheres *via* Thiol-Ene-Chemistry and Alkyne-Azide Click Reactions

The functionalization of crosslinked poly(divinylbenzene) (pDVB) microspheres using the thiol-ene and azide-alkyne click reactions is presented. The RAFT technique was used to synthesize SH-functionalized poly(N-isopropylacrylamide) (pNIPAAm) and utilized to generate surface-modified microspheres via thio-click modification (thiol-ene reaction, Figure 2.3., A). In a second approach, pDVB microspheres were grafted with poly(2-hydroxyethyl methacrylate) (pHEMA). For this purpose, the residual double bonds on the microsphere surface were modified with azide groups via the thio-click approach of a thiol-azide compound. In a second step, the alkyne endgroup functionalized pHEMA was used to graft PHEMA to the azide-modified surface via click-chemistry (Figure 2.3., B).

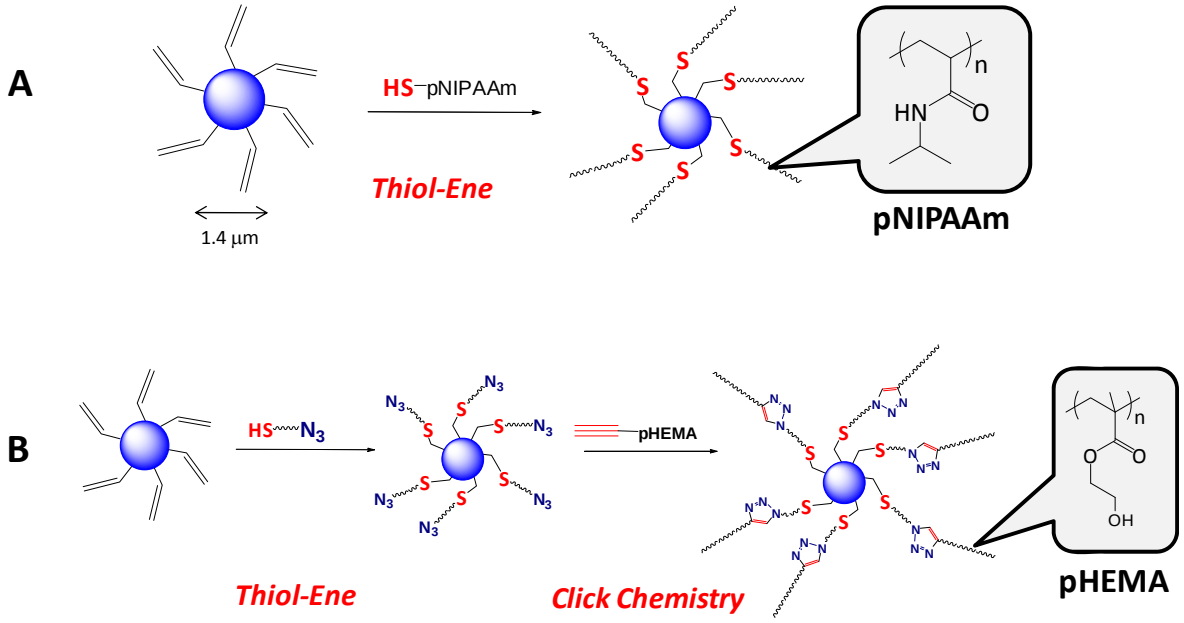

Figure 2.3. A: Thio-click modification of pDVB80 microspheres with pNIPAAm$_{45}$ in a one-step approach. B: PHEMA grafted microspheres via Huisgen 1,3-dipolar cycloaddition.

Successful grafting via the click approach was demonstrated by surface characterization methods, SEM and confocal fluorescence microscopy. Figure 2.4 represents a cross-sectional slice of fluorescence-labeled pHEMA microspheres. It clearly shows the fluorescence in the outer shell (and no fluorescence in the core of the particle) and therefore confirms the exclusive functionalization with pHEMA on the surface of the microspheres.

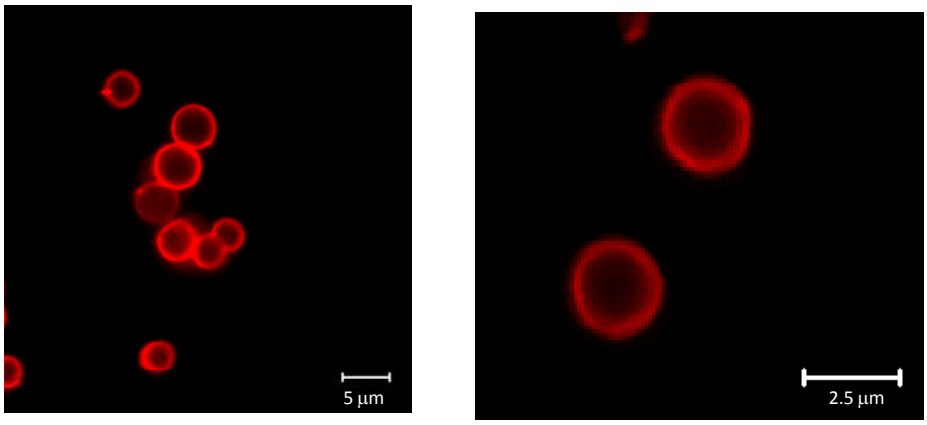

Figure 2.4. Confocal microscopy image of pDVB80-g-pHEMA microspheres functionalized with a Rhodamine B- fluorescent tag.

3.3. Biomimetic Mussel Adhesive Inspired Clickable Anchors Applied to the Functionalization of Fe_3O_4 Nanoparticles

Herein, I investigated the surface-functionalization of Fe_3O_4 magnetic nanoparticles, employing a dopamine-derived inspired biomimetic anchor strategy of the clickable group. The strategy illustrated is applicable to many surfaces and therefore broadens the scope of surface functionalization methods by click chemistry. The ability of catechols (e.g., dopamine) to bind to a large variety of inorganic surfaces, the biomimetic anchoring strategy is an interesting and versatile tool for surface modification of different particles. Fe_3O_4 magnetic nanoparticles were chosen as a model substrate to demonstrate the versatility of the click-functionalized alkyne-dopamine.

The synthesis of click-functionalized Fe_3O_4 nanoparticles (NPs) is reported as a unique route towards clickable magnetic nanoparticles. Therefore, fluorescent azido-Rhodamine was used to visualize the click-modification of Fe_3O_4 magnetic NPs. Fluorescence spectroscopy and confocal fluorescence microscopy are explicit methods to prove the effective surface functionalization. We demonstrate the synthetic strategy of alkyne-surface modified Fe_3O_4 magnetic particles as well as the click-reaction with the fluorescent compound. The general synthetic strategy is shown in Figure 2.5.

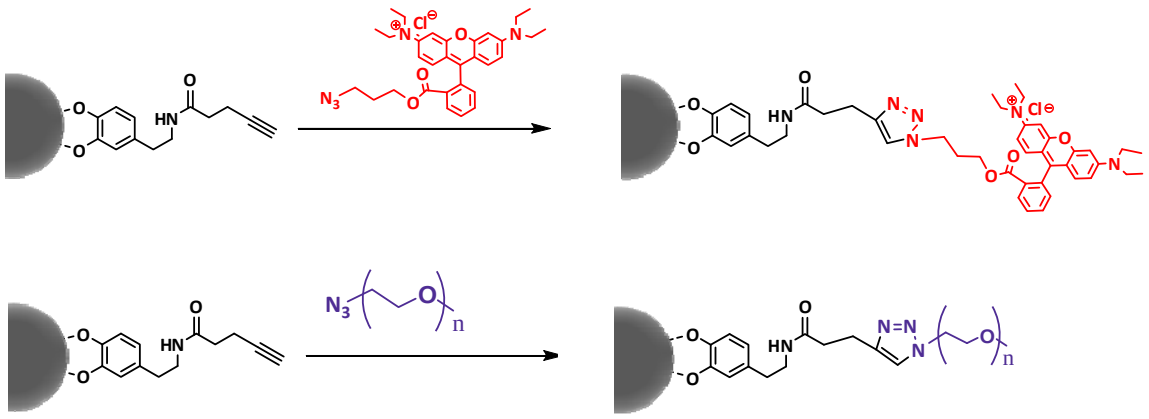

Figure 2.5. Synthetic strategy for clickable, mussel adhesive inspired fluorescent Fe_3O_4 nanoparticles. A: TEM image of oleic acid stabilized Fe_3O_4 nanoparticles in n-hexane. B: TEM image of dopamine-stabilized fluorescent Fe_3O_4 nanoparticles (THF) C: Confocal Fluorescence Microscopy image of aggregated dried dopamine-stabilized fluorescent Fe_3O_4 nanoparticles.

The synthesis of the Fe_3O_4 particles and the alkyne-dopamine are described as well as the characterization of the fluorescent nanoparticles. Confocal fluorescence microscopy visualizes the successful attachment of alkyne-dopamine and therefore effective click-chemistry.

3.4. Individual Contributions to Joint Publications

The results presented in this thesis were obtained in collaboration with others, and have been published or will be submitted to publication as indicated below. In the following, the contributions of all the coauthors to the different publications are specified. The asterisk denote the corresponding author.

Chapter IV

This work is published in ***Polymer*** **2008**, *49*, 2274 under the title:

"Access to Cyclic Polystyrenes *via* a Combination of Reversible Addition Fragmentation Chain Transfer (RAFT) Polymerization and Click Chemistry"

by Anja S. Goldmann, Damien Quémener, Pierre-Eric Millard, Thomas P. Davis, Martina H. Stenzel, Christopher Barner-Kowollik and Axel H. E. Müller**

I conducted all experiments and wrote the publication.
Damien Quémener was involved in discussion.
Pierre-Eric Millard was involved in discussions and conducted the LACCC measurements.
Thomas P. Davis and Martina H. Stenzel were involved in discussions.
Christopher Barner-Kowollik and Axel H. E. Müller were involved in scientific discussion and correcting this manuscript.

Chapter V

This work is published in ***Macromolecules*** **2009**, *42*, 3707 under the title:

"Surface Modification of Poly(divinylbenzene) Microspheres via Thiol-Ene-Chemistry and Alkyne-Azide Click Reactions"

by Anja S. Goldmann, Andreas Walther, Leena Nebhani, Raymond Joso, Dominique Ernst, Katja Loos, Leonie Barner, Christopher Barner-Kowollik and Axel H. E. Müller**

I conducted all experiments and wrote the publication.

Andreas Walther was involved in discussion.

Leena Nebhani conducted the synthesis of the p(DVB) microspheres.

Raymond Joso was involved in discussions.

Dominique Ernst accomplished the fluorescence microscopy measurements.

Katja Loos conducted the XPS measurements.

Leonie Barner, Christopher Barner-Kowollik and Axel H. E. Müller were involved in scientific discussion and correcting this manuscript.

Chapter VI

This work was submitted to **Macromolecular Rapid Communications** under the title:

"Biomimetic Mussel Adhesive Inspired Clickable Anchors Applied to the Functionalization of Fe_3O_4 Nanoparticles"

*by Anja S. Goldmann, Christine Schödel, Andreas Walther, Jiayin Yuan, Katja Loos and Axel H. E. Müller**

I performed most of the experiments and wrote the manuscript.

Christine Schödel was involved in the synthesis of alkyne-dopamine and fluorescence measurements.

Katja Loos conducted the XPS measurements.

Andreas Walther, Jiayin Yuan and Axel H. E. Müller were involved in scientific discussion and correcting this manuscript.

Access to Cyclic Polystyrenes *via* a Combination of Reversible Addition Fragmentation Chain Transfer (RAFT) Polymerization and Click Chemistry

Anja S. Goldmann,[1] Damien Quémener,[§,2] Pierre-Eric Millard, [1] Thomas P. Davis,[2] Martina H. Stenzel,[,2] Christopher Barner-Kowollik,*[,2] and Axel H. E. Müller*[,1]*

[1] Makromolekulare Chemie II and Zentrum für Kolloide und Grenzflächen, Universität Bayreuth, 95440 Bayreuth, Germany

[2] Centre for Advanced Macromolecular Design, School of Chemical Engineering and Industrial Chemistry, The University of New South Wales, Sydney, NSW 2052, Australia, Email: axel.mueller@uni-bayreuth.de, m.stenzel@unsw.edu.au, c.barner-kowollik@unsw.edu.au

[§] current address: Institut Européen des Membranes, UMR 5653, CNRS-ENSCM-UM II, 2 Place E Bataillon, 43095 Montpellier, France

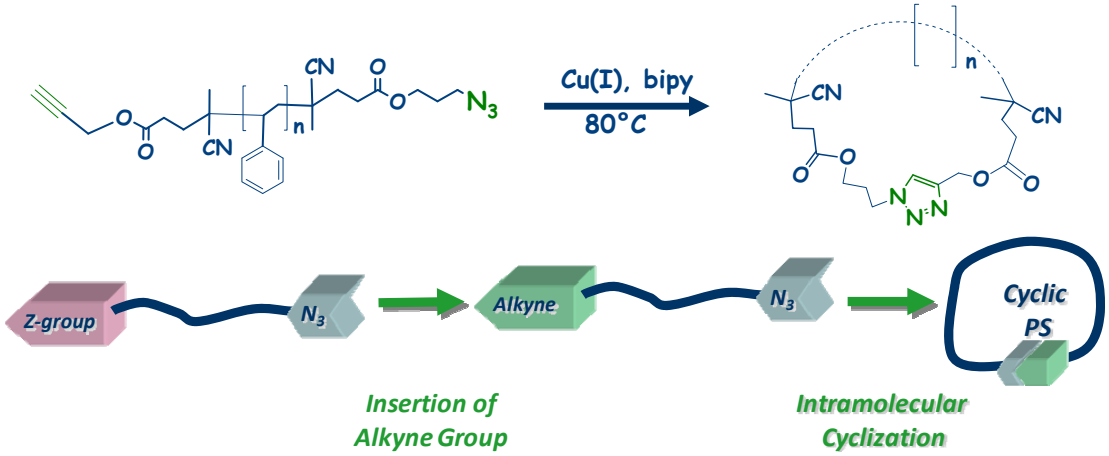

Abstract

The coupling of the reversible addition-fragmentation chain transfer (RAFT) polymerization technique with the copper catalyzed Huisgen 1,3-dipolar cycloaddition ("click chemistry") as a simple and effective way to generate polystyrene (PS) macrocycles is presented. The novel strategy entails the synthesis of linear PS backbones followed by endgroup modification to facilitate click chemistry for the formation of ring shaped polymers. An azido group modified 4-cyanopentanoic acid dithiobenzoate is employed as the chain transfer agent in the RAFT mediated polymerization of styrene to form PS with M_n from 2000 g mol^{-1} to 6000 g mol^{-1} and *PDI* < 1.2. To facilitate the cyclization of the polystyrene chains by click coupling, the thiocarbonyl thio endgroup is removed and concomitantly replaced by an alkyne bearing function. This is carried out *via* the radical decomposition of excess azobis(4-cyano valeric acid) (ACVA) modified with an alkyne endgroup in the presence of the thiocarbonylthio-capped PS. The successful click endgroup modifications of several polystyrenes along with the results from the cyclization of a PS with M_n = 4300 g mol^{-1} are discussed in detail. This improved method avoids the presence of thiocarbonylthio functions in the macrocycle, thus considerably increasing the chemical stability of these polymers.

Keywords: Reversible Addition Fragmentation Chain Transfer (RAFT), macrocyclic polymers, copper catalyzed Huisgen 1,3-dipolar cycloaddition, click chemistry.

Introduction

Numerous synthetic methods have been explored by several groups for optimizing the control over polymer architecture[1-5] as a prerequisite to manipulating the material properties. In particular, cyclic polymers have become increasingly attractive over the past years due to their unique architecture and their novel properties[6] (due to the absence of endgroups), potentially simple bond cleavage,[7] bond interchange reactions[8,9] or the formation of catenanes,[10-12] , rotaxanes[12-15] or knots[12,16-18] In the past, cyclic oligomers have been identified as side products in step-growth polymerizations, formed by ring-opening through backbiting reactions[19-21] or ring-chain equilibrium reactions.[22] However, several challenges exist in controlling the molecular weights and polydispersity in order to obtain well-defined cyclic macromolecules. Significant efforts have been dedicated to preparation and characterization of cyclic homopolymers *via* anionic polymerization using bifunctional initiators and bifunctional coupling agents.[23-26] In an alternative approach, Deffieux and his coworkers,[27] employed a coupling reaction under conditions of extreme dilution for the synthesis of vinyl type polymers. Their work involved direct coupling of a heterotelechelic linear polymer precursor previously prepared by living polymerization. In an alternative approach, Cramail and coworkers used linear PS featuring two living endgroups with 1,3-bis(1-phenylethylenyl)benzene (DDPE) as a coupling agent.[28] Hemery *et al*. detailed a synthetic route to heterotelechelic PS *via* nitroxide-mediated radical polymerization and its cyclization by intramolecular esterification.[28,29] Some of these earlier syntheses often involve incomplete cyclizations or undesired side reactions which require tedious purification procedures to remove the impurities. Grayson *et al.*[30] demonstrated a strategy to achieve cyclization *via* the combination of ATRP and click chemistry. In their work, PS prepared by ATRP was selected because the terminal benzylic bromide represents a good substrate for a nucleophilic displacement with an azide. The synthetic strategy for the synthesis of cyclic polymers and block copolymers by monomer insertion into a cyclic chain transfer agent was successfully prepared by Pan *et al*.[31] Monteiro *et al.*[32] achieved formation of unique monocyclic polystyrene chains by polymerizing styrene in the presence of a difunctional RAFT agent and subsequent conversion of the dithioester end groups to thiols. Monocyclic polymer was obtained by oxidation under dilute conditions. Xu *et al.*[33] reported the preparation of cyclic poly(N-isoproypacrylamide) (PNIPAAm) using an approach similar to the one published by Grayson[30] by combining ATRP and click chemistry using propargyl 2-

chloropropionate as the initiator, followed by reacting with NaN_3 to transform the terminal chloride into azide group. The subsequent end-to-end intramolecular coupling reaction was conducted under high dilution. Recently, Winnik *et al.*[34-36] prepared cyclic PNIPAM in aqueous solution synthesized by reversible addition fragmentation chain transfer polymerization (RAFT) carrying an azidoethoxyethyl group on one end. The propargyl group was inserted by a one-pot aminolysis/Michael addition sequence. Click cyclization leads to a polymer with a carbon-sulfur bond in the macrocycle, which makes the ring potentially unstable toward chemical attack.

In comparison, the present approach for cyclization of linear polystyrene chains also provides ready accessibility towards ring-closure due to suitable insertion of the prerequisite alkyne- and azido functional groups, which are required for click chemistry (Scheme 1) and at the same time provides a macrocyle with higher chemical stability.

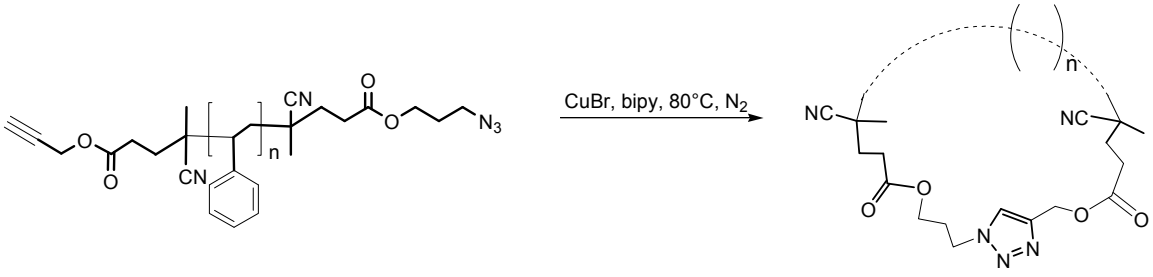

Scheme 1. Click-cyclization procedure of telechelic polystyrenes

In the current study, the RAFT polymerization technique is combined with click chemistry to obtain the ring shaped polymers. RAFT is a particularly attractive approach for synthesizing macrocyclic precursors because of the easy amenability of the azido endgroup functionality using a recently developed azido dithiobenzoate RAFT agent[37] followed by the exchange of the Z-group with an alkyne-functionalized initiator (Scheme 2).

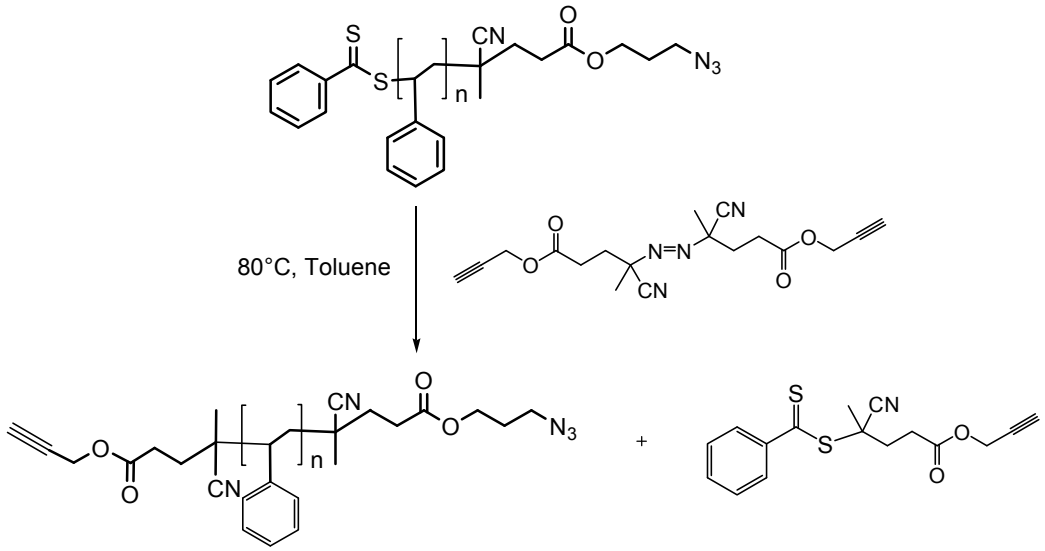

Scheme 2. Endgroup modification of the PS chain via removal of the thiocarbonyl-thio functionality to obtain telechelic homopolymers

The basic mechanism involved in the click reaction, employed for the preparation of our ring shaped polymers, is the copper-catalyzed Huisgen 1,3-dipolar cycloaddition of a terminal alkyne and an azide to form a 1,4-disubstituted 1,2,3-triazole.[38] The challenge in preparing cyclic polymers *via* RAFT was to synthesize the alkyne-terminated initiator to obtain the required end functionality for the click cyclization and to find the best conditions to achieve cyclization in high yields.

Experimental Part

Materials

All chemicals and solvents where purchased from Sigma-Aldrich, Acros and Fluka at the highest available purity and used as received unless otherwise noted. Styrene was purified by passing through a basic alumina column. Dimethylformamide (DMF) was dried over molecular sieve or distilled. The thermally decaying initiator 2,2´-azoisobutyronitrile (AIBN, Aldrich, 99%) was purified by crystallization from ethanol. The synthesis of the azido dithiobenzoate RAFT agent (**Scheme 2**) was undertaken according to the previously reported protocols.[37,39]

Measurements

The ^{1}H NMR and ^{13}C NMR spectra were recorded on a Bruker ACF300 300-MHz spectrometer with $CDCl_3$ as the solvent. 2D NMR measurements (HMBC and HSQC) were performed using a Bruker 500 MHz spectrometer. The SEC setup was performed in pure THF at an elution rate of 1 mL min^{-1} using PSS SDVgel columns (300 × 8 mm, 5μm): 10^5, 10^4, 10^3, and 10^2 Å with RI and UV (260 nm) detection. Polystyrene standards were used to calibrate the columns. Samples from preparative SEC were analysed using THF SEC with a precolumn (SDV-Gel (PSS), L: 5cm, D: 0.8cm, particle size: 5 μm, pore size: 100 Å) and analytical columns (PL-Gel (PL), L: 2 × 60cm; D: 0.8 cm, particle size: 5μm, pore size 100 Å) with THF as eluent and a flow rate of 0.5 mL min^{-1}. The calibration is based on PS standards. Preparative SEC was carried out on an instrument with a precolumn: SDS (PSS), 5μm, and analytical columns: PL-Gel (PL), L: 30 cm, D: 2.5 cm, 10 μm, 10^4 Å, L: 30 cm, D: 2.5 cm, 10 μm, 10^3 Å, 2 × 10 μm, 100 Å, L: 60 cm, D: 2.5 cm and L: 30 cm, D: 2.5 cm). VISCO-SEC was conducted on an Agilent HPLC system (1200 series) with a flow rate of 0.8 mL min^{-1} in THF (HPLC grade) at room temperature. Four detectors were used for the Visco-SEC: UV (260 nm), RI, Viscometer, Model 250 (Viscotek), (Columns: PSS-SDV), 10^6 Å, 5 μm, 10^5 Å, 5 μm, 10^3 Å, 5 μm). Liquid adsorption chromatography under critical conditions (LACCC) was conducted on a HPLC system at a flow rate of 0.5 mL/min. An Evaporative Light Scattering detector (ELSD, PL-EMD 960) operating at 80 °C with a gas flow rate of 6.8 L/min was used for mass detection. Then 10 μL samples of ca. 0.5 wt % polymer solutions were injected. All measurements were carried out at a constant column temperature of 25 °C. Two reversed phase columns (YMC, 250 × 4 mm) with 5 μm average particle size and 100 and 300 Å pore diameters were used. The critical solvent composition for PS is THF/hexane 43:57 (v/v). Premixing of the mobile phase by weight is necessary for a constant and exact composition. The FT-NIR and ATR-FTIR measurements were performed using a Bruker IFS66\S FTIR spectrometer equipped with a tungsten halogen lamp, a CaF_2 beam splitter and a liquid nitrogen-cooled InSb detector (FT-NIR). For ATR-FTIR a KBr beam splitter was used. Each spectrum in the spectroscopic region of 4000-500 cm^{-1} was calculated from the co-added interferograms of 16 scans with a resolution of 4 cm^{-1}. UV-VIS measurements were carried out on a CARY 300 double-beam spectrophotometer.

*Mass analysis***.** ESI-MS experiments were carried out using a Thermo Finnigan LCQ Deca ion trap mass spectrometer (Thermo Finnigan, San Jose, CA) equipped with an atmospheric

pressure ionization source operating in the nebulizer-assisted electrospray mode. The instrument was calibrated with caffeine, MRFA, and Ultramark 1621 (all from Aldrich) in the mass range 195-1822 Da. All spectra were acquired in positive ion mode with a spray voltage of 5 kV, a capillary voltage of 44 V and a capillary temperature of 225 °C. Nitrogen was used as sheath gas (flow: 50% of maximum) while helium was used as auxiliary gas (flow: 5% of maximum). The eluent was a 6:4 v/v mixture of THF/methanol. All reported molecular weights were calculated *via* the program package CS ChemDraw 6.0 and are monoisotopic. MALDI-TOF mass spectra were recorded on a Bruker Reflex III operated in linear mode using a nitrogen laser (337 nm) and an accelerating voltage of 20 kV. Dithranol was used as matrix and silver trifluoracetate as salt. Samples were prepared from THF solution by mixing matrix (20 mg mL^{-1}), sample (10 mg mL^{-1}) and salt (10 mg mL^{-1}) in a ratio 20:5:1. The instrument was calibrated with a peptide calibration standard from Bruker (part no. 206195) containing a mixture of different peptides in the mass range from $[M+H]^+$=1047.20 to $[M+H]^+$=3149.61. For the medium range protein calibration standard I was used (part no. 206355) in the mass range from $[M+H]^+$=5734.56 to $[M+H]^+$=16952.55. As titration device a Metrohm automatic 809 Titrando system was used with a 20 mL dosing unit (800 Dosino).

Polymerization Procedures

All polymerizations were carried out using the conditions described in Table 1. During the polymerizations, samples were taken at predetermined time intervals so as to monitor the monomer to polymer conversion as well as the molecular weight evolution with the monomer conversion. For the described cyclization procedures, linear PS chains with molecular weights in the range from 2000 – 5000 g mol^{-1} were used.

Table 1. RAFT polymerizations of styrene with azido dithiobenzoate click-RAFT agent

Exp.	[Mon]:[CTA]:[Ini]	Time (min)	Temp. (°C)	Solv.	$M_{n,th}$ [c] (g mol^{-1})	M_n, [a] (g mol^{-1})	*PDI* [a]	Conv.[b] (%)
1	150:5:1	1260	60	-	5100	5300	1.08	30
2	150:5:1	590	60	-	3200	3500	1.09	17.5
3	150:5:1	820	60	-	3500	3700	1.19	20
4	200:1:0.2	510	80	DMF	3100	4800	1.11	13
5	250:5:1	330	60	-	2800	2900	1.08	9
6	500:5:1	180	60	-	2500	1900	1.05	4

[(a)]The experimental number-average molecular weight, $M_{n,exp}$ and the polydispersity index, *PDI*, were measured by size-exclusion chromatography (SEC) using polystyrene standards in THF. [(b)]Conversion was determined by gravimetry. [(c)]The theoretical number average molecular weight was calculated according to the equation, $M_{n,th}=M_M \times \text{conv.} \times [M]_0/[CTA]_0 + M_{CTA}$ where $M_{n,th}$ is the theoretically calculated molecular weight of the polymer, M_M is the molecular weight of the monomer, $[M]_0$ and $[CTA]_0$ the concentration of the monomer and the concentration of the RAFT agent, M_{CTA} is the molecular weight of the RAFT agent.

Synthesis of the alkyne endgroup modified initiator (propargyl initiator) (1)

Azobis(4-cyano valeric acid) (ACVA) (1.5 g, 5.35×10^{-3} mol, 1 equiv.) and propargyl alcohol (3.0 g, 5.35×10^{-2} mol, 10 equiv.) were dissolved in a mixture of THF (30 mL) and water (20 mL). This solution was cooled to 0°C and *N*-Ethyl-*N*'-(3-dimethylaminopropyl)carbodiimide hydrochloride (EDC, 3.08 g, 1.61×10^{-2} mol, 0.33 equiv.) and 4-Di(methylamino)pyridine (DMAP, 0.65 g, 5.35×10^{-3} mol, 1 equiv.) were subsequently added. The mixture was stirred at 0°C for 2 h and then at ambient temperature overnight. The reaction mixture was washed with CH_2Cl_2 (3 × 50 mL) and the combined organic layers were dried over $MgSO_4$. The product was purified by column chromatography using dichloromethane as the eluent. The volatiles were removed under reduced pressure and the product was isolated as a white powder (1.6 g, 84 %).

^{1}H NMR ($CDCl_3$, δ in ppm): 4.7 (t, 4H, C$\underline{H_2}$O), 2.5-2.4 (m, 10H, C≡$\underline{H}$, CO$\underline{CH_2}$C) 1.72 (s, 3H, CH_3), 1.67 (s, 3H, CH_3). ^{13}C NMR ($CDCl_3$, δ in ppm): 170.4 (2C, C=O), 117.3 (2C, CN), 77.2 (2C, CH), 75.3 (2C, $\underline{C}HCH_2$), 71.7 (2C, $\underline{C}CN$), 52.4 (2C, CH_2O), 32.9 (2C, $\underline{C}H_2CO$), 28.9 (2C, $\underline{C}H_2C$), 23.8 (2C, $\underline{C}H_3$); ESI-MS $[C_{18}H_{20}N_4O_4]Na^+$, Calc.: 379.1 g mol^{-1}, Found.: 379.1 g mol^{-1}.

Preparation of azide functionalized polystyrenes (dithio-PS-N_3)

A master batch solution of styrene (7.2 g, 6.9 $\times 10^{-2}$ mol), dithiobenzoate RAFT azido (0.05 g, 1.38 $\times 10^{-4}$ mol) and AIBN (0.046 g, 2.80 $\times 10^{-4}$ mol) was prepared and aliquots were placed in a Schlenck tube. The solution was mixed thoroughly and subsequently degassed by four freeze-pump-thaw cycles to remove any residual oxygen. The polymerization reaction was performed at 60°C unless indicated otherwise. In order to monitor the progress in the polymerization, samples were withdrawn with a gas-tight syringe at predetermined time intervals and the polymerizations were quenched by cooling the solutions at 0 °C in an ice bath. The molecular weights and polydispersity indices were obtained using SEC. The monomer-to-polymer conversion was determined by gravimetry. The residual monomer in the samples taken at predetermined time intervals was evaporated under vacuum at room temperature. It should be noted that at low monomer conversions, low molecular weights were obtained (< 800 g mol^{-1}) which could not be quantified and therefore were omitted from the linear fit (see Figure 1).

General endgroup modification of dithio-PS-N_3 with propargyl initiator (alkyne-PS-N_3)

In a Schlenck tube, dithio-PS-N_3 (0.1 g, 4 × 10^{-5} mol) and the alkyne modified initiator (0.284 g, 8 × 10^{-4} mol) were dissolved in 3 mL Toluene. The solution was degassed by purging with N_2 for 30 minutes followed by stirring at 80°C for several hours. The endgroup conversion was indicated by a change in color of the solution from pink to yellow. After completion of the reaction, the solution was cooled to ambient temperature and the solution was added dropwise into cold hexane. The resulting white polymer was filtered and dried.

Click Cyclization procedure

To a 250 mL custom-built flask, DMF (180 mL) was added and was degassed using 2 freeze-pump-thaw cycles. 0.16 g (1.0 × 10^{-3} mol) CuBr and 0.45 g (2.0 × 10^{-3} mol) 2,2′ bipyridyl (bipy) were added to the DMF. The flask was then resealed and degassed with N_2 while connected to the Titration system (Metrohm, 809 Titrando). The dosing unit containing alkyne-PS-N_3 (0.06 g, 2.0 × 10^{-5} mol, M_n = 3000 g mol^{-1}) dissolved in 20 mL DMF was degassed by bubbling nitrogen. This solution was then transferred to the CuBr/bipy reaction solution at 80 °C *via* a dosing unit at a rate of 0.01 mL min^{-1}. Once the polymer addition to the catalyst solution was completed, the reaction was allowed to proceed at 80 °C for 2 h. After

cooling to ambient temperature the DMF was removed and column chromatography in THF was used to remove the catalyst. The crude polymer was precipitated in methanol and dried *in vacuo*.

Results and Discussion

The dithiobenzoate RAFT agent[37] was designed to entail the prerequisite functionality for the click chemistry. This modified RAFT agent carrying an azide group (azido dithiobenzoate click-RAFT agent, Scheme 2) was employed in the polymerization reaction. RAFT polymerizations of styrene were carried out in bulk at 60 °C using AIBN as the initiator. The azido dithiobenzoate click-RAFT agent has been shown to provide good control of the polymerization of styrene as demonstrated previously by Quémener[37] as well as Gondi *et al*.[39] As shown in Figure 1, the molecular weight increases linearly with the monomer conversion while the polydispersity indices remain less than 1.2 indicating effective living/controlled polymerization leading to homopolymers with molecular weight close to that theoretically expected and low *PDI* (Table 1).

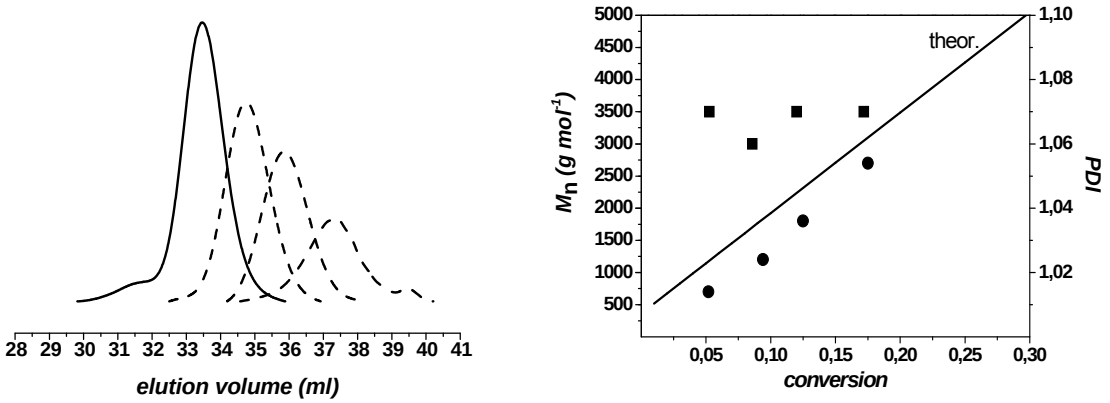

Figure 1. left: SEC traces of the evolution of the molecular weight for RAFT polymerization with azide dithiobenzoate RAFT agent at 60 °C (Exp. 2, reaction terminated after 17.5 % conversion); right: Evolution of the number-average molecular weight with monomer conversion. The solid line shows the theoretical number-average molecular weight, taking the molecular weight of the transfer agent into account.

To facilitate the cyclization of the PS chain by click coupling, the thiocarbonyl thio endgroup was modified with the required acetylene functionality as shown in Scheme 2. The insertion of the alkyne group at the PS chain end was accomplished by the removal of the

thiocarbonylthio endgroup from the polymeric chains according to the method described by Perrier and coworkers.[40] Using this method, the carboxylic acid groups of azobis(4-cyano valeric acid) (ACVA) were converted to alkyne esters to obtain the modified initiator. The alkyne-modified initiator decomposes in solution to form two propargyl 4-cyanovalerate radicals. These radicals react with the C=S of the thiocarbonylthio moiety in the polymer chain. Under conditions of an excess of the initiator radicals, the equilibrium between the formation of free leaving group radicals (R-group) and the fragmentation of the original attacking radicals, is displaced towards the formation of the R-group radical. The R-group radical can subsequently react with the free initiator radicals and the dithio moiety of the polymer chains with the alkyne initiator fragments is substituted.

The alkyne modified initiators were characterized by ^{1}H NMR, ^{13}C NMR, 2D NMR (HMBC, HSQC) and ESI-MS spectrometry (see Supporting Information, Figure S1). The theoretically calculated molecular weights of the alkyne modified initiator correlates well with the experimental values determined by ESI-MS *i.e.* $M_{n,calc}$ = 379.1 g mol^{-1} while $M_{n,exp}$ = 379.1 g mol^{-1}.

After the reaction with the alkyne modified initiator, the polymer was isolated by precipitation in cold hexane resulting in a white powder indicating the removal of the dithio moiety. To confirm this observation, UV/VIS measurements were carried out before and after treatment with the alkyne modified initiator, which indicated the loss of the characteristic peak of the dithiobenzoate moiety (500 – 510 nm) (Figure 2). The complete removal of the dithio moiety was further corroborated by the elemental analysis data that resulted in sulfur composition in the modified PS below the detection limit (< 10 ppm).

The SEC trace of alkyne modified PS samples (alkyne-PS-N_3) with different molecular weights is given in Figure 2a along with that of the unmodified polymer (dithio-PS-N_3), indicating no significant change in the molecular weight upon endgroup functionalization.

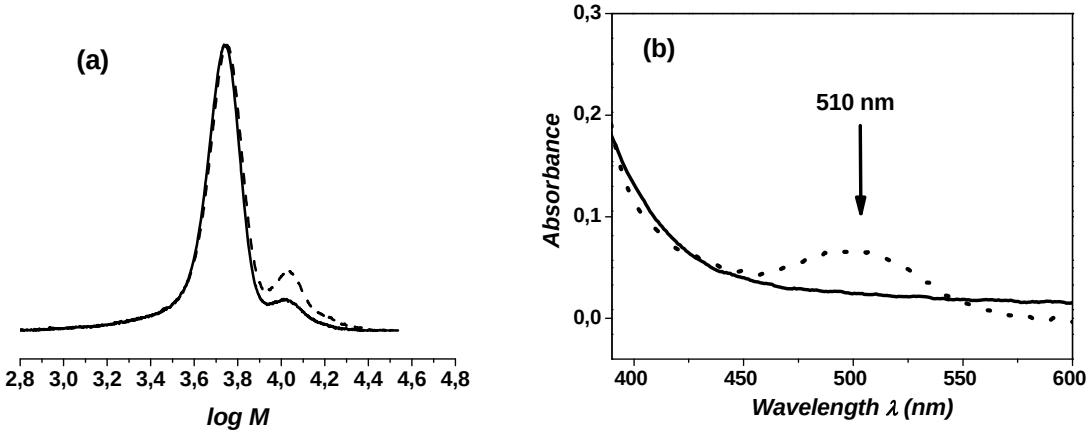

Figure 2. (a) SEC traces for PS synthesized with azido dithiobenzate agent (Exp. 1, solid line, M_n = 5300 g mol^{-1}, PDI = 1.08) and PS sample after treatment with alkyne functionalized cleavage initiator (dashed line, M_n = 5300 g mol^{-1}, PDI = 1.15) (b) UV/VIS spectra of dithio-PS-N_3 (dotted line) and after treatment with alkyne functionalized initiator (alkyne-PS-N_3, (solid line)) showing the complete disappearance of the characteristic peak for the dithio moiety at 510 nm in tetrahydrofuran.

The non-modified PS shows a small shoulder at higher molecular weights, which is due to the formation of coupled polymer chains during the synthesis. It can be seen that this shoulder slightly increased in area after the endgroup modification. Such an observation may be attributed to the coupling of the PS-N_3 radicals generated during the synthesis, leading to a higher molecular weight shoulder in the SEC trace as well as higher polydispersity index.

Linear PS chains with molecular weights below 5000 g mol^{-1}, which did not show coupling during the polymerization, also showed coupling products after the reaction with the alkyne functionalized initiator. Any changes in the reaction conditions, such as increasing the temperature or increasing the amount of the alkyne functionalized initiator, did not reduce the formation of the coupling products. The complete removal of the dithio moiety was further confirmed by ^{1}H NMR spectroscopy (Figure 3) of the polymers before and after the treatment with alkyne functionalized initiator. The characteristic resonance peaks for the aromatic protons of the dithio moiety (δ = 7.3 – 8.0 ppm) disappeared completely after reaction with the alkyne functionalized initiator (Figure 3, insets). Also, a new resonance peak at 4.7 ppm (H_c) could be detected after the reaction which corresponds to the CH_2-group adjacent to the alkyne group.

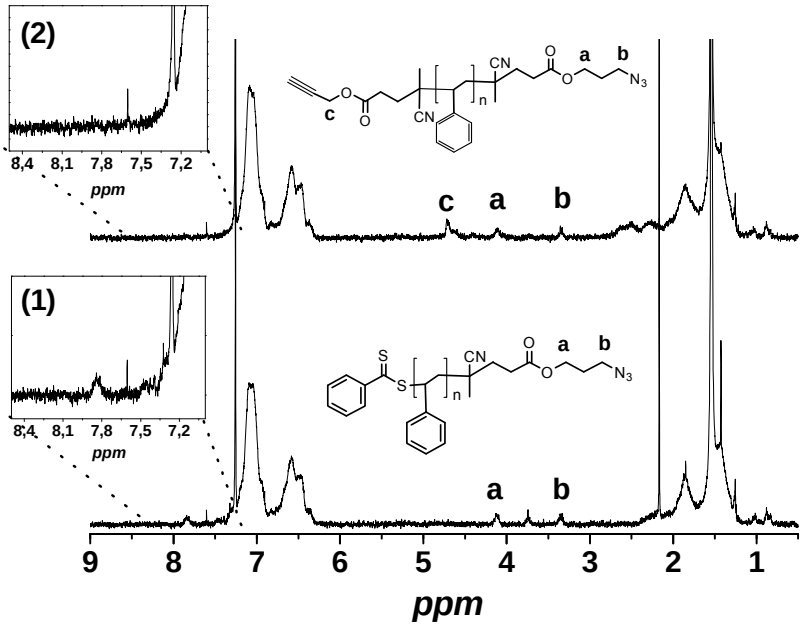

Figure 3. ^{1}H NMR spectra of (1) dithio-PS-N_3 and (2) alkyne-PS-N_3. Aromatic protons of the dithio endgroup before and after the treatment with alkyne functionalized initiator are shown in the insets.

The polymers were subjected to preparative SEC fractionation to separate the coupling product from the main product. Several samples were taken manually at constant intervals and for each sample an SEC trace was taken to identify the region of the main product. All fractions of the main peak were combined and concentrated by solvent evaporation followed by drying. The molecular weight distributions of the purified PS and the coupling product are shown in Figure 4, which confirms a monomodal distribution of the PS. Thus fractionation is a very efficient method to obtain linear polystyrene with the desirable click functionalities with low polydispersity.

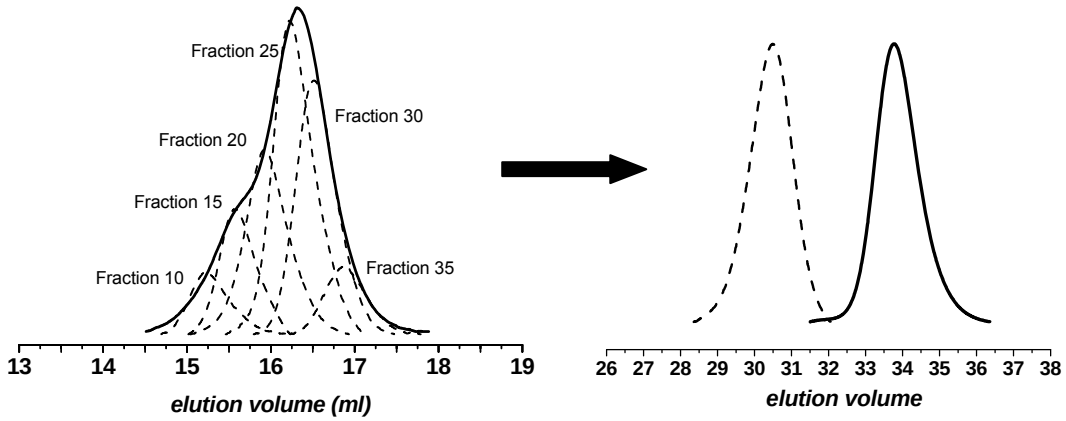

Figure 4. Separation of coupling product from main product with preparative SEC, Exp. 3, left: original trace and some fractions of the polymer separated by preparative SEC. Right: Analytical SEC traces of the cumulated fractions 25-35 (solid line) and the coupling product (fractions 1-12; dashed line). Before fractionation: M_n = 3700 g mol^{-1}, PDI = 1.19; cumulated fractions 25-35: M_n = 3000 g mol^{-1}, PDI = 1.05.

To establish the feasilbility of the polymeric click cyclization, a copper catalysed model click cycloaddition reaction using low molecular weight alcohols (3-azido-1-propanol and propargyl alcohol) was carried out. The click reaction was conducted using copper(I) bromide as catalyst and 2,2´-bipyridyl as ligand in dimethylformamide (DMF) at 80°C, for 20 h. Conditions similar to this reaction were used for the polymeric click-cyclization as well. The progress of the click reaction was monitored by ^{1}H NMR (supporting information, Figure S2) as well as Fourier transform infrared spectroscopy (FT-IR) for the condition employed (80°C). FT-IR analysis showed the characteristic peaks at 3300 cm^{-1} (alkyne) and 2100 cm^{-1} (azide)[41] for propargyl alcohol and azidopropanol. The relative concentration of the functional group after reaction can be followed *via* the appearance of the triazole stretches (C=C: 1650 cm^{-1} and =C-H: 2800 cm^{-1}) and the disappearance of the alkyne- and azide stretch (3300 cm^{-1} (alkyne) and 2100 cm^{-1} (azide)) indicating a complete conversion of the azido and alkyne endgroups to triazole rings.

After the above-mentioned pre-investigation, cyclization was attempted at 80°C by the end-to-end ring closure of alkyne-PS-N_3. To verify the successful click cyclization, ^{1}H NMR, SEC and IR spectroscopies were used. The SEC trace (solid line, Figure 5) of the cyclized PS showed a shift to higher elution volumes due to the more compact structure of the macrocycles[33,42,43] and therefore lower hydrodynamic volume. This shift corresponds to a lower apparent molecular weight due to the ring formation. Both traces show a small peak due to dead polymers formed during endgroup modification (see above). Afer endgroup modification the coupling peak is also shifted towards lower molecular weight which may be attributed to the formation of dimeric cycles. The small peak includes both dead polymers formed during endgroup modification and dimeric cycles. Hence, the small peak is also shifted towards higher elution volume.

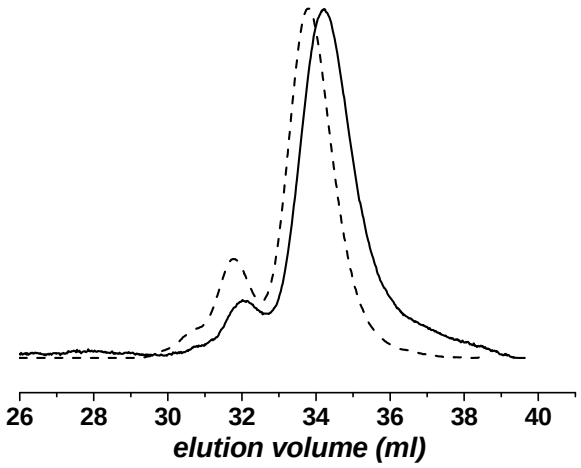

Figure 5. SEC trace of linear alkyne-PS-N_3 (Exp. 1, M_n = 5300 gmol^{-1}, dotted line) and of cyclic alkyne-PS-N_3 (M_n = 4300 gmol^{-1}, solid line).

Liquid chromatography at critical conditions of adsorption (LACCC) is a powerful method for the characterization of cyclic and linear polymers according to the chemical heterogeneity. Separation of polymers on porous separation phases using mixed mobile phases at critical conditions of adsorption allows the elution of homopolymers independent of their molar mass. Under these conditions, homopolymers can be separated according to the number and nature of functional groups, e.g. end groups. Because of a better separation, LACCC is more sensitive for a quantitative determination of the topology of the polymer. Pasch et al.[44] and Takano et al.[45] already analyzed cyclic polymers with LACCC. Figure 6 shows the LACCC traces of the dithio-PS-N_3 precursor, linear alkyne-PS-N_3 and cyclic polystyrenes at critical conditions of alkyne-PS-N_3. Four different alkyne-PS-N_3 with a molecular weight in the range from 2000 – 10000 g mol^{-1} were used to find the critical conditions, THF/hexane = 43:57 (v/v) on an RP (reversed phase) column set.

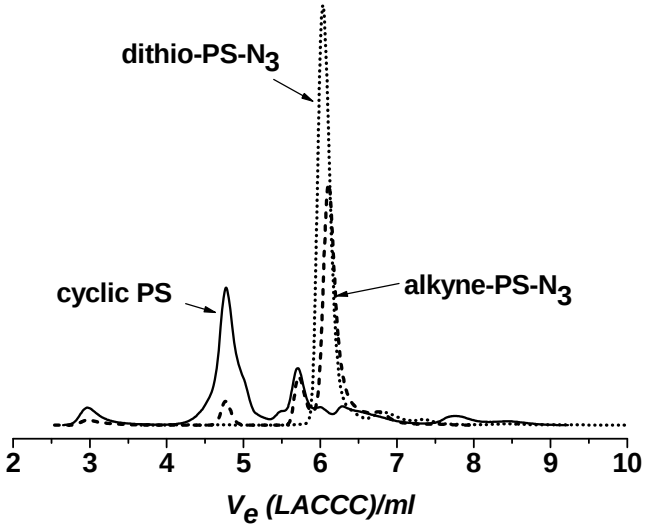

Figure 6. LACCC chromatograms at critical conditions of alkyne-PS-N_3 (ELSD detector) for linear dithio-PS-N_3 precursor (dotted line, Exp.1), linear alkyne-PS-N_3 (dashed line) and cyclic polystyrenes (solid line) measured by SEC with viscosity detection in tetrahydrofuran.

Both linear samples, dithio-PS-N_3 precursor (6.0 mL) and alkyne-PS-N_3 (6.1 mL) elute nearly at the same elution volume. However, the cyclic PS elutes significantly earlier (4.7 mL) than the linear counterparts due to the absence of end groups and therefore loss of the polarity. Alkyne-PS-N_3 exhibit few shoulders due to side reactions during endgroup modification. The shoulder at 5.7 mL can be attributed to the recombination product formed during insertion of the alkyne group. These dead polymers also show up for the cycle. This liquid chromatography method clearly underlines the formation of cycles.

MALDI-TOF measurements were carried out to determine the absolute molecular weight. Identical absolute molecular weights were detected for the linear precursor (Exp. 1, $M_{w,lin}$ = 3150 g mol^{-1}) and the cyclized PS ($M_{w,cyc}$ = 3200 g mol^{-1}), which corroborates the successful ring formation. Unfortunately, efforts towards characterization of the side products with MALDI-TOF analysis did not give distinct information because of overlapping of several peaks. ATR-FTIR analysis provided further proof of ring formation, where a peak at 2096 cm^{-1}, corresponding to the N_3 group of the dithio-PS-N_3 and alkyne-PS-N_3 completely disappeared in the cycle due to formation of the triazole group (Figure 7).

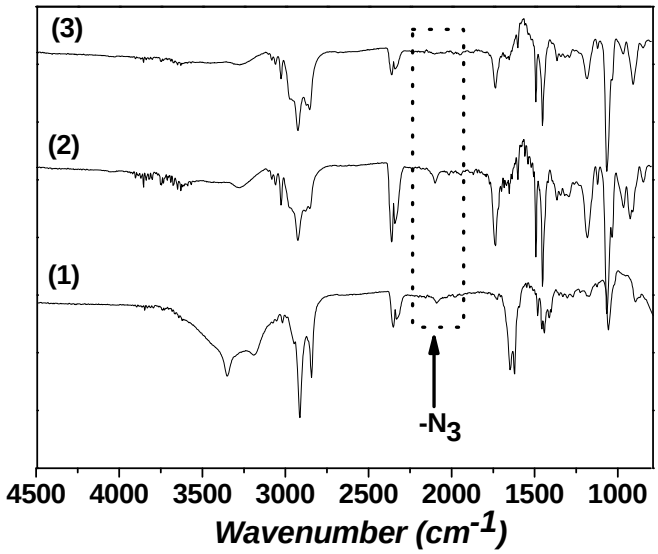

Figure 7. ATR-FTIR spectra for (1) dithio-PS-N_3 (Exp.1), (2) alkyne-PS-N_3 and (3) cyclic PS showing the loss of the azido group at 2099 cm^{-1}.

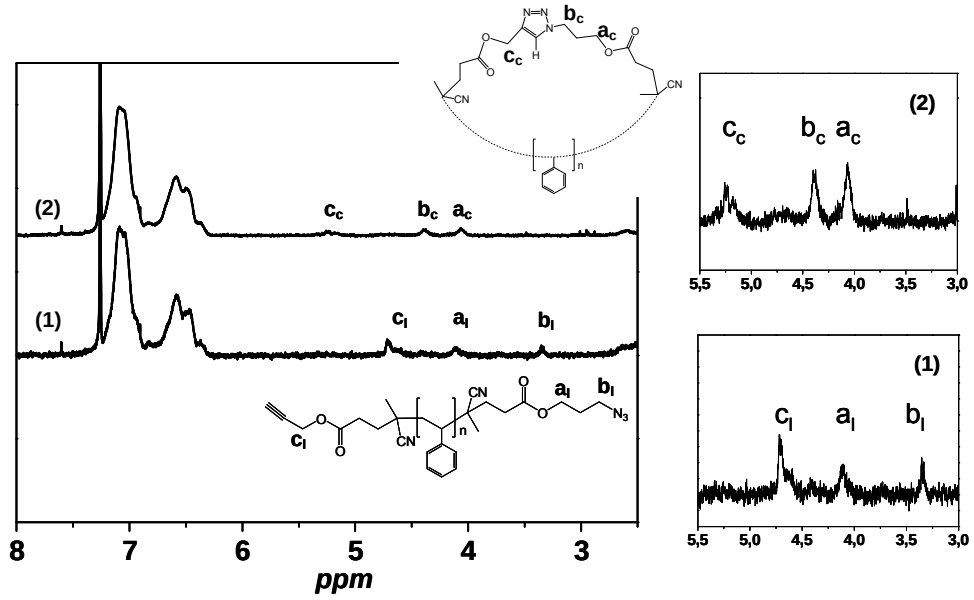

Figure 8. ^1H NMR for the heterotelechelic linear alkyne-PS-N_3 (Exp.1) (1) and the cyclic product (2).

NMR measurements provide further evidence for the triazole formation and therefore intramolecular ring closure. The shift of the methylene protons adjacent to the azido group was observed from δ = 3.3 ppm (b_l) to δ = 4.3 ppm (b_c) (*Figure 8*) due to triazole formation. The disappearance of protons c adjacent to the alkyne moiety for the linear poymer chain at δ = 4.7 ppm (c_l) and the appearance of a new peak at δ = 5.2 ppm (c_c) are also observed (see

Figure 8), which results as a effect of the formation of the heterocycle. The proton of the triazole ring was detected at δ = 8.0 ppm with a Bruker DPX 300 instrument.

Intrinsic viscosities were obtained from SEC measurements in THF using a viscosity detector. The Mark-Howink plots of log[η] versus log *M* for linear and cyclic PS samples result in straight though not quite parallel lines (Figure 9). The Mark-Houwink exponents are found to be a = 0.74 for the cycles and a = 0.69 for the linear chains, which is in good agreement with earlier studies of linear and cyclic polystyrenes.[28,42] From the viscosity measurements a contraction factor of $g' = [\eta]_{cyc}/[\eta]_{lin}$, can be calculated, which was predicted by Bloomfield and Zimm[42] and Casassa[46] to be g'= 2/3 for θ–conditions. Depending on the nature of the polymer, molecular weight and solvent used, contraction factors in the literature range from 0.64 to 0.71.[22,28,47] The value obtained by us in the good solvent THF, g´= 0.70 – 0.74, is consistent with these previous results obtained for polymers in solution.

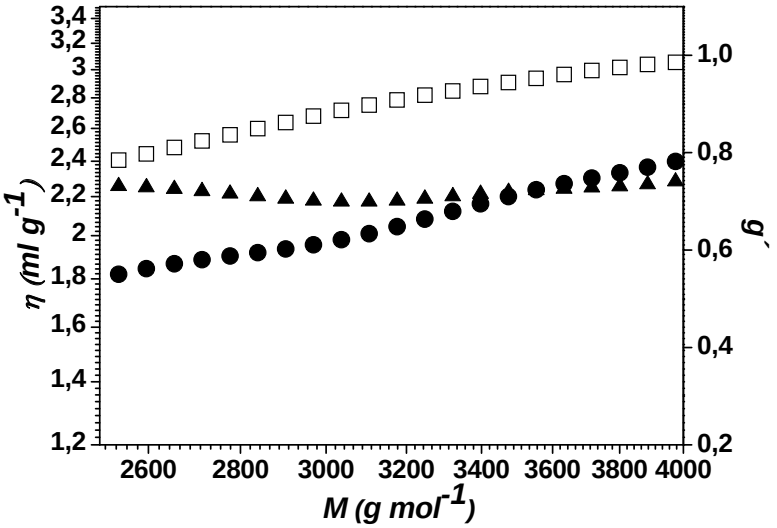

Figure 9. Mark-Houwink plots of intrinsic viscosity versus molecular weight, for linear (□, Exp.1) and cyclic (●) polystyrenes measured by SEC with viscosity detection in tetrahydrofuran. (7): contraction factors, g'.

Conclusions

The combination of RAFT and copper catalyzed Huisgen 1,3-dipolar cycloaddition (click chemistry) is an efficient strategy to synthesize ring shaped polymers. An azido dithiobenzoate click RAFT agent was employed as chain transfer agent in the RAFT polymerization of styrene resulting in low molecular weight azido-terminated polymers. The exchange of the dithio moiety of the polymeric chains was carried out efficiently by using an

alkyne-modified initiator, leading to the appropriate endgroup modifications of polystyrene for the click chemistry. Intramolecular cyclization was successfully carried out and the ring formation was assertively evaluated by ^{1}H NMR, ATR-FTIR measurements, MALDI-TOF, SEC, VISCO-SEC and LACCC. The present route towards ring shaped polymers represents a versatile approach for the preparation of cyclic polymers and the approach is in principle applicable for polymers derived from acrylates as well, which can be further functionalized to grow polymer brushes on the cyclic backbone. Studies towards such new architecture of ring shaped polymer brushes are currently in progress in our laboratories.

Acknowledgements

Financial support by the Australian Research Council (ARC) and the Deutsche Forschungsgemeinschaft (DFG) within an International Linkage Grant is gratefully acknowledged. We would like to thank Sabine Wunder, Andreas Walther and Jiayin Yuan (MC II, University of Bayreuth), Dr. Tara Lovestead and Till Gründling (CAMD, University of New South Wales) for valuable assistance with analytical measurements. The fruitful discussions with Dr. Chakravarthy Gudipati (IMRE, Singapore) are also acknowledged. C. B.-K. acknowledges receipt of an Australian Professorial Fellowship (ARC) and T.P.D. acknowledges receipt of a Federation Fellowship (also ARC).

Supporting Information

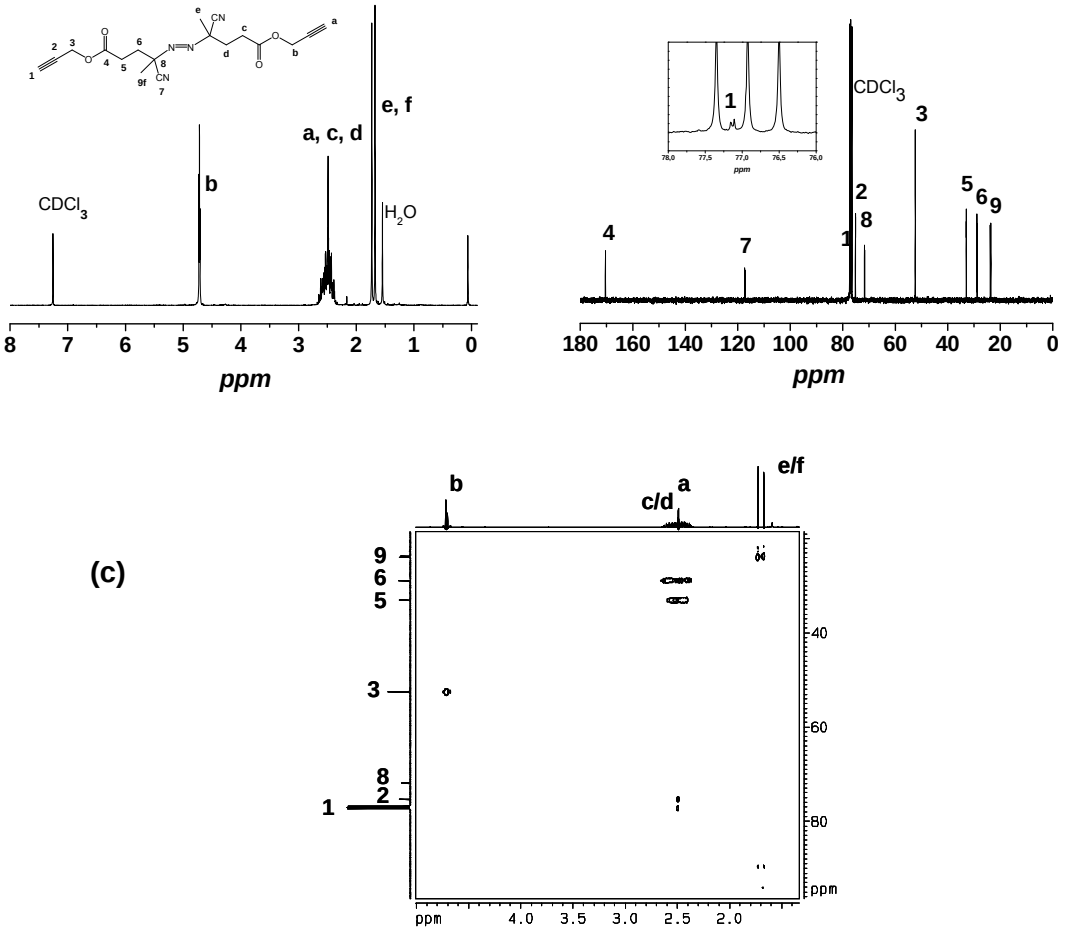

Figure S1. (a) ^{1}H NMR, (b) ^{13}C NMR and (c) 2D NMR, HSQC (heteronuclear single quantum correlation) spectra of alkyne endgroup modified initiator (propargyl initiator).

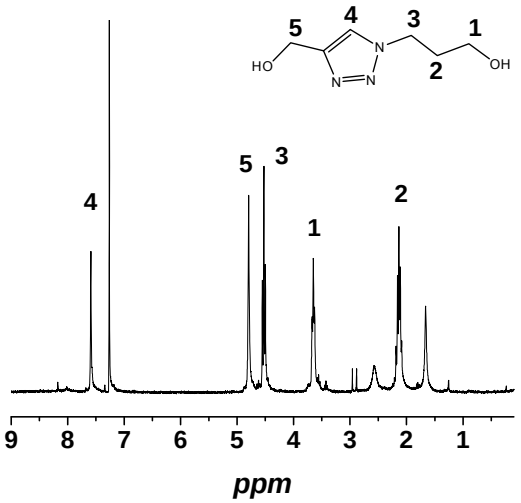

Figure S2. ^{1}H NMR spectrum of the model compound prepared by the click reaction of 3-azido-1-propanol and propargyl alcohol. The characteristic resonance peaks corresponding to the triazole ring (H_4) were earmarked for the characterization of the click-cyclized PS rings.

References

(1) Barner, L.; Davis, T. P.; Stenzel, M. H.; Barner-Kowollik, C. *Macromolecular Rapid Communications* **2007**, *28*, 539.

(2) Barner-Kowollik, C.; Davis, T. P.; Heuts, J. P. A.; Stenzel, M. H.; Vana, P.; Whittaker, M. *Journal of Polymer Science Part A: Polymer Chemistry* **2003**, *41*, 365.

(3) Perrier, S.; Takolpuckdee, P. *Journal of Polymer Science Part A: Polymer Chemistry* **2005**, *43*, 5347.

(4) Quémener, D.; Hellaye, M. L.; Bissett, C.; Davis, T. P.; Barner-Kowollik, C.; Stenzel, M. H. *Journal of Polymer Science Part A: Polymer Chemistry* **2007**, *46*, 155.

(5) Takolpuckdee, P.; Westwood, J.; Lewis, D. M.; Perrier, S. *Macromolecular Symposia* **2004**, *216*, 23.

(6) Semlyen, J. A. *Cyclic Polymers*; Elsevier Applied Science: London, New York, 1986.

(7) Kelen, J.; Schlotterbeck, D.; Jaacks, V.; IUPAC Conference on Macromolecules: Boston, 1971.

(8) Eisenberg, A. *Inorg. Macromolecules Rev.* **1970**, *1*, 75.

(9) Thilo, E. *Advances in Inorganic Chemistry and Radiochemistry*; Academic Press: New York, 1962.

(10) Schill, G. *Catenanes, Rotaxanes and Knots*; Academic Press: New York, London, 1971.

(11) Schill, G.; Zürcher, C. *Angewandte Chemie* **1969**, *81*, 996.

(12) Wasserman, E. *Journal of the American Chemical Society* **2002**, *82*, 4433.

(13) Harrison, I. T. *Chem. Comm.* **1972**, *4*, 231.

(14) Harrison, I. T. *J. Chem. Soc., Perkin I* **1974**, 301.

(15) Schill, G.; Zürcher, C.; Vetter, W. *Chem. Ber.* **1973**, *106*, 228.

(16) Brochard, F.; de Gennes, P. G. *Macromolecules* **2002**, *10*, 1157.

(17) Gooden, J. K.; Gross, M. L.; Mueller, A.; Stefanescu, A. D.; Wooley, K. L. *Journal of the American Chemical Society* **1998**, *120*, 10180.

(18) Roovers, J.; Toporowski, P. M. *Macromolecules* **2002**, *16*, 843.

(19) Clarkson, S. J.; Semlyen, J. A.; Horska, J.; Stepto, R. F. T. *Polymer* **1986**, *27*, 31.

(20) Fawcett, A. H.; Mee, R. A. W.; McBride, F. V. *Macromolecules* **2002**, *28*, 1481.

(21) Sigwalt, P.; Masure, M.; Moreau, M.; Bischoff, R. *Macromolecular Rapid Communications* **1993**, *73*, 146.

(22) Geiser, D.; Höcker, H. *Macromolecules* **2002**, *13*, 653.

(23) Hild, G.; Hohler, A.; Rempp, P. *Eur. Polym. J.* **1980**, *16*, 525.

(24) Hogen-Esch, T. E.; Sundarajan, J. *Polym. Prepr. (Am. Chem. Soc. Div. Polym. Chem.)* **1991**, *32*, 604.

(25) Hogen-Esch, T. E.; Sundararajan, J.; Toreki, W. *Makromol. Chem., Macromol. Symp.* **1991**, *47*, 23.

(26) Vollmert, B.; Huang, J. X. *Die Makromolekulare Chemie, Rapid Communications* **1981**, *2*, 467.

(27) Rique-Lurbet, L.; Schappacher, M.; Deffieux, A. *Macromolecules* **2002**, *27*, 6318.

(28) Lepoittevin, B.; Dourges, M.-A.; Masure, M.; Hemery, P.; Baran, K.; Cramail, H. *Macromolecules* **2000**, *33*, 8218.

(29) Lepoittevin, B.; Perrot, X.; Masure, M.; Hemery, P. *Macromolecules* **2001**, *34*, 425.

(30) Laurent, B. A.; Grayson, S. M. *Journal of the American Chemical Society* **2006**, *128*, 4238.

(31) He, T.; Zheng, G.-H.; Pan, C.-y. *Macromolecules* **2003**, *36*, 5960.

(32) Whittaker, M. R.; Goh, Y.-K.; Gemici, H.; Legge, T. M.; Perrier, S.; Monteiro, M. J. *Macromolecules* **2006**, *39*, 9028.

(33) Xu, J.; Ye, J.; Liu, S. *Macromolecules* **2007**, *40*, 9103.

(34) Qiu, X.-P.; Tanaka, F.; Winnik, F. M. *Macromolecules* **2007**, *40*, 7069.

(35) Barner-Kowollik, C.; Davis, T. P.; Heuts, J. P. A.; Stenzel, M. H.; Vana, P.; Whittaker, M. *J. Pol. Sci.* **2003**, *41*, 365.

(36) Qiu, X.-P.; Tanaka, F.; Winnik, F. M. *Macromolecules* **2007**, *40*, 7069.

(37) Quémener, D.; Davis, T. P.; Barner-Kowollik, C.; Stenzel, M. H. *Chem. Comm.* **2006**, 50561.

(38) Huisgen, R. *1,3-Dipolar Cycloaddition Chemistry*; Padwa, A.: New York, 1984.

(39) Gondi, S. R.; Vogt, A. P.; Sumerlin, B. S. *Macromolecules* **2007**, *40*, 474.

(40) Perrier, S.; Takolpuckdee, P.; Mars, C. A. *Macromolecules* **2005**, *38*, 2033.

(41) Ladmiral, V.; Mantovani, G.; Clarkson, G. J.; Cauet, S.; Irwin, J. L.; Haddleton, D. M. *Journal of the American Chemical Society* **2006**, *128*, 4823.

(42) Bloomfied, V.; Zimm, B. H. *J. Chem. Phys.* **1966**, *44*, 315.

(43) Dodgson, K.; Semlyen, J. A.; , P.-. *Polymer* **1977**, *18*, 1265.

(44) Pasch, H.; Deffieux, A.; Ghahary, R.; Schapacher, M.; Rique-Lurbet, L. *Macromolecules* **1997**, *30*, 98.

(45) Takano, A.; Kushida, Y.; Aoki, K.; Masuoka, K.; Hayashida, K.; Cho, D.; Kawaguchi, D.; Matsushita, Y. *Macromolecules* **2007**, *40*, 679.

(46) Casassa, E. F. *J. Polym. Sci., Part A* **1965**, *3*, 605.

(47) Lutz, P.; McKenna, G. B.; Rempp, P.; Strazielle, C. *Die Makromolekulare Chemie, Rapid Communications* **1986**, *7*, 599.

Appendix

Synthesis of bifunctional azide endgroup modified initiator

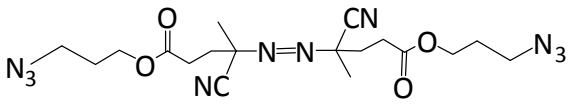

Azobis(4-cyano valeric acid) (ACVA) (1.5 g, 5.35×10^{-3} mol, 1 equiv.) and azido propanol (5.41 g, 5.35×10^{-2} mol, 10 equiv.) were dissolved in a mixture of THF (30 mL) and water (20 mL). This solution was cooled to 0°C and *N*-Ethyl-*N*′-(3-dimethylaminopropyl)-carbodiimide hydrochloride (EDC, 3.08 g, 1.61×10^{-2} mol, 0.33 equiv.) and 4-Di(methylamino)pyridine (DMAP, 0.65 g, 5.35×10^{-3} mol, 1 equiv.) were subsequently added. The mixture was stirred at 0°C for 2 h and then at ambient temperature overnight. The reaction mixture was washed with CH_2Cl_2 (3 × 50 mL) and the combined organic layers were dried over $MgSO_4$. The product was purified by column chromatography using dichloromethane as the eluent. The volatiles were removed under reduced pressure and the product was isolated as a yellowish liquid (2.0 g, 81 %).

^{1}H NMR ($CDCl_3$, δ in ppm): 4.1 (t, 4H, $N_3C\underline{H_2}$), 3.3 (t, 4H, $O\underline{CH_2}$) 2.3-2.5 (m, 8H, $CO\underline{CH_2}\underline{CH_2}$), 1.9 (t, 4H, $CH_2\underline{CH_2}CH_2$) 1.66 (s, 3H, $C\underline{H_3}$), 1.61 (s, 3H, $C\underline{H_3}$). ^{13}C NMR ($CDCl_3$, δ in ppm): 170.2 (2C, C=O), 116.5 (2C, CN), 70.8 (2C, $\underline{C}CN$), 61.1 (2C, $N_3\underline{C}$), 47.1 (2C, $O\underline{C}H_2$), 32.1 (2C, $\underline{C}H_2C$), 28.0 (2C, $\underline{C}H_2CO$), 27.0 (2C, $CH_2\underline{C}H_2CH_2$), 22.7 and 22.9 (2C, $\underline{C}H_3$).

Surface Modification of Poly (Divinylbenzene) Microspheres *via* Thiol-Ene-Chemistry and Alkyne-Azide Click Reactions

Anja S. Goldmann,[1] Andreas Walther,[1] Leena Nebhani,[6] Raymond Joso,[2] Dominique Ernst,[3] Katja Loos,[4] Christopher Barner-Kowollik,[,5] Leonie Barner*[,6] and Axel H. E. Müller*[,1]*

[1]Makromolekulare Chemie II and Zentrum für Kolloide und Grenzflächen, Universität Bayreuth, 95440 Bayreuth, Germany, e-mail: axel.mueller@uni-bayreuth.de

[2]Centre for Advanced Macromolecular Design, School of Chemical Sciences and Engineering, The University of New South Wales, Sydney, NSW 2052, Australia

[3]Experimentalphysik IV and Bayreuther Institut für Makromolekülforschung (BIMF), Universität Bayreuth, 95440 Bayreuth, Germany

[4]Department of Polymer Chemistry & Zernike Institute for Advanced Materials, University of Groningen, 9747AG Groningen, The Netherlands

[5]Preparative Macromolecular Chemistry, Institut für Technische und Polymerchemie, Universität Karlsruhe (TH)/Karlsruhe Institute of Technology (KIT), Engesserstr. 18, 76128 Karlsruhe, Germany, e-mail: christopher.barner-kowollik@polymer.uni-karlsruhe.de

[6]Fraunhofer Institut für Chemische Technologie, Joseph-von-Fraunhofer-Str. 7, 76327 Pfinztal (Berghausen), Germany, e-mail: Leonie.Barner@ict.fraunhofer.de;

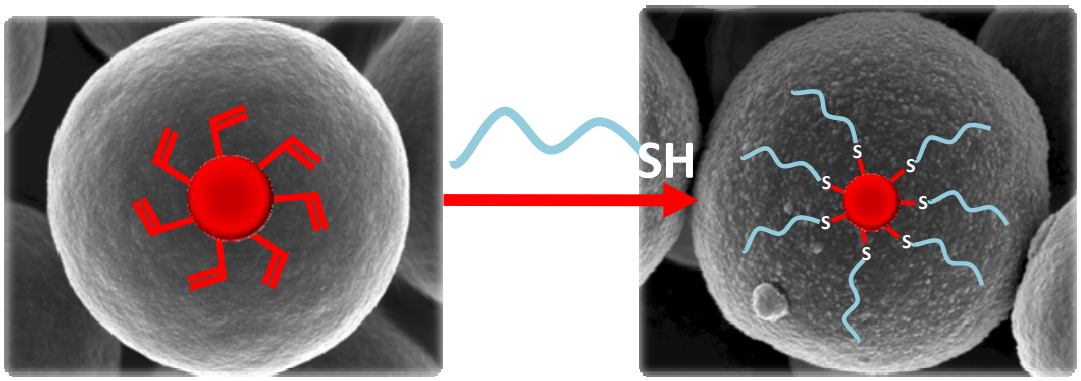

Summary

We report the functionalization of crosslinked poly(divinylbenzene) microspheres using both thiol-ene chemistry and azide-alkyne click reactions. The RAFT technique was carried out to synthesize SH-functionalized poly(*N*-isopropylacrylamide) (pNIPAAm) and utilized to generate pNIPAAm surface-modified microspheres via thiol-ene modification. The accessible double bonds on the surface of the microspheres allow the direct coupling with thiol-end functionalized pNIPAAm. In a second approach, pDVB microspheres were grafted with poly(2-hydroxyethyl methacrylate) (pHEMA). For this purpose, the residual double bonds on the microspheres surface were used to attach azide groups via the thiol-ene approach of 1-azido-undecane-11-thiol. In a second step, alkyne endfunctionalized pHEMA was used to graft pHEMA to the azide-modified surface via click-chemistry (Huisgen 1,3 dipolar cycloaddition).

The surface-sensitive characterization methods X-ray photoelectron spectroscopy, scanning-electron microscopy and FT-IR transmission spectroscopy were employed to characterize the successful surface modification of the microspheres. In addition, fluorescence microscopy confirms the presence of grafted pHEMA chains after labeling with Rhodamine B.

Introduction

In recent years, grafting techniques have been employed to affect the attachment of polymers onto surfaces of nano- and microparticles.[1,2] Surface modification of microspheres to obtain shell-functionalized microspheres is an interesting tool for modifying their properties.[3] Various approaches towards the surface-modification of poly(divinyl benzene) microspheres (pDVB) have been published over the past years. In general, two different approaches can be categorized, the "*grafting to"* and the "*grafting from"* approach. Several groups chose the "*grafting from*" technique because it allows growing polymer chains from the initiators on the substrate, leading to high grafting densities because the monomer units can easily diffuse to the propagating sites. Various living/controlled free polymerizations techniques can be employed for this purpose, e.g. the reversible addition fragmentation chain transfer (RAFT) process or atom transfer radical polymerization (ATRP). In the "*grafting to"* technique, the polymer chains carry an active terminal group and are coupled to the active surface. Such an approach allows the characterization of the polymer chains before coupling but tends to suffer both from low grafting rates[4] and from low final grafting densities.

The immense amount of scientific interest in "click"-chemsitry in the past years – especially for the Huisgen cycloaddition – shows the efficiency and the versatile applicability of this reaction.[5,6] The ease of synthesis of the alkyne and azide functionalities, coupled with tolerance to a wide variety of functional groups, stability and reaction conditions, make this coupling process highly attractive for the modification of polymeric materials. Concomitantly, the thiol-ene reaction may be – under certain conditions – an efficient way to couple polymer strands. Therefore, the thiol–ene reaction has started to attract researchers in various areas of material synthesis.[7-13] In our laboratories, the copper-catalyzed Huisgen 1,3-dipolar azide/alkyne cycloaddition process[14-18] as well as the equally effective hetero Diels-Alder conjugation chemistries[19-21] have been used successfully for a number of efficient coupling reactions.

In addition, several groups have applied the *"grafting from"* approach for the modification of microspheres. Zheng and Stöver reported the ring-opening polymerization (ROP) of ε–caprolactone catalyzed by $Al(Et)_3$ and $Al[OCH(CH_3)_2]_3$ from lightly cross-linked poly(DVB80-*co*-HEMA) microspheres[22] as well as the grafting of polystyrene from narrow disperse polymer particles by surface-initiated atom transfer radical polymerization.[23] Barner and co-

workers employed RAFT polymerization to exert additional control over the design of core-shell pDVB microspheres and functional particles.[19,24,25] Furthermore, Barner and co-workers applied anionic ring opening polymerization of ethylene oxide to synthesize hydroxyl-functionalized core/shell microspheres.[26]

Even though "*grafting to*" techniques can suffer from lower grafting-densities, we demonstrate in here the versatility and success of these two click-techniques via the efficient surface-modification of pDVB microspheres in combination with controlled radical polymerization techniques (ATRP and RAFT).

Experimental Section

Materials

11-Bromo-1-undecanol (98%, Aldrich), methanol (Merck), tetrahydrofuran (Merck), acetonitrile (Sigma-Aldich), 1,4-Dioxane (Fisher Scientific), anisole (99%, Sigma Aldrich), dimethyformamide (BDH, Prolabo), CuBr (99,999%, Aldrich), 2-Bromo-2-isobutyrate, *N*,*N*,*N´*,*N´*,*N´´*-Pentamethyldiethylenetriamine (PMDETA, Aldrich), 2-(Trimethylsilyloxy)ethyl methacrylate (TMS-HEMA, 96%, Aldrich), sodium azide (Sigma-Aldrich), sodium ascorbate (Sigma), *N*,*N´*-Dicyclohexylcarbodiimide (99%, Sigma-Aldrich), 4-(Dimethylamino)pyridine (99%, Aldrich), Rhodamin B base (97%, Aldrich), phosphorus oxychloride (98%, Fluka) and copper sulfate (Sigma), tris(2-carboxyethyl)phosphine (TCEP, powder, Aldrich), *N*-(1-pyrenyl)maleimide (PM, Sigma) were purchased and used as received. 2,2'-Azoisobutyronitrile (AIBN) was recrystallized from methanol. NIPAAm (*N*-Isopropylacrylamide) was recrystallized from a mixture of benzene and hexane (2:1). The synthesis of the RAFT agent 3-benzylsulfanylthiocarbonylsulfanyl propionic acid (BPATT) has been described elsewhere.[27]

Synthesis

Synthesis of 1-azido-undecane-11-thiol

This compound was synthesized by adapting the method by Oyelere et al. ^{1}H-NMR ($CDCl_3$, 300 MHz): 3.24 (t, 2H); 2.51 (q, 2H); 1.59 (m, 4H); 1.22-1.41 (m, 14H).[28]

Synthesis of azido-functionalized pDVB80 microspheres (pDVB-N_3)

Poly(divinylbenzene) microspheres (pDVB80) were prepared as described by Bai et al.[29] (DVB80, which is composed of isomers of DVB (meta and para), 80%, and 3- and 4-ethylvinyl styrene 20%, is used for the synthesis of the microspheres). 1 g of pDVB80 microspheres were mixed with 1-Azidoundecan-11-thiol ($1\cdot10^{-5}$ mol) and AIBN ($1\cdot10^{-4}$ mol) in acetonitrile (10 mL) as solvent. The reaction mixture was stirred for 72 h under reflux. The functionalized microspheres were then isolated by filtration through a 0.45 μm membrane and washed thoroughly with tetrahydrofuran, ethanol and acetone. Soxhlet extraction has been carried out in acetonitrile for 5 d to remove any unreacted compounds. The microspheres were dried under vacuum before characterization.

Synthesis of α-alkyne poly(HEMA) with ATRP (alkyne-pHEMA)

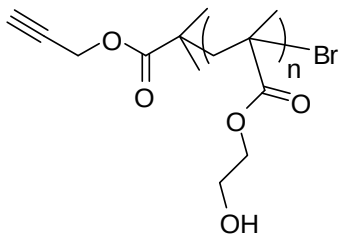

The pHEMA polymer (M_n=21000 g·mol^{-1}, M_w/M_n = 1.77) was prepared via the ATRP of TMS-HEMA followed by a deprotection of the TMS groups. The ATRP of TMS-HEMA in anisole runs as follows: after filtration through a silica column, 53.34 g of TMS-HEMA (0.26 mol) monomer was placed in a flask equipped with 164.4 g of anisole, 53.6 mg of CuBr (0.37 mmol), 54.0 mg of 2-propynyl 2-bromo-2-methyl propanoate (0.26 mmol) and a magnetic stirrer bar. The flask was then sealed with a septum and bubbled with nitrogen for 30 min. Then it was heated to 80°C and 66 mg of PMDETA (0.38 mmol) was injected under argon to start the polymerization. After 48 h, the reaction was stopped at a conversion of 47.5%. The reaction mixture was purified by filtration over a silica column and dialyzed against THF for 2 weeks.

The cleavage of the TMS protecting groups was carried out by precipitating the p(TMS-HEMA) solution from THF into water in the presence of several drops of concentrated HCl aqueous solution. The white precipitate was freeze-dried from dioxane.

Synthesis of poly(HEMA) functionalized pDVB80 (pDVB-*g*-pHEMA)

pDVB-N_3 (0.02 g) was mixed with alkyne-pHEMA (0.2 g, $9.5 \cdot 10^{-6}$ mol) in dimethylformamide in a Schlenck flask. Sodium ascorbate (0.19 g, $9.5 \cdot 10^{-5}$ mol) dissolved in 1 mL of distilled water was added immediately to the solution. The solution is degassed with nitrogen for 20 min. A degassed flask containing copper sulfate (0.51 mg, $3.2 \cdot 10^{-6}$ mol) in distilled water was transferred via a cannula to the Schlenck flask. The solution was stirred for 24 h at 70°C. Any unreacted compounds were removed by Soxhlet extraction in THF and water.

Synthesis of Rhodamine B Chloride

A solution of Rhodamine B base (2.5 g, 5.6 mmol) in 1,2 dichloromethane (20 mL) – dried over molecular sieve (3Å) over night – was stirred under nitrogen, and phosphorus oxychloride (0.98 mL, 10.6 mmol) was slowly added dropwise over 5 min. The solution was refluxed for 5 h. The color turned from dark red to dark purple. Thin layer chromatography (MeOH 100%) indicated full conversion after 4 h. After filtering the dark purple solution by syringe filters and evaporation of the solvent, the dark purple oily product was dried under vacuum (4.5 mbar) at 45°C over night resulting in a dark-bronze colored solid as crude product that was not purified further.

Rhodamine B Chloride-labeling of pHEMA-functionalized microspheres

To fluorescence label the pDVB-*g*-pHEMA, 1 mg of pDVB-*g*-pHEMA grafted microspheres were added to a solution of *N*,*N*'-dicyclohexylcarbodiimide (DCC) as a dehydrating agent (5.0 mg, $5.8 \cdot 10^{-6}$ mol), 4-dimethylamino pyridine (1.0 mg, $8.2 \cdot 10^{-6}$ mol) and Rhodamine B acid chloride (5.2 mg, 1.1×10^{-5} mol) in 2 mL THF. The degassed mixture was stirred for 24 h at room temperature. Particles were washed thoroughly with THF, water and ethanol. As a control experiment, pDVB80 microspheres were submitted to the same reaction conditions.

Synthesis of pNIPAAm$_{45}$

In a round bottom flask, 4.53 g of N-isopropylacrylamide (NIPAAm, 40 mmol), 242.1 mg of 3-benzylsulfanylthiocarbonylsulfany propionic acid (BPATT, $8.9 \cdot 10^{-4}$ mol) and 72.99 mg ($4.5 \cdot 10^{-4}$ mol) of AIBN were dissolved in 27 mL of dioxane. The flask was sealed with a rubber septum and the solution was degassed by nitrogen bubbling for 20 min. Then the flask was put in an oil bath at 60°C for 24 h. The polymerization was stopped by cooling the reaction to room temperature under air exposure. The solution was concentrated under vacuum and precipitated in diethyl ether. After filtration the yellow powder was dried overnight under vacuum. A conversion of 82% was determined by gravimetric measurement. By analysis of the obtained polymer with a NMP SEC, a molecular weight of 5300 g·mol^{-1} and a PDI of 1.14 were determined based on a polystyrene calibration.

SH-endgroup modification of pNIPAAm$_{45}$ (pNIPAAm$_{45}$-SH)

Thiol-modification was followed by the procedure published by McCormick and co-workers.[30] To a 50 mL round-bottom flask were added pNIPAAm homopolymer (M_n = 5 300 g·mol^{-1}, M_w/M_n = 1.14) and 15 mL of deionized water. The resulting solution was further diluted with an additional 15 mL solution of 1 M $NaBH_4$, and the mixture was allowed to react for 2 h. Following reduction, the homopolymer solution was dialyzed against water for 3 d and subsequently lyophilized. The resulting dried polymer was then dissolved in DMF, and a solution of tris(2-carboxyethyl phosphine) (TCEP) in DMF was added to yield a 150:1 mole ratio of TCEP to polymer. This solution was allowed to react for 24 h, after which it was charged with a solution of *N*-(1-pyrenyl)maleimide (PM) in DMF to yield a 150:1 mole ratio of PM to polymeric thiol (pNIPAAm-SH).

Thiol-ene Reaction between pNIPAAm-SH and pDVB80 (pDVB-*g*-pNIPAAm)

pDVB80 (0.05 g) was mixed with pNIPAAm-SH (0.25 g, $4.9 \cdot 10^{-5}$ mol) in 10 mL acetonitrile in a Schlenck flask. AIBN (0.025 g, $1.5 \cdot 10^{-4}$ mol) was added immediately to the solution. The solution was degassed with nitrogen for 20 min. Subsequently, the solution was stirred for 48 h at 70°C to ensure complete conversion. Particles were washed thoroughly with acetonitrile and water by Millipore filtration.

Characterization

NMR Spectroscopy. ^{1}H NMR spectra were recorded on a Bruker ACF300 300-MHz spectrometer.

SEC measurements were performed at room temperature on an apparatus equipped with PSS GRAM columns (30 × 8mm, 7 μm particle size) with 100 Å and 1000 Å pore sizes and a pre-column using RI (Bischoff) and UV (270 nm, Waters) detection. NMP with 0.05 M LiBr was used as an eluent in the case of pNIPAAm and DMAC in the case of pHEMA. The flow rate was 1.0 mL·min^{-1} and the WinGPC software was used for evaluation of the obtained data.

X-ray Photoemission Spectroscopy. The samples were introduced through a load look system into an SSX-100 (Surface Science Instruments) photoemission spectrometer with a monochromatic Al K_α X-ray source (E = 1 486.6 eV). The base pressure in the spectrometer during the measurements was 10^{-10} mbar. The photoelectron takeoff angle was 37°. The energy resolution was set to 1.3 eV to minimize measuring time. Sample charging was compensated for by directing an electron flood gun onto the sample. Spectral analysis included a Shirley background subtraction and a peak deconvolution that employed Gaussian and Lorentzian functions in a least-square curve-fitting program (WinSpec) developed at the LISE, University of Namur, Belgium.

Fourier Transform Infrared (FT-IR) transmission spectra were recorded using a Bruker IFS 66v/s spectrometer under vacuum at a resolution of 4 cm^{-1} using the KBr pellet technique. Spectra were recorded and evaluated with the software OPUS version 4.0 (Bruker).

Scanning Electron Microscopy (SEM) images were recorded on a LEO 1530 (Zeiss) instrument, applying the InLens detector with a slow acceleration voltage of 2 kV and sputtering the microspheres with lead to a sufficient material contrast.

Fluorescence Microscopy. The fluorescence microscope (Leica DMRX) was operated with a HBO lamp as an excitation light source and a filter cube consisting of an excitation bandpass-filter (BP 450-490 nm), a dichroic beamsplitter with a cut off wavelength of 510 nm and a detection filter (LP 515 nm). With this combination we could observe the emission of the

microspheres. We used objectives with several magnifications (20×, C Plan; 63×, HCX PL Fluotar; 100×, PL Fluotar; Leica). For each CCD-recorded frame (ColorView III, Soft imaging system) we chose an integration time of 50 s for all measured samples.

Confocal fluorescence microscopy images were captured using a Zeiss LSM 510 confocal laser scanning microscope. All images were captured using an oil immersion lens NA 1.3 (Objective Plan-Neofluar 40×/1.3 oil). Rhodamine B was excited by a 488 nm Argon laser. A main beam splitter (MFT) was used with a long pass filter (488 nm/543 nm). Emission was captured by a spectral detection unit set 560 nm (LP).

Turbidity study: A titration device, Metrohm automatic 809 Titrando system, was used and a temperature ramp from 20°C to 70°C was applied with a temperature increase of $1°C \cdot min^{-1}$.

Elemental analysis was performed using a Thermo Flash Elemental Analyser (1112 Series), D,L-methionin was used for calibration.

Results and Discussion

In the following section, we describe in detail the characterization of the core-shell microspheres which were synthesized via two approaches. For both approaches, poly(divinylbenzene) (pDVB80) particles were prepared by precipitation polymerization, having diameters of 1.3 μm. These microspheres have a thin surface layer consisting of lightly crosslinked and swellable poly (divinylbenzene)[31] and contain vinyl groups on their surfaces which are accessible for modification, i.e. direct surface modification via *"grafting to"* techniques. The RAFT technique was used to synthesize SH-functionalized poly(*N*-isopropylacrylamide) (pNIPAAm-SH) polymers to generate surface-modified microspheres via thiol-ene reaction (**Scheme 1**). In a second approach, pDVB80 microspheres were grafted with alkyne-functionalized pHEMA (**Scheme 2**). For this purpose, the residual double bonds on the microsphere surface were converted into azide groups via a thio-click approach using a thiol-azide compound (1-azido-undecane-11-thiol). In a second step, the alkyne end-functionalized pHEMA was grafted to the azide-modified surface via click chemistry.

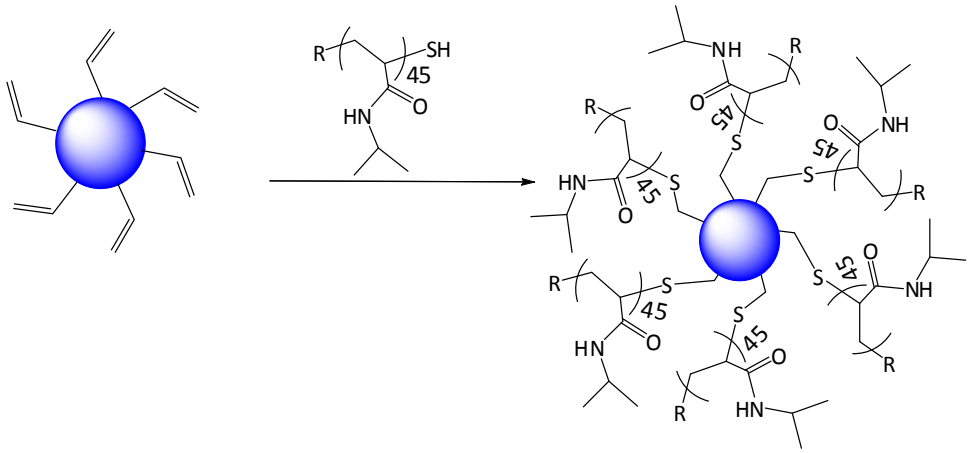

Scheme 1. Thiol-ene modification of pDVB80 microspheres with pNIPAAm$_{45}$ in a one-step approach (Approach 1).

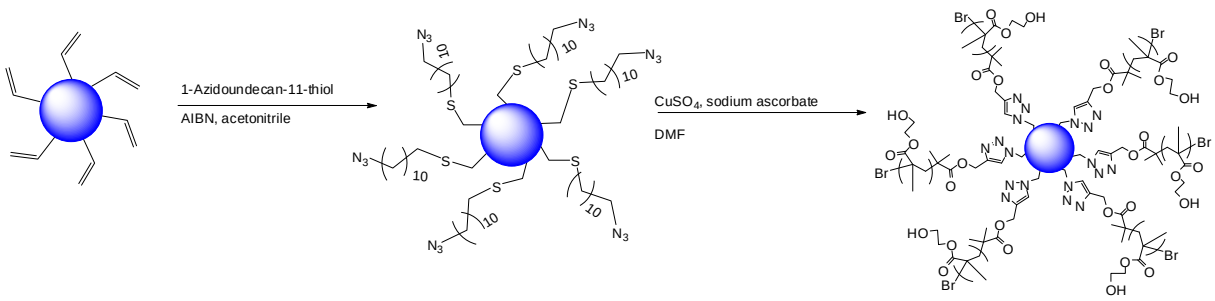

Scheme 2. PHEMA grafted microspheres via Huisgen 1,3-dipolar cycloaddition (Approach 2).

PDVB-*g*-pNIPAAm$_{45}$

Approach 1 results in pDVB-*g*-pNIPAAm$_{45}$ microspheres. This approach is a simple way to modify pDVB80 microspheres due to the direct coupling of thiol-modified polymer to the residual free and accessible double bonds on the surface. The surface-modified microspheres were characterized with elemental analysis, SEM, FT-IR transmission spectra and XPS. PNIPAAm is a stimuli-responsive polymer which shows response to change in temperature resulting in an LCST (lower critical solution temperature) around 32°C. On the one hand, it has an expanded conformation due to hydration below 32°C. On the other hand, it contracts in aqueous solution above the LCST. Among diverse stimuli as temperature, pH, solvent composition, and electric fields, temperature is one of the most broadly used stimulus in environment-responsive polymer systems because it is easy to control.

XPS was used to identify the chemical composition at the surface of the modified microspheres. Figure 1a shows the XPS spectra of the pDVB80 microspheres and Figure 1b the spectra of the pDVB80-*g*-pNIPAAm$_{45}$ microspheres. Inspection of the Figures clearly shows that the poly(divinyl benzene) microspheres only display a signal for carbon while the grafted microspheres display additional signals for nitrogen, sulfur and oxygen atoms as expected for a pNIPAAm-containing surface. Thus the XPS data clearly confirm the attachment of pNIPAAm onto the surface of the microspheres.

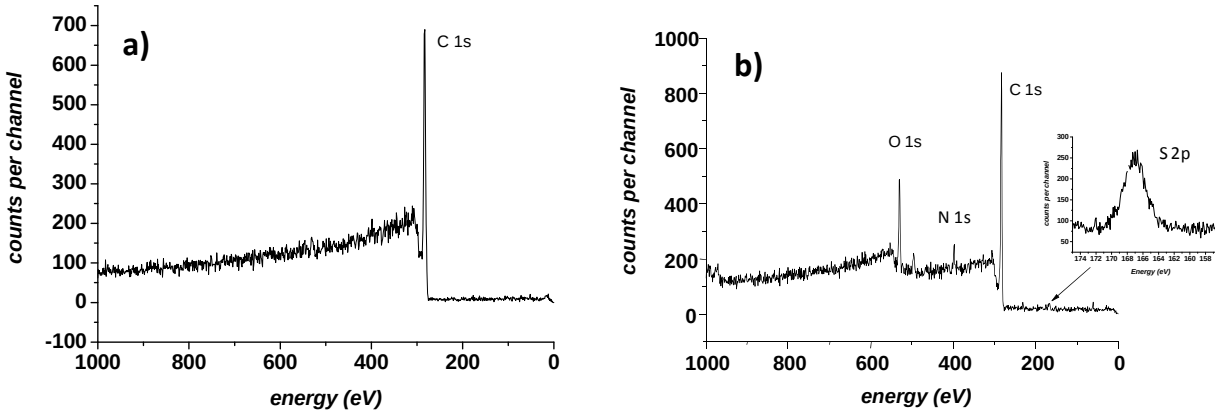

Figure 1. XPS spectrum of a) poly(divinyl benzene) microspheres (pDVB80) and b) pDVB80-g-pNIPAAm$_{45}$ microspheres. The inset shows the S2p XPS spectrum.

Figure 2 shows the FT-IR transmission spectra of (a) pDVB80 microspheres, (b) pDVB80-*g*-pNIPAAm$_{45}$ microspheres and (c) pNIPAAm$_{45}$. Clearly, characteristic peaks of pNIPAAm can be detected in the spectrum of the surface modified microspheres, indicating the successful grafting (3 435 cm^{-1} (ν(N-H)$_{free,}$ (ν (N-H)$_{bonded}$, amide), 1 705 cm^{-1} (amide stretch), 1 169 cm^{-1} (CH_3 and CH_2 skeletal).[22]

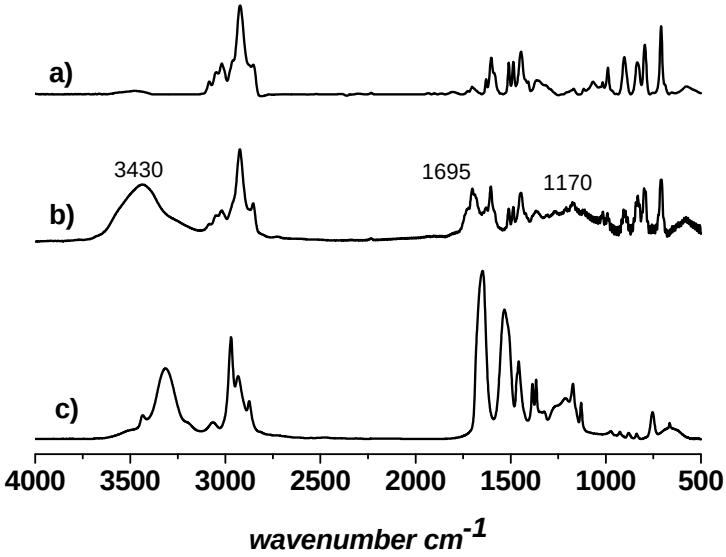

Figure 2. FT-IR transmissions spectra of a) pDVB80 microspheres, b) pDVB80-g-pNIPAAm$_{45}$ microspheres and c) pNIPAAm$_{45}$ as reference.

Suspension studies of pDVB80-*g*-pNIPAAm$_{45}$ microspheres demonstrate an appealing gain of hydrophilicity when grafted with pNIPAAm$_{45}$. PDVB80 and pDVB80-*g*-pNIPAAm$_{45}$ microspheres were stirred vigorously in deionized water. Prior to their functionalization, the particles show hydrophobicity, accumulate on the water surface, and adhere to the wall of the glass vial. However, pNIPAAm-grafted particles can easily be suspended in water due to their hydrophilic outer pNIPAAm-layer. This clearly indicates the disparate behavior of modified and unmodified microspheres. As mentioned above, pNIPAAm exhibits a lower critical solution temperature (LCST) in aqueous solution and a sharp reversible phase transition is observed at 32°C in water.[24] Above the LCST of PNIPAAm (32°C) the hydrophobic pDVB80-*g*-pNIPAAm$_{45}$ microspheres are sticking to the glass vial due to increasing hydrophobicity. The hydrophobicity of the microspheres leads to the continuous adsorption of the particles to the glass vial (see arrows in Figure 3).

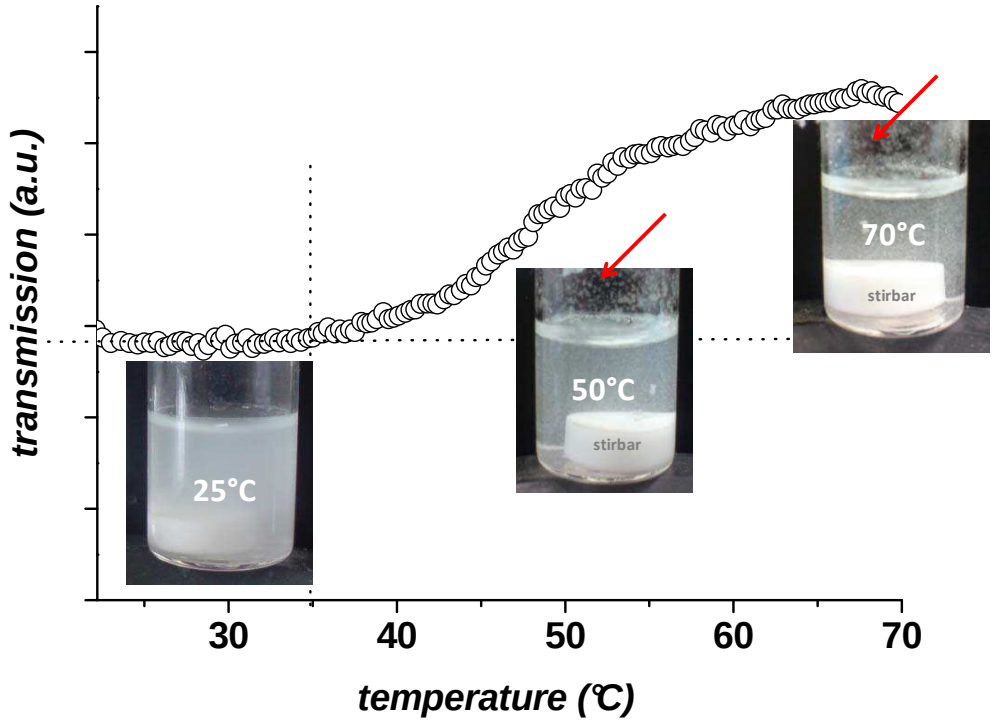

Figure 3. Temperature-dependent turbidity measurement of pDVB80-g-pNIPAAm$_{45}$ microspheres (20-70°C)). Suspension study in water for pDVB80-g-pNIPAAm$_{45}$ microspheres clearly showing the dispersability of pDVB80-g-pNIPAAm$_{45}$ microspheres and increasing transmission with increasing temperature.

This observation was supported by a turbidimetric study from 20°C to 70°C. Up to approximately 40°C a slight increase in transparency is detected. Above 40°C, which is slightly higher than the LCST of pNIPAAm (32°C), a sharp increase of the transmission is observed (Figure 3). Near or above the LCST the pNIPAAm chains collapse and induce a more hydrophobic environment and therefore decrease the dispersibility of the microspheres. At this transition point, the microspheres aggregate and move to the water surface leading to a more transparent solution. As can be seen in Figure 3, the microspheres adhere to the glass vial above the LCST as a result of the increasing hydrophobicity. Even if "grafting to" approaches tend to suffer both from low grafting rates and from low final grafting densities, the grafting density of PDVB80-*g*-pNIPAAm$_{45}$ is sufficient for the stimuli-responsive behavior. In addition, the microspheres were visualized by scanning electron microscopy (SEM). Figure 4a shows an image of a single pDVB80 microsphere. pNIPAAm-grafted particles (Fig. 4b) clearly show a significantly more coarse and rough surface which is due to the attached polymer on the surface.

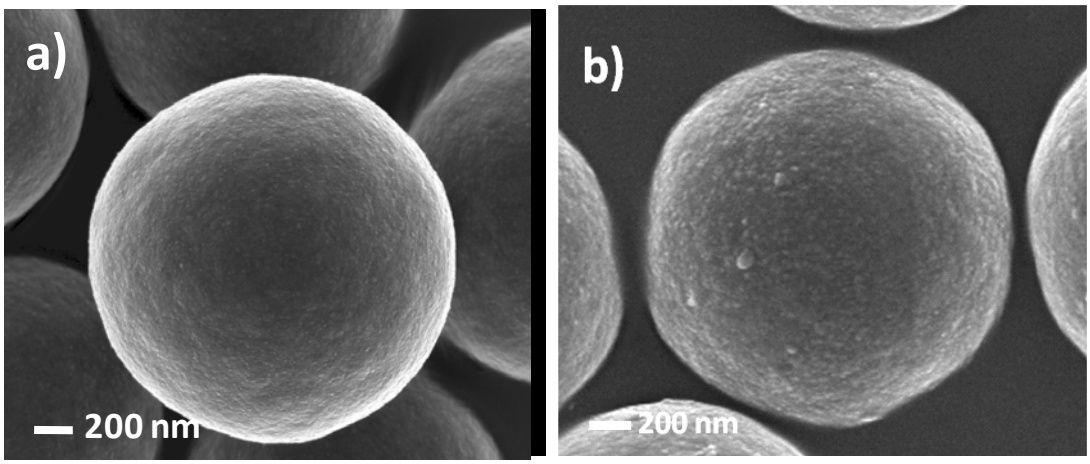

Figure 4. SEM images of a) poly(divinyl benzene) microspheres (pDVB80) and b) pDVB80-g-pNIPAAm$_{45}$ core-shell microspheres. The surface structure of pNIPAAm grafted microspheres is distinctly coarser compared to the blank microspheres.

pDVB-*g*-pHEMA

Approach 2. In a second study, we describe the synthesis and characterization of polyHEMA grafted pDVB80 microspheres (Scheme 2). Here, the Huisgen 1,3-dipolar cycloaddition is used to attach azido-functionalized pHEMA to the surface.

This approach is a very versatile and orthogonal method to attach any compound, polymer, or biomacromolecule carrying an alkyne-group to a surface. Therefore, multifunctional azido-microspheres (pDVB-N_3) were synthesized via the thiol-ene reaction. The surface-modified microspheres were characterized by elemental analysis, SEM, FT-IR, fluorescence spectroscopy and XPS. XPS analysis of the pDVB80-*g*-pHEMA microspheres (Figure 5c) exhibits the characteristic signals for bromine, nitrogen, sulfur and oxygen atoms.

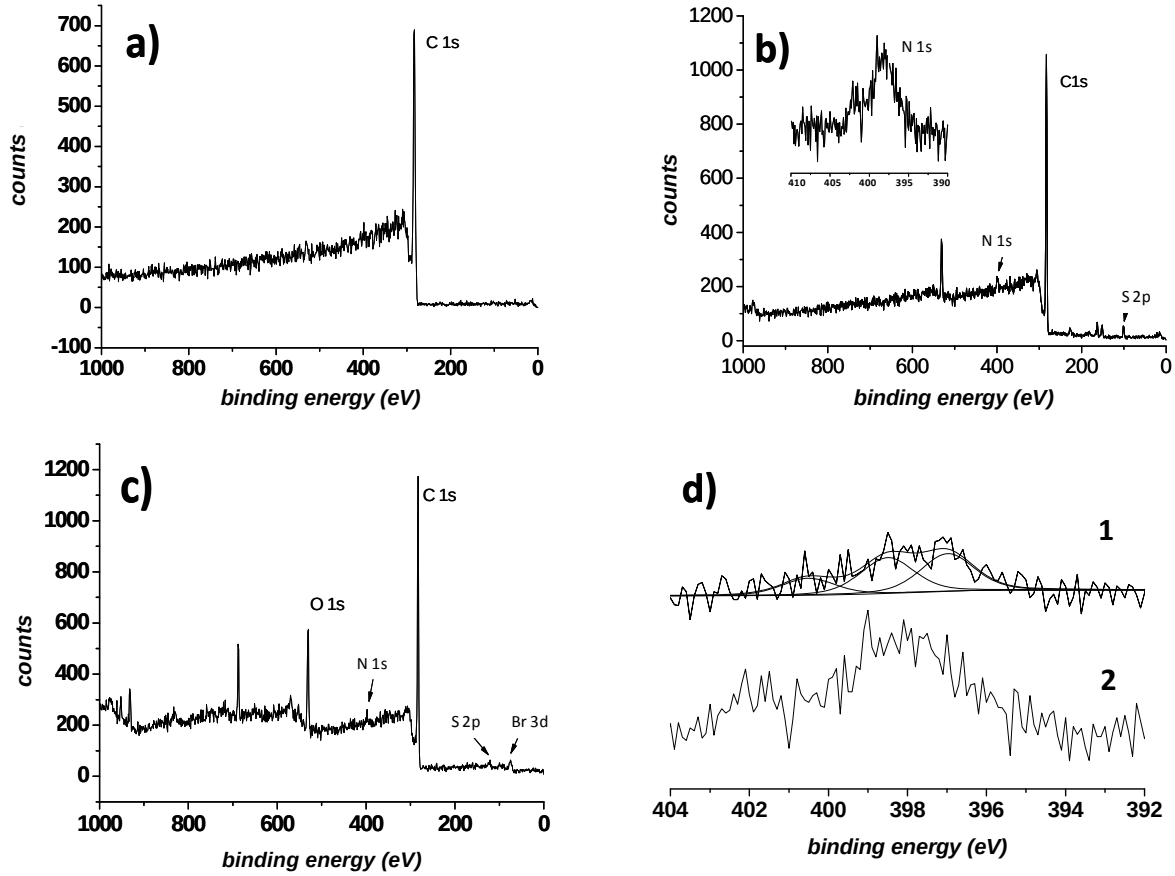

Figure 5. XPS spectra of a) pDVB80 b) pDVB-N_3 and b) pDVB80-g-pHEMA microspheres. The inset shows the N1s XPS spectrum. The peak at 688 eV results from residual $CuSO_4$ from click-reaction (Cu2p). d) shows the N1s XPS spectra of (1) pDVB-N_3 and (2) pDVB80-g-pHEMA microspheres.

The N1s spectra of pDVB-N_3 shows two peaks at 402 eV and 399 eV (see Figure 5d). The ratio of the areas of these two peaks is approximately 2:1. The peak at 402 eV corresponds to the relatively electron poor middle N atom of the azide group[32] (Please note that the peaks are shifted due to charging effects). After reaction of the pHEMA with pDVB-N_3 only one N1s signal can be observed at 397 eV. This is in accordance with previous results by Collman et al.[33] and London et al.[34] proving that the reaction took place. The N1s signal at 397 eV observed in the case of pDVB80-*g*-pHEMA microspheres is quite broad which is caused by a high binding energy shoulder due to unreacted azide groups. Fitting the N1s spectrum (see Figure 5d) shows that 41% of all azide groups have reacted. This is in good accordance with the values found with FT-IR spectroscopy.

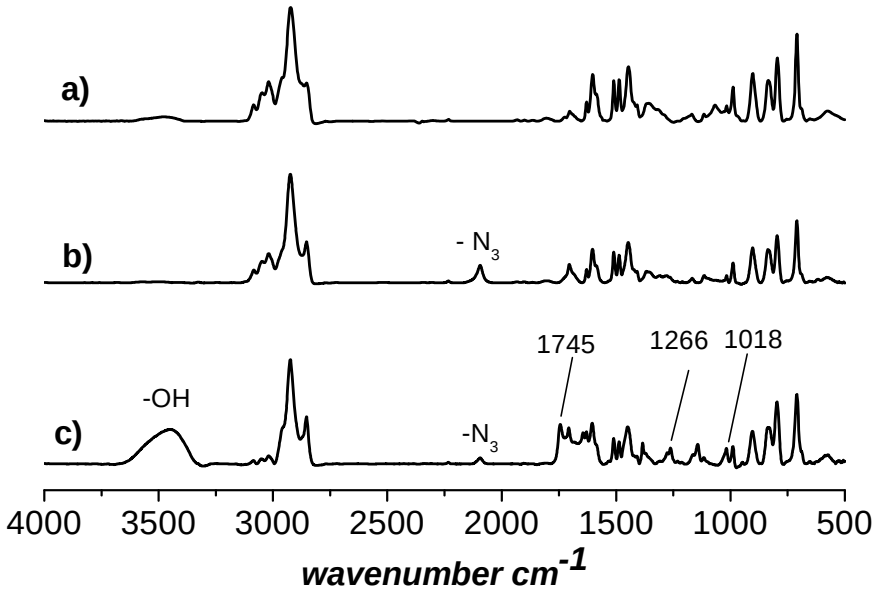

Figure 6. FT-IR transmission spectra of a) pDVB80 microspheres, b) pDVB80-N_3 and c) pDVB80-g-pHEMA.

Figure 6 shows the FT-IR transmission spectra of a*)* pDVB80-*g*-pHEMA, b) pDVB80-N_3 and c) pDVB80 microspheres. The spectrum of the pDVB80-N_3 microspheres clearly shows the characteristic N_3-vibration at 2 100 cm^{-1}. After reaction with alkyne-modified pHEMA, the peak decreases significantly but not completely. This indicates that not all azide groups have reacted. Comparing the areas under the N_3-vibration peaks at 2 100 cm^{-1} before and after reaction shows that about 39% of all azide groups have reacted which is in good accordance with the XPS results. The increase in grafting density hinders further grafting in the vicinity of grafted polymer chains. Characteristic peaks for pHEMA after the click-reaction with N_3-functionalized microspheres can also be detected (3500 cm^{-1} (OH stretching), 1745 cm^{-1} (C=O), 1640 cm^{-1}, 1266 cm^{-1} (CH_2), 1018 cm^{-1} (CO(H) stretching)) proving a successful grafting.

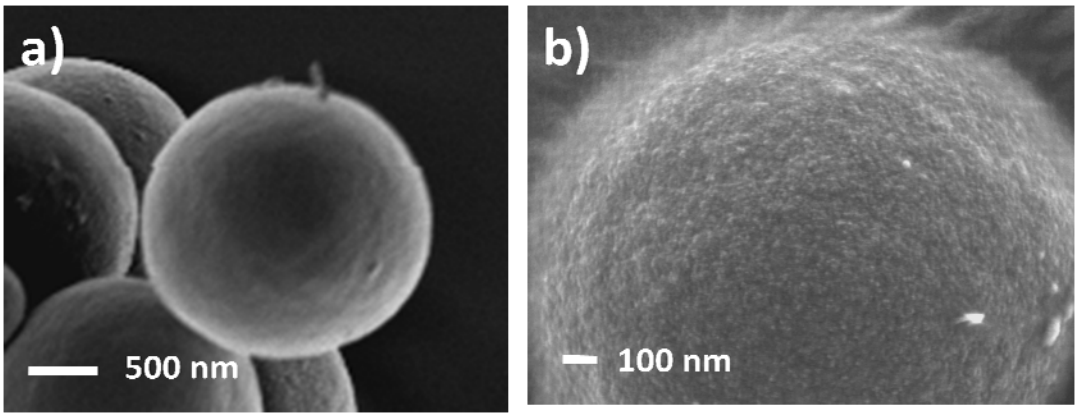

Figure 7. SEM images of pDVB-g-pHEMA , b) magnified SEM image of pDVB-g-pHEMA

In order to prove the effective attachment of the pHEMA chains to the surface of the azido-functionalized microspheres, the functional OH-groups of the pHEMA chains were used to label them with a fluorescent dye, e.g. Rhodamine B. This fluorescent tag has a functional carboxyl group which can react with hydroxy-functional end groups.

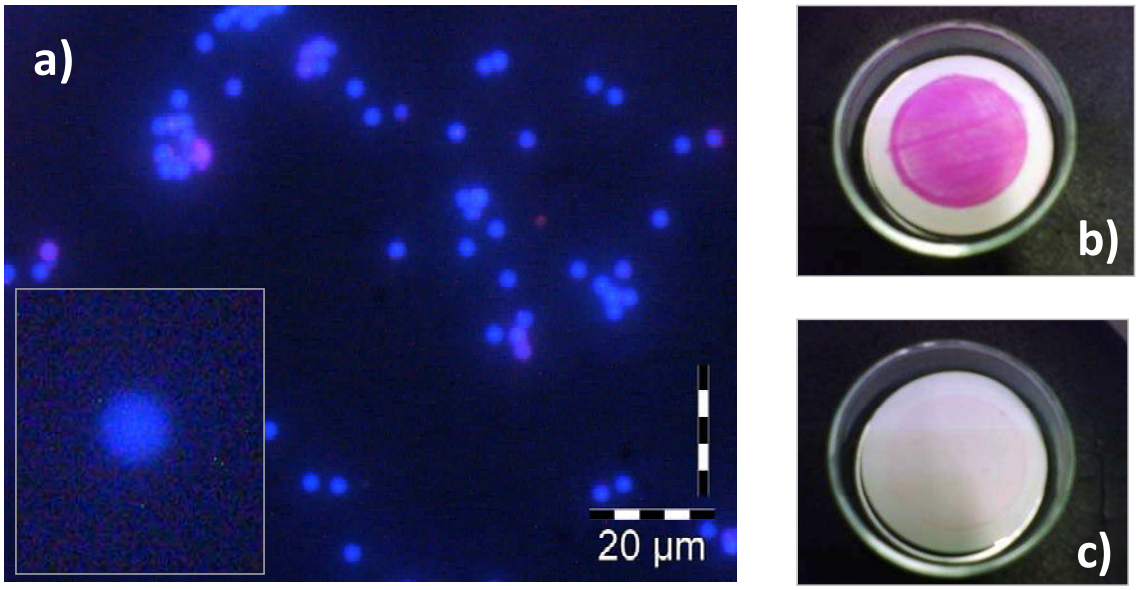

Figure 8. a) Wide-field fluorescence microscopy images of Rhodamine B-labeled pDVB80-g-pHEMA (excitation filter: 450-490 nm) b) Rhodamine B-labeled microspheres on a filter paper (pink). The pink color results from the covalently bounding of the Rhodamine B c) control experiment: identical conditions for ungrafted pDVB80 microspheres on a filter paper (white).

Figure 8a represents a fluorescence image of the pDVB80-*g*-pHEMA microspheres measured with a Leica DMRX. The homogeneous fluorescence clearly confirms that the microspheres

were functionalized with pHEMA. The control experiment with pDVB80 microspheres under identical conditions shows no fluorescence. Moreover, the fluorescent derivatization of the particles demonstrated a homogeneous distribution of OH-groups on the surface of the particle (Figure 8a). Figure 8b shows the Rhodamine B-labeled microspheres on a filter paper after intensive washing. The particles have a pink color due to the covalently bound Rhodamine B to the pHEMA chains attached to the pDVB80 surface. As expected, the control experiment which was carried out under identical conditions with pDVB80 microspheres, results in non-fluorescent particles. Furthermore, the microspheres keep their white color, which indicates that no Rhodamine B is attached to the surface (Figure 8c).

Additionally, the Rhodamine B tagged microspheres were studied via confocal microscopy. Hence, it is possible to select the Z-dimension (three-dimensional function) which provides image depth and enables the fabrication of cross-sectional slices of the images. The image shown in Figure 9 represents a cross-sectional slice of fluorescence-labeled pHEMA microspheres. It clearly shows the fluorescence in the outer shell (and no fluorescence in the core of the particle) and therefore confirms the exclusive functionalization with pHEMA on the surface of the microspheres. Furthermore, the control experiment with non-functionalized pDVB80 microspheres under identical reaction conditions with Rhodamine B shows no fluorescence.

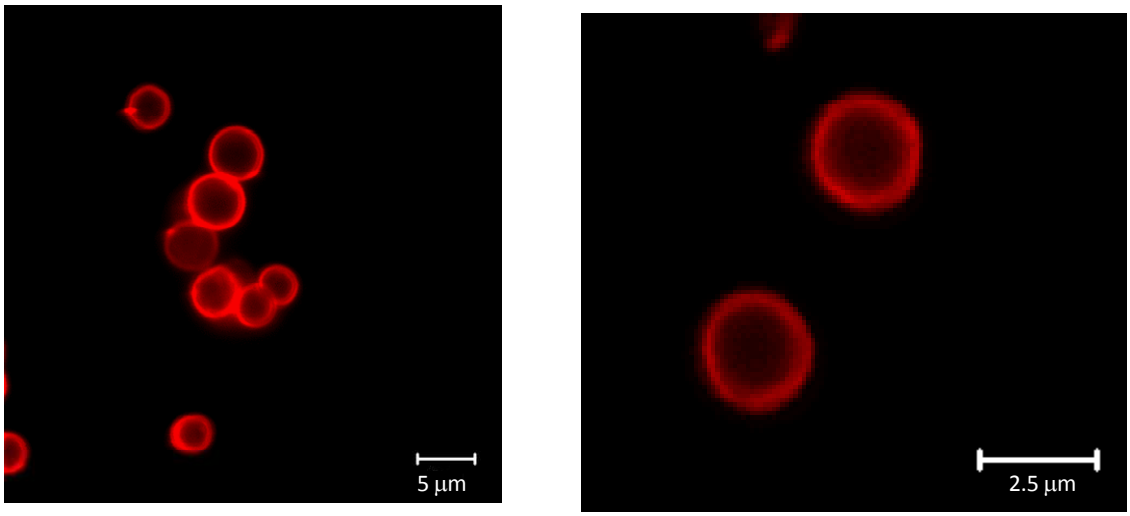

Figure 9. Confocal microscopy image of pDVB80-g-pHEMA microspheres functionalized with a Rhodamine B fluorescent tag.

Conclusions

We demonstrate the successful grafting of polymer chains via thiol-ene chemistry and azide-alkyne click-reactions. The thiol-ene approach for grafting thiol-endgroup functionalized polymers is a straight forward and effective method to directly graft polymers to the residual accessible double bonds of pDVB80 microspheres in a one-step process. As a model reaction, we chose SH-functionalized pNIPAAm, synthesized via RAFT polymerization. This approach can be extended towards the attachment of any thiol-functionalized compound to the surface (e.g. various thiol-end group functionalized responsive polymers and proteins). We showed the successful grafting via surface analysis methods (FT-IR transmission spectroscopy and XPS) and temperature dependent turbidity studies. The visualization of the particles was carried out with Scanning Electron Microscopy (SEM).

In an alternative approach, the 1,3 Huisgen dipolar cycloaddition was used to click alkyne-functionalized pHEMA to N_3-functionalized pDVB80. This approach sufficiently extends our *"grafting to"* approach to further agents not carrying a thiol group. For this purpose multi-functional azido-functionalized microspheres were prepared via the thiol-ene reaction of 1-azido-undecane-11-thiol with residual double bonds on the surface. These surface-modified particles are grafted with pHEMA and characterized with FT-IR transmission spectroscopy, XPS, SEM and fluorescence microscopy. The presented grafting techniques therefore provide a facile and near global access to an enormous variety of functional grafted microspheres. Grafting of hydrophilic polymers to hydrophobic particles can truly enhance the suspension properties of the particles in aqueous environment.

Acknowledgements

AG acknowledges Jiayin Yuan, Pierre-E. Millard and Andreas Hanisch (Macromolecular Chemistry II, University of Bayreuth) for polymer synthesis and Rhodamine B Chloride preparation. Sabine Wunder (Macromolecular Chemistry II, University of Bayreuth) is thanked for SEC measurements, Ingrid Otto (Chair of Materials Processing, University of Bayreuth) for Confocal Microscope images, Werner Reichstein (Experimentalphysik IV, University of Bayreuth) for SEM images, Brigit Brunner (Chemische Verfahrenstechnik, University of Bayreuth) for elemental analysis measurements and Prof. P. Rudolf and the group of Surfaces and Thin Films (Zernike Institute for Advanced Materials) for access to the X-ray photoelectron spectrometer. CBK acknowledges funding from the Karlsruhe Institute

of Technology (KIT) in the context of the German Excellence Initiative for leading German universities. DE acknowledges financial support by the Deutsche Forschungsgemeinschaft (FOR 608). LB and AHEM acknowledge financial support from the Australian Research Council (DP0877122) and the Fraunhofer Institute for Chemical Technology.

References and Notes

1. Li, Y.; Schadler, L. S.; Benicewicz, B. C., Surface and Particle Modification via the RAFT Process: Approach and Properties. In *Handbook of RAFT Polymerization*, Barner-Kowollik, C., Ed. Wiley-VCH: Weinheim 2008; p. 423.

2. Advincula, R. C.; Brittain, W. J.; Caster, K. C.; Rühe, J., *Polymer Brushes*. Wiley-VCH: Weinheim, 2004.

3. Barner, L. *Advanced Materials*, **2009**, in press, DOI: 10.1002/adam.200900373.

4. Deutsch, A. A.; Myers, E.; Stern, H. *Digestive Surgery* **1991**, 8, (4), 236-237.

5. Kolb, H. C.; Finn, M. G.; Sharpless, K. B. *Angewandte Chemie International Edition* **2001**, 40, (11), 2004-2021.

6. Binder, W. H.; Sachsenhofer, R. *Macromolecular Rapid Communications* **2007**, 28, (1), 15-54.

7. Gress, A.; Völkel, A.; Schlaad, H. *Macromolecules* **2007**, 40, (22), 7928-7933.

8. Dondoni, A. *Angewandte Chemie* **2008**, 120, (47), 9133-9135.

9. ten Brummelhuis, N.; Diehl, C.; Schlaad, H. *Macromolecules* **2008**, 41, (24), 9946-9947.

10. Killops, K. L.; Campos, L. M.; Hawker, C. J. *Journal of the American Chemical Society* **2008**, 130, (15), 5062-5064.

11. Qiu, X. P.; Winnik, F. M. *Macromolecular Rapid Communications* **2006**, 27, (19), 1648-1653.

12. Li, M.; De, P.; Gondi, S. R.; Sumerlin, B. S. *Journal of Polymer Science Part A-Polymer Chemistry* **2008**, 46, (15), 5093-5100.

13. J.-F. Lutz, H. Schlaad *Polymer* **2008**, 49, 817.

14. Goldmann, A. S.; Quémener, D.; Millard, P.-E.; Davis, T. P.; Stenzel, M. H.; Barner-Kowollik, C.; Müller, A. H. E. *Polymer* **2008**, 49, (9), 2274-2281.

15. S. Sinnwell; A. J. Inglis; M. H. Stenzel; Barner-Kowollik, C. *Macromolecular Rapid Communications* **2008**, 29, (12-13), 1090-1096.

16. Ting, S.; Quémener, D.; Granville, A.; Davis, T. P.; Stenzel, M. H.; Barner-Kowollik, C. *Aust. J. Chem.* **2007**, *60*, 405-409.

17. Quémener, D.; Davis, T. P.; Barner-Kowollik, C.; Stenzel, M. H. *Chem. Comm.* **2006**, 5051-5053.

18. Quémener, D.; Le Hellaye; M.; Bissett, C.; Davis, T. P.; Barner-Kowollik, C.; Stenzel, M. H. *J. Polym. Sci. Polym. Chem.* **2008**, *46*, 155–173.

19. Nebhani, L.; Sinnwell, S.; Inglis, A. J.; Stenzel, M. H.; Barner-Kowollik, C.; Barner, L. *Macromolecular Rapid Communications* **2008**, 29, (17), 1431-1437.

20. Inglis, A. J.; Sinnwell, S.; Stenzel, M. H.; Barner-Kowollik, C. *Angewandte Chemie* **2009**, 48, (13), 2411-2414.

21. Sinnwell, S.; Inglis, A. J.; Davis, T. P.; Stenzel, M. H.; Barner-Kowollik, C. *Chem. Comm.* **2008**, 2052-2054.

22. Zheng, G. D.; Stöver, H. D. H. *Macromolecules* **2002**, 35, (20), 7612-7619.

23. Zheng, G.; Stöver, H. D. H. *Macromolecules* **2002**, 35, (18), 6828-6834.

24. Barner, L.; Li, C. E.; Hao, X.; Stenzel, M. H.; Barner-Kowollik, C.; Davis, T. P. *Journal of Polymer Science Part A: Polymer Chemistry* **2004**, 42, (20), 5067-5076.

25. Joso, R.; Stenzel, M. H.; Davis, T. P.; Barner-Kowollik, C.; Barner, L. *Australian Journal of Chemistry* **2005**, 58, (6), 468-471.

26. Joso, R.; Reinicke, S.; Walther, A.; Schmalz, H.; Müller, A. H. E.; Barner, L. *Macromolecular Rapid Communication* **2009**, DOI: 10.1002/marc.200900031.

27. Lai, J. T.; Filla, D.; Shea, R. *Macromolecules* **2002**, 35, (18), 6754-6756.

28. Oyelere, A. K.; Chen, P. C.; Huang, X. H.; El-Sayed, I. H.; El-Sayed, M. A. *Bioconjugate Chemistry* **2007**, 18, (5), 1490-1497.

29. Bai, F.; Yang, X.; Huang, W. *Macromolecules* **2004**, 37, (26), 9746-9752.

30. Scales, C. W.; Convertine, A. J.; McCormick, C. L. *Biomacromolecules* **2006**, 7, (5), 1389-1392.

31. Yang, H.; Cheng, R. S.; Wang, Z. L. *Polymer* **2003**, 44, (23), 7175-7180.

32. Wollman, E. W.; Kang, D.; Frisbie, S: D.; Lorkovic, I. M.; Wrighton, M. S. *Journal of the American Chemical Society*, **1994**, 116, (10), 4395-4404.

33. Collman, J. P.; Devaraj, N. K.; Eberspacher, N. P. A.; Chidsey, C. E. D. *Langmuir* **2006**, 22, 6, 2456-2464.

34. London, G.; Carroll, G. T.; Landaluce, T. F.; Pollard, M. M.; Rudolf, P.; Feringa, B. L. *Chem. Commun.* **2009**, 1712–1714.

Biomimetic Mussel Adhesive Inspired Clickable Anchors Applied to the Functionalization of Fe_3O_4 Nanoparticles

Anja S. Goldmann,[a] Christine Schödel,[a] Andreas Walther,[b] Jiayin Yuan,[a] Katja Loos[c] and Axel H. E. Müller,[a]*

[a] *Makromolekulare Chemie II and Bayreuther Zentrum für Kolloide und Grenzflächen, Universität Bayreuth, 95440 Bayreuth, Germany. Fax. +49 921 553393, e-mail: axel.mueller@uni-bayreuth.de*

[b] *Molecular Materials, Department of Applied Physics, School of Science and Technology, Aalto University, Puumiehenkuja 2, FIN-00076 Aalto, Finland*

[c] *Polymer Chemistry & Zernike Institute for Advanced Materials, University of Groningen, 9747AG Groningen, The Netherlands*

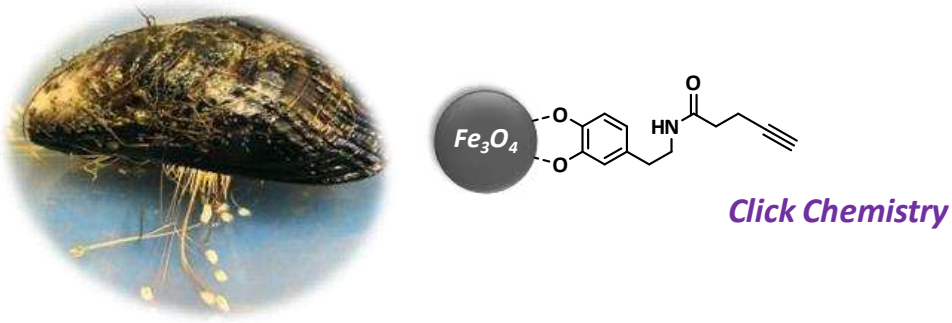

We report the functionalization of magnetite (Fe_3O_4) nanoparticles with dopamine-derived clickable biomimetic anchors. Herein, an alkyne-modified catechol-derivative was employed as the anchor, as (i) the catechol-functional anchor groups possess irreversible covalent binding affinity to Fe_3O_4 nanoparticles and (ii) the alkyne terminus enables further functionalization of nanoparticles via the grafting-onto approach with various possibilities offered by click chemistry. In the present work, azido-end group functionalized Rhodamine and poly(ethylene glycol) (PEG) were utilized for coating the iron oxide nanoparticles to make them fluorescent and water-soluble.

Introduction

Recently, it has become obvious that strategies employed by biological organisms can raise inspiration for new approaches to graft polymers onto surfaces. Of particular interest are unusual amino acids found in marine adhesive proteins, used to secure robust attachment to wet surfaces. Marine mussels adhere firmly to a variety of material surfaces such as rocks, wood, animals, and shells even in a wet and turbulent environment. Dopamine contributes noteworthy adhesive properties, forming strong chemical interactions with both organic and inorganic surfaces.[1] Messersmith and coworkers[2] demonstrated the first example of using a catecholic initiator for surface-initiated polymerization from metal surfaces to create antifouling polymer coatings. A new bifunctional initiator inspired by mussel adhesive proteins was synthesized, which strongly adsorbs to titanium and stainless steel substrates, providing an anchor for surface immobilization of grafted polymers. They presented the ability of catechols (e.g., dopamine) to bind to a large variety of inorganic surfaces. This biomimetic anchoring strategy is expected to be a highly versatile tool for polymer thin film surface modification for biomedical and other applications. Xu et al.[3] described a general strategy that used dopamine as a stable anchor to attach functional molecules on the surface of iron oxide nanostructures. They reported an easy method that employed dopamine as a robust anchor to immobilize functional molecules on the surfaces of magnetic nanoparticles (Fe_2O_3). The use of nitrilotriacetic acid as the functional molecule for protein separation demonstrates the robustness and specificity of nanostructures created by this method.

Up to now, only few efforts have been made to modify the surface of nanoparticles using click chemistry. The click-functionalization of SiO_2 particles was investigated several times in recent studies.[4,5] Even less studies have been performed to functionalize magnetic nanoparticles. Turro and coworkers[6] modified γ-Fe_2O_3 nanoparticles with click chemistry. Ligand exchange was performed with two types of ligands: phosphonic acid-azide and carboxylic acid-alkyne. The resultant particles were submitted to Cu(I)-catalyzed azide–alkyne cycloaddition (CuAAC) reactions with organic substrates. Prosperi and coworkers[7] reported a versatile, one-pot biofunctionalization of γ-Fe_2O_3 by CuAAC reaction. They demonstrated that this method is particularly suitable for protein immobilization, resulting in a site-specific anchorage onto the nanoparticle surface, which prevents loss of protein bioactivity. He et al.[8] have developed a methodology to prepare magnetic nanohybrids from clickable magnetic nanoparticles and polymer-coated nanomaterials by CuAAC click chemistry. They demonstrated that a soft polymer interlayer was indispensable for the surface click reactions between hard nanoparticles. Von Maltzahn et al.[9] demonstrated that click chemistry may be used to develop superparamagnetic iron oxide nanoparticles that seek out specific cells in vivo based on their surface expression of protein markers. These findings suggest that click chemistry meets the criteria of being applicable under aqueous conditions, efficient, orthogonal to thiol- and amine-containing targeting motifs, and stable in the complex in vivo environments of the blood and tumor milieu.

Because of the increasing usage of iron oxide nanoparticles in biomedical research, the ease of linking other biomolecules to iron oxide surfaces through a versatile anchor, such as dopamine, is expected to lead to useful applications of magnetic nanostructures in several areas, e.g. cell biology, biotechnology, and environment monitoring. Xie et al.[10] showed the functionalization of iron oxide nanoparticles with dopamine linked to human serum albumin which are highly efficient in labeling various types of cell lines. Click chemistry is a suitable procedure in biomedical and biochemistry applications.

We herein present the merger of click chemistry and mussel protein inspired anchor which we believe to open up new and versatile avenues for functional nanoparticles. We report the surface-functionalization of Fe_3O_4 nanoparticles (NPs) with an alkyne-functionalized dopamine

as mussel adhesive inspired clickable biomimetic anchors. Azido-Rhodamine was utilized as a technique to visualize the click-modification of Fe_3O_4 magnetic NPs. The Huisgen [2+3] cycloaddition was used to attach clickable fluorescent linkers to alkyne-modified Fe_3O_4 NPs. Furthermore iron oxide nanoparticles were coated with azido-end group functionalized polyethylene glycol (PEG) by click chemistry. Due to the fact that click-functionalities are easy accessible, the strategy is applicable to an immense number of attachable groups like functional polymers, biomolecules or fluorescent linkers.

Experimental Section

Materials

$Fe(CO)_5$ (Aldrich), octylether (Aldrich), oleic acid (90%, ABCR), (+)-sodium-L-ascorbate (Sigma), copper(II)sulfate (Sigma), 3-hydroxytyramine hydrochloride (dopamine, Sigma), Rhodamine B (Sigma), sodium azide (Sigma), 4-dimethylaminopyridin (99%, Aldrich), 3,4-dihydroxyphenylacetic acid (97%, TCI Europe), 3-bromo-1-propanol (97%, Aldrich), N_3-PEG (Mn = 1000 g mol^{-1}, creative PEGworks).

Synthesis

Oleic acid stabilized particles were synthesized according to a modified procedure described by Hyeon et al.[11] To prepare monodisperse Fe_3O_4 iron nanoparticles, 2 mL of $Fe(CO)_5$ (1.52 mmol) was added under nitrogen atmosphere to a mixture containing 200 mL of octylether and 12.8 g of oleic acid (4.56 mmol) at 100 °C. The resulting mixture was heated to reflux and kept at that temperature for approximately 4 h until the solution gets black. The resulting black solution was cooled to room temperature and kept at the air. Ethanol was added to yield a black precipitate, which was then separated by a magnet. The resulting black powder can easily be redispersed in solvents, such as hexane, octane, and toluene.

Synthesis of pentynoic acid chloride

2 g (20.4 mmol) of pentynoic acid was dissolved in dichloromethane under argon atmosphere. Then 2.62 mL (30.6 mmol) of oxalyl dichloride was added. The reaction mixture was stirred at room temperature for 15 h under argon atmosphere. The solvent and the residual oxalyl dichloride were evaporated and the yellow liquid was purified by distillation to give a colorless liquid and was stored under inert gas.

^{1}H-NMR (CD_2Cl_2, 300 MHz) δ 2.09 (t, J = 2.7 Hz, 1H), 2.56 (dt, J = 2.7, 7.0 Hz, 2H), 3.15 (t, J = 7.0 Hz, 2H) 1H-NMR (CD_2Cl_2, 300 MHz) δ 2.09 (t, J = 2.7 Hz, 1H), 2.56 (dt, J = 2.7, 7.0 Hz, 2H), 3.15 (t, J = 7.0 Hz, 2H).

Synthesis of alkyne-functional dopamine (Alkyne-Dopa)

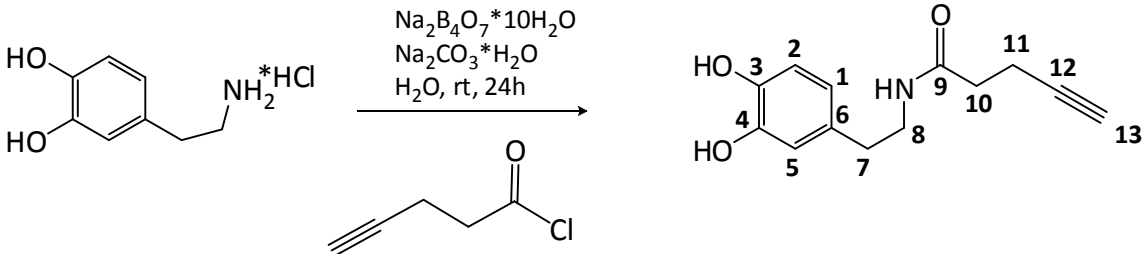

The synthesis was adopted from a modified procedure described by Messersmith and coworkers.[2] A 250 mL round-bottomed flask was charged with borax ($Na_2B_4O_7$ 10 H_2O, 3.83 g, 10 mmol) and 100 mL of water. The solution was degassed with argon for 30 min, and dopamine·HCl (1.9 g, 10 mmol) was added. The reaction mixture was stirred for 15 min and the pH was adjusted to pH 9-10 with $Na_2CO_3·H_2O$. The resulting solution was cooled in an ice bath, and pentynoic acid chloride (10 mmol) was added. The reaction mixture was allowed to reach room temperature and stirred for 24 h under argon. The pH of the solution was maintained at pH 9-10 with $Na_2CO_3·H_2O$ during the reaction. The reaction solution was then acidified to pH = 2 with aqueous HCl solution, and extracted with EtOAc (3 × 100 mL). The combined organic layers were dried over $MgSO_4$, and the solvent was evaporated under reduced pressure to give a brownish liquid. The crude product was purified by silica gel column chromatography (4% MeOH in $CHCl_3$) to give a colorless viscous liquid. (0.96 g, yield 41 %).

^{13}C and 2D NMR (gs-HSQC-^{1}H/^{13}C) are provided in the supporting information.

^{1}H NMR ($CDCl_3$, δ in ppm): 8.0 (-NH, broad, 1H); 6.8-6,4 (aromatic protons, 3H); 3.35 (-C<u>H$_2$</u>-NH-, 2H); 2.65 (-C<u>H$_2$</u>-CH$_2$-NH-, 2H); 2.41 (CO-C<u>H$_2$</u>-CH$_2$-, 2H); 2.31 (CO-CH$_2$-C<u>H$_2$</u>-, 2H); 2,19 (-CH$_2$-C<u>ΞH, 1H</u>). ^{13}C NMR ($CDCl_3$, δ in ppm): 174.1 (C9); 146.4 (C3); 144.9 (C4); 132.2 (C6); 121.3 (C1); 117.1 (C5); 116.5 (C2); 83.7 (C12); 70.5 (C13); 42.5 (C8); 36.3 (C10); 36.1 (C7); 15.9 (C11).

Mass spectrometric analysis: $M_{exp.}$233.26 gmol^{-1} ($M_{theor.}$233.26 gmol^{-1}).

Synthesis of N_3-Rhodamine B

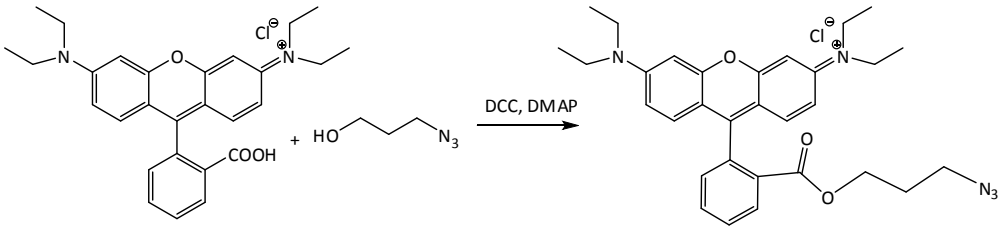

3-bromo-1-propanol (5g, 36 mmol) and sodium azide (3.83 g, 59 mmol) were dissolved in a mixture of acetone (60 mL) and water (10 mL) and the resulting solution was refluxed overnight. Acetone was then removed under reduced pressure, 50 mL of water were added and the mixture was extracted with diethyl ether (3 × 50 mL). The collected organic layers were dried over $MgSO_4$ and, after removal of the solvent under reduced pressure, 3-azido-1-propanol was isolated as a colorless oil (2.2 g, 60%).

1 g (0.01 mol) of 3-azido-1-propanol, 5.3 g (0.011 mol) of Rhodamine B, 4.12 g (0.02 mol) of *N*,*N*′-Dicyclohexylcarbodiimide (DCC) and catalytical amounts of DMAP were dissolved in 100 mL of dichloromethane. The reaction was allowed to stir over night (18 h). After removal of the solvent, the resulting dark red liquid was purified via column chromatography.

Surface functionalization of Fe_3O_4 nanoparticles with alkyne-dopamine (Alkyne-Fe_3O_4)

To 40 mg of oleic acid stabilized Fe_3O_4 nanoparticles, dispersed in hexane, alkyne-dopamine was added in excess. The dispersion was treated with a sonifier (45 minutes, settings: 20% amplitude, 3 seconds on and 2 seconds off). The particles were dialysed for 7 days to remove any unreacted alkyne-dopamine.

Click-reaction of alkyne-Fe_3O_4 and N_3-Rhodamine

Alkyne-modified Fe_3O_4 nanoparticles, dispersed in DMSO (0.5 mg mL^{-1}) were treated with ultrasound for 15 min. $CuSO_4$ ($1.25 \cdot 10^{-3}$ mol) and sodium ascorbate ($7.07 \cdot 10^{-4}$ mol) were added in excess to the solution. 20 mg of N_3-Rhodamine was added and the dispersion was stirred at room temperature for 48 h. The particles were washed several times with DMSO and deionized water until the washing solution showed no sign of fluorescence and were separated magnetically. The particles were redispersed in THF. In a control experiment blank oleic acid stabilized Fe_3O_4 nanoparticles were treated under identical conditions.

Click-reaction of alkyne-Fe_3O_4 and N_3-PEG

Alkyne-modified Fe_3O_4 nanoparticles, dispersed in DMSO (approx. 5 mg mL^{-1}) were treated with ultrasound for 15 min. $CuSO_4$ and sodium ascorbate were added in excess to the solution. 0.05 g of N_3-PEG (1000 g mol^{-1}) was added and the dispersion was stirred at 50 °C for 48 h. The particles were washed with DMSO repetitively after dialyzing against DMSO for 14 days.

Characterization

Nuclear Magnetic Resonance (NMR) Spectroscopy. ^{1}H-NMR and ^{13}C-NMR spectra were recorded on a Bruker ACF300 300-MHz spectrometer. Gs-HSQC-^{1}H/^{13}C were recorded on a Bruker Avance 300 300-MHz spectrometer.

X-ray Photoemission Spectroscopy. The samples were introduced through a load look system into an SSX-100 (Surface Science Instruments) photoemission spectrometer with a monochromatic Al K_α X-ray source (*E*=1486.6 eV). The base pressure in the spectrometer during the measurements was 10^{-10} mbar. The photoelectron takeoff angle was 37°. The energy resolution was set to 1.3 eV to minimize measuring time. Sample charging was compensated by directing an electron flood gun onto the sample. Spectral analysis included a Shirley background subtraction and a peak deconvolution that employed Gaussian and Lorentzian functions in a least-square curve-fitting program (WinSpec) was developed at the LISE, University of Namur, Belgium. Atomic compositions were calculated in a semi-quantitative approach with the atomic sensitivity factors of the XPS system.[12]

Fourier Transform Infrared (FT-IR) transmission spectra were recorded using a Bruker IFS 66v/s spectrometer under vacuum at a resolution of 4 cm^{-1} using the KBr pellet technique. Spectra were recorded and evaluated with the software OPUS version 4.0 (Bruker).

Scanning Electron Microscopy (SEM) images were recorded on a LEO 1530 (Zeiss) instrument, applying the InLens detector with a slow acceleration voltage of 2 kV and sputtering the microspheres with lead to a sufficient material contrast.

Dynamic light scattering (DLS) measurements were performed on an ALV DLS/SLS-SP 5022F compact goniometer system with an ALV 5000/E correlator and a He-Ne laser. CONTIN analysis of the obtained autocorrelation functions was carried out.

Confocal fluorescence microscopy images were captured using a Zeiss LSM 710 confocal laser scanning microscope. All images were captured using an oil immersion lens NA 1.3 Objective Plan-Apochromat 63×/1.4 Oil DIC M27). Rhodamine B was excited by a 543 nm HeNe laser. A main beam splitter was used with a long pass filter (485 nm/543 nm). Emission was captured by a spectral detection unit set 625 nm (LP).

Mass spectrometry

Mass spectra were recorded using a MAT 8500 instrument (Finnigan).

Sonication treatment was performed with a Branson model-250 digital sonifier equipped with 1/8 in. diameter tapered microtip (200 watt at 20% amplitude).

Results and discussion

Fe_3O_4 nanoparticle synthesis

Fe_3O_4 nanoparticles were prepared by the thermal decomposition of iron pentacarbonyl in the presence of oleic acid at 100 °C[11] yielding near monodisperse iron oxide without a further size selection process. The obtained nanoparticles were characterized by TEM and DLS (Figure 1).

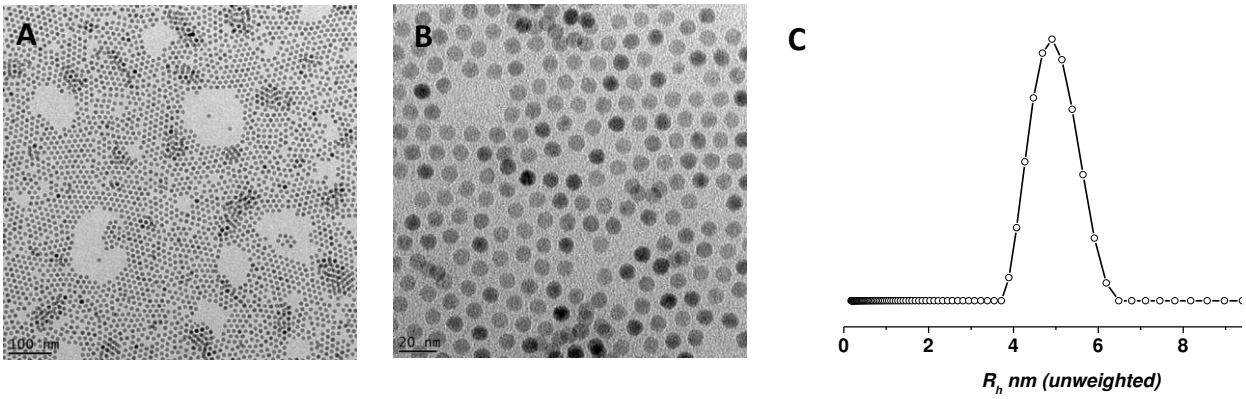

Figure 1. A, B) TEM images of a two-dimensional hexagonal assembly of near monodisperse Fe_3O_4 nanoparticles synthesized via the thermal decomposition of iron pentacarbonyl in the presence of oleic acid; C). DLS CONTIN plot (unweighted) of oleic-acid stabilized Fe_3O_4 nanoparticles (hexane).

The TEM image of the iron oxide nanoparticles exhibitis that nanoparticles are near monodisperse with a diameter of 8.52 nm ± 0.66 nm, which is further confirmed by Dynamic light scattering (DLS). The z-average hydrodynamic radius of the particles in hexane is found to be 4.9 nm which is in good accordance to the average diameter found in a statistical evaluation of the TEM images (8.52 nm ± 0.66 nm).

Fe_3O_4-alkyne

An alkyne-modified dopamine derivative was synthesized as a stable biomimetic anchor to stabilize the magnetic iron oxide particles. As mentioned before, dopamine-derivatives act as adhesive and stick to virtually any kind of surface. Alkyne-dopamine was utilized to create

multi-click functional Fe_3O_4 NPs as demonstrated in Scheme 1. These nanoparticles act as scaffold for further modification via click chemistry.

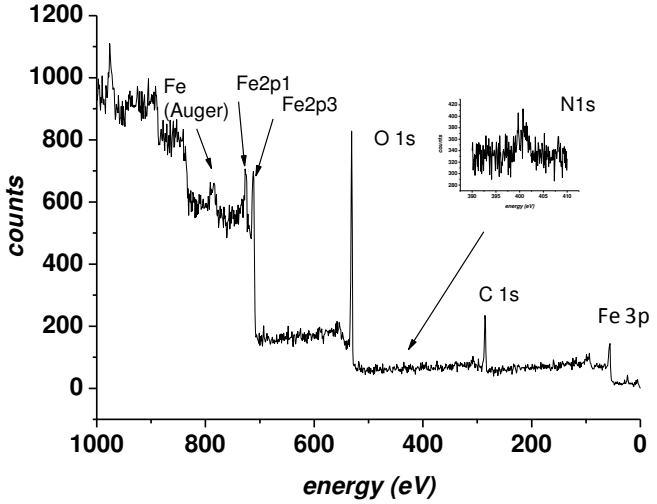

Figure 2. XPS spectrum of alkyne-modified Fe_3O_4 magnetic nanoparticles (Fe_3O_4-alkyne).

XPS was used to identify the chemical composition at the surface of the modified iron oxide NPs. Figure 2 clearly shows that the signals for iron, carbon, oxygen and nitrogen are displayed as expected for a dopamine-coated surface. Different signals for the iron-containing core can be assigned to the Fe-Auger signal at 784 eV, as well as the Fe2p1 (720 eV), Fe2p3 (707 eV) and Fe3p (60 eV) signals. The inset shows the nitrogen signal at 402 eV and therefore indicates the successful binding of alkyne-dopamine to the surface. The atomic compositions of C and N can be calculated in a semi-quantitative approach with the atomic sensitivity factors of the XPS system allowing the determination of the elemental ratio and additional proof for the successful ligand exchange with alkyne-dopamine. The calculated value (average value of three measurements) of C:N, 11.3:1, is in good accordance with the theoretical calculations of the element ratio (11:1). This proves a quantitive exchange of the oleic acid ligands by alkyne-Dopa.

Fe_3O_4-Rhodamine

To demonstrate the activity of alkyne groups at the outer layer azido-Rhodamine was used to visualize the click chemistry. This fluorescent tag binds covalently to the dopamine shell via click chemistry under adequate reaction conditions. The synthesis is presented in Scheme 1. The

excess of N_3-Rhodamine was removed by intensive washing with DMSO and the pure functionalized particles were separated magnetically.

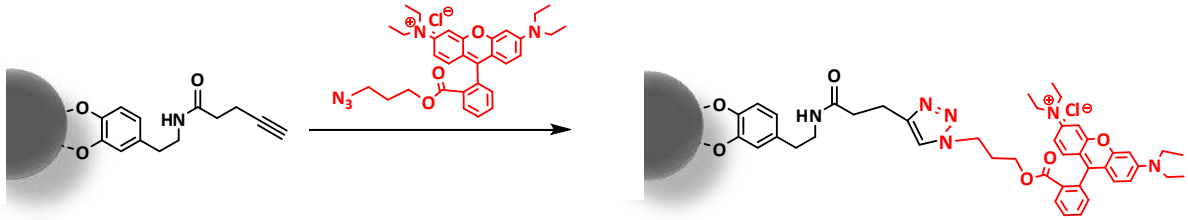

Scheme 1. Strategy for Rhodamine-labeling of Fe_3O_4 nanoparticles with click chemistry.

Due to the modification of the surface, the color of the particle solution changed from brownish to brownish-red. The color results from the Rhodamine B dye covalently bound to the particles (Figure 3D). UV light exposure (366 nm) induces fluorescence of the labeled NPs in THF solution.

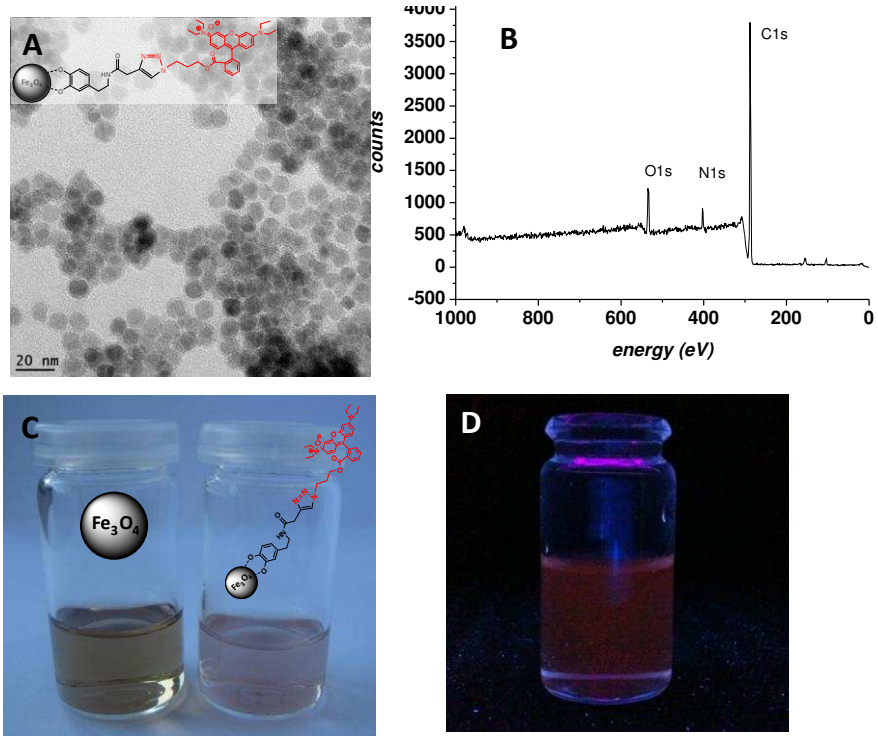

Figure 3. TEM (A) and XPS (B) analysis of fluorescently modified Fe_3O_4 nanoparticles; Optical images (C) of oleic acid (left) and alkyne-dopamine (right) stabilized Fe_3O_4 nanoparticles in THF; (D) Photograph showing the fluorescence of Rhodamine-labeled NPs in THF (UV lamp 366 nm).

XPS measurements of Rhodamine-labeled magnetic particles illustrate the signals for carbon, oxygen and nitrogen. Interestingly the characteristic signals for iron are missing. The inelastic mean free path of a photoelectron in a solid is generally smaller that 10 – 20 Å. Therefore only the elements of the dopamine-Rhodamine shell (C, N, O) are detectable as the organic shell is too thick to allow photoelectrons of Fe be emitted. The calculated ratio of C:N (average value of three measurements) is 8.4:1 which is in good accordance with the theoretical calculations of the element ratio (7:1). The FT-IR spectrum of N_3-Rhodamine shows a characteristic peak for the azido-group at 2120 cm^{-1}. After click-reaction this vibration peak has vanished indicating that the reaction took place completely and no free N_3-Rhodamine remains in solution (see Figure 4 A).

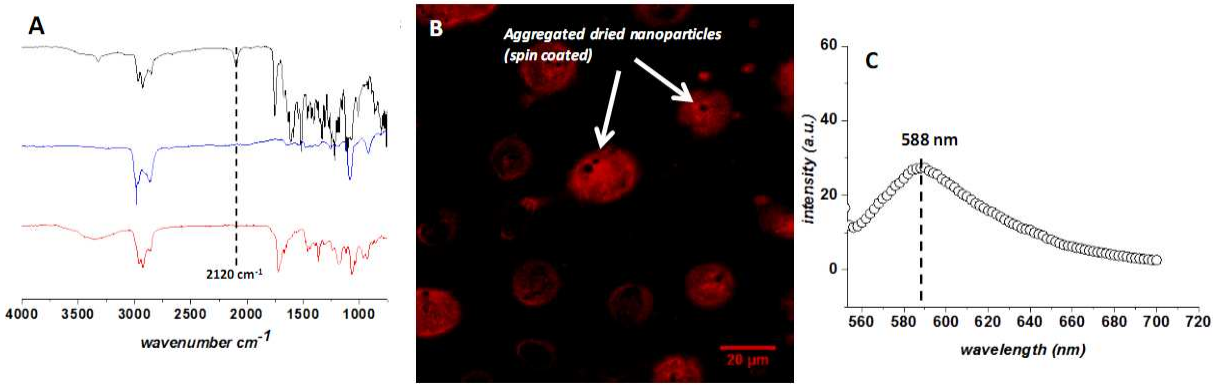

Figure 4. A) FT-IR spectra of Fe_3O_4-Rhodamine (red), Fe_3O_4-alkyne-dopamine stabilized particles (blue) and N_3-Rhodamine (black) as reference. B) Confocal fluorescence micrograph of spin-coated fluorescent Fe_3O_4 nanoparticles. The fluorescent spherical parts are aggregates of magnetic iron oxide nanoparticles. C) Fluorescence emission spectrum of Rhodamine-labeled Fe_3O_4 nanoparticles dissolved in THF (excitation wavelength 543 nm).

Figure 4 B shows a confocal fluorescence micrograph (CFM) and the fluorescence spectrum of Rhodamine-labeled Fe_3O_4 particles. The NPs were spin-coated from THF solution. As expected, large spherical aggregates are formed while spin-coating the samples. Nevertheless, the fluorescence confirms the exclusive functionalization with azido-Rhodamine on the surface via click chemistry. Due to resolution limit of CFM and the small size of the particles, single particles cannot be resolved. The emission spectrum shows the maximum fluorescence intensity at 588

nm which is in accordance with the azide-Rhodamine spectrum (see supporting informations). The control experiment, which was carried out under identical conditions with non-functionalized dopamine coated particles, does not show fluorescence. Additionally, the color of the dispersed particles in THF did not change compared to the starting material, which indicates that no Rhodamine is attached or adsorbed.

Fe_3O_4-*g*-PEG

Furthermore, click-modified iron oxide nanoparticles were modified with poly(ethylene glycol) (PEG) via copper-catalyzed Huisgen [2+3] cycloaddition. For that purpose, azido-endgroup functionalized PEG (N_3-PEG, 1000 g mol-1, DP_n = 23) as hydrophilic polymer was used. The coating strategy is outlined in Scheme 1. The excess of N_3-PEG was removed by several washing cycles with DMSO and subsequent dialysis for 14 days. With this approach, hydrophobic Fe_3O_4 nanoparticles can be converted into water-soluble biocompatible particles. With our method PEG is anchored covalently onto the monodisperse Fe_3O_4 NPs and can be redispersed in water due to the hydrophilic PEG shell which corroborates the successful grafting.

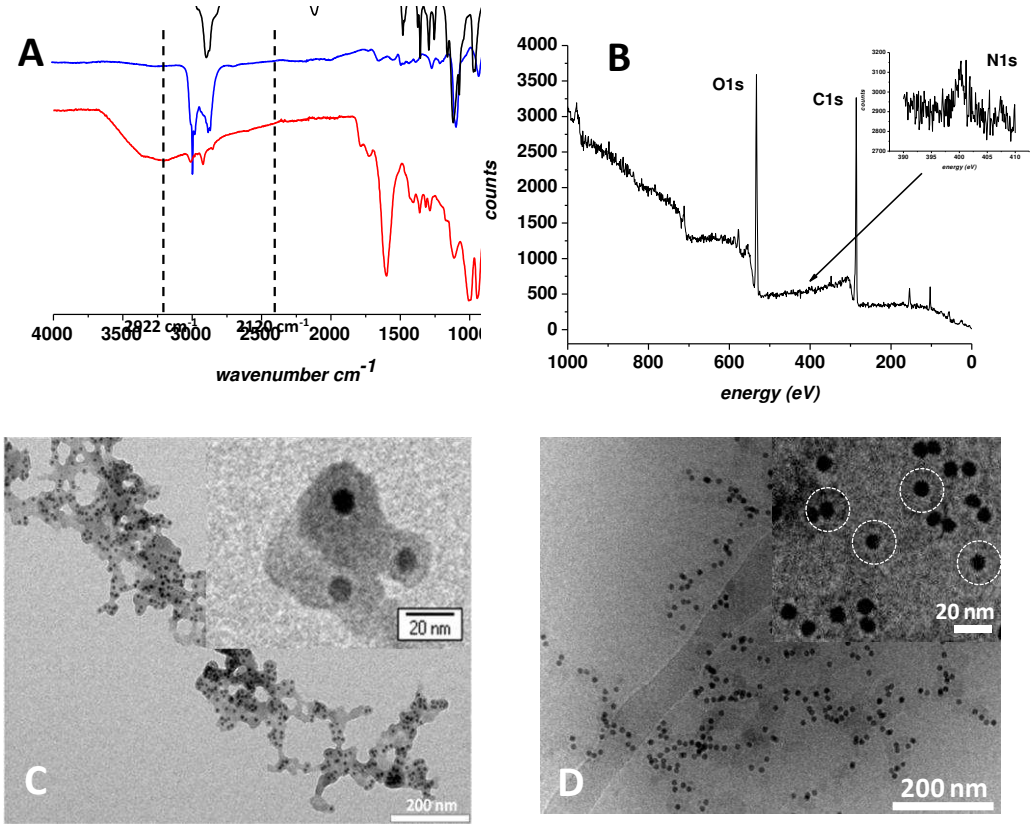

Figure 5. A) FT-IR spectra of Fe_3O_4-g-PEG (red), Fe_3O_4-alkyne-dopamine stabilized particles (blue) and N_3-PEG (black) as reference B) XPS measurements of PEG-coated Fe_3O_4 nanoparticles C: TEM image of PEG-coated Fe_3O_4 nanoparticles obtained from DMSO by drop coating on a carbon-coated cupper grid. D: Cryo-TEM image of PEG-coated Fe_3O_4 nanoparticles obtained from water.

Figure 5 B shows the FT-IR spectra of dopamine-coated and PEG-functionalized iron oxide particles as well as the spectrum of N_3-PEG as reference. The spectra provide evidence for successful click-grafting. For the PEG-coated particles the vibration peaks of the methylene hydrogen, originating from the PEG repeating units can be found at 2922 cm^{-1}. On the contrary, the dopamine-stabilized particles do not show this vibration peak. N_3-PEG has a characteristic peak for the azido-group at 2120 cm^{-1}. After click-reaction this vibration peak vanishes indicating that the reaction took place completely and no free N_3-PEG remains in solution. The XPS measurement of PEG-coated iron oxide nanoparticles (Figure 5 A) shows the characteristic

elements C, N and O of the PEG shell. Again, no iron signals can be detected due to the dense polymer layer. Figure 5 C represents a typical TEM image of PEG-coated nanoparticles obtained by drop-coating from DMSO solution. Clearly the polymer shell of the iron oxide particles can be detected. The PEG coated particles are seen to agglomerate, which might be attributed to drying effects. Single, non aggregated particles are also found on the grid as presented in the inset in (C). A cryogenic TEM images of PEG-coated nanoparticles in water is shown in Figure 5 D. The grey halos around the Fe_3O_4 core represent the PEO coronas. Surprisingly, aggregates are still seen in solution. The reason for this is yet unclear and will be investigated in the future. As a control experiment, oleic acid stabilized Fe_3O_4 nanoparticles, which do not contain an alkyne-functionality, were dispersed with N_3-PEG and treated under the same conditions for the click reaction between click-dopamine-coated particles and N_3-PEG. After purification by dialysis TEM images demonstrate absence of any corona around the iron oxide particles (see Figure S5). This control experiment corroborates the successful coating of click-dopamine coated particles. Additionally, the particles agglomerate strongly in solution (DMSO) due to the lack of the stabilizing PEG shell.

Conclusion

We demonstrated the successful combination of click chemistry with biomimetic mussel-adhesive protein inspired anchors. This merges two important and versatile strategies of modern nanochemistry. We used iron oxide nanoparticles as a model system to demonstrate several facile conjugations. The irreversible binding affinity of the dopamine-derivative serves as scaffold for the click reaction of various clickable ligands. As a model reaction, we chose N_3-Rhodamine as fluorescent dye. Confocal fluorescence micrographs demonstrate the successful click reaction. Furthermore, this approach was corroborated by the attachment of azidofunctionalized PEG. This method can be extended to the attachment of any suitable click-functionalized compound to the Fe_3O_4 surface (e.g. various N_3-end group functionalized responsive polymers and proteins). The successful grafting was demonstrated by surface analysis methods and TEM to visualize the particles. Looking out to the future, our click-

functionalized dopamine units can be very versatile building blocks for the orthogonal, easy and rapid functionalization of virtually any surface.

Acknowledgements

The authors thank Markus Müllner for N_3-Rhodamine synthesis and Andrea Wolf, Melanie Förtsch, Annika Ochs and Dr. Markus Drechsler for TEM and cryo-TEM measurements (Macromolecular Chemistry II, University of Bayreuth). Melanie Pretzl (Physical Chemistry II, University of Bayreuth) is thanked for Confocal Microscope images. Prof. P. Rudolf and the group of Surfaces and Thin Films (Zernike Institute for Advanced Materials, Groningen) arre thanked for access to the X-ray photoelectron spectrometer.

References and Notes

(1) Lee, H.; Dellatore, S. M.; Miller, W. M.; Messersmith, P. B. Science 2007, 318, 426.

(2) Fan, X.; Lin, L.; Dalsin, J. L.; Messersmith, P. B. Journal of the American Chemical Society 2005, 127, 15843.

(3) Xu, C.; Xu, K.; Gu, H.; Zheng, R.; Liu, H.; Zhang, X.; Guo, Z.; Xu, B. Journal of the American Chemical Society 2004, 126, 9938.

(4) Ranjan, R.; Brittain, W. J. Macromolecules 2007, 40, 6217.

(5) Lu, X.; Sun, F.; Wang, J.; Zhong, J.; Dong, Q. Macromolecular Rapid Communications 2009, 30, DOI: 10.1002/marc.200900356.

(6) White, M. A.; Johnson, J. A.; Koberstein, J. T.; Turro, N. J. Journal of the American Chemical Society 2006, 128, 11356.

(7) Polito, L.; Monti, D.; Caneva, E.; Delnevo, E.; Russo, G.; Prosperi, D. Chem. Comm. 2008, 621.

(8) He, H.; Zhang, Y.; Gao, C.; Wua, J. Chem. Comm. 2009, 1655

(9) von Maltzahn, G.; Ren, Y.; Park, J.-H.; Min, D.-H.; Kotamraju, V. R.; Jayakumar, J.; Fogal, V.; Sailor, M. J.; Ruoslahti, E.; Bhatia, S. N. Bioconjugate Chemistry 2008, 19, 1570.

(10) Xie, J.; Chen, K.; Lee, H.-Y.; Xu, C.; Hsu, A. R.; Peng, S.; Chen, X.; Sun, S. Journal of the American Chemical Society 2008, 130, 7542.

(11) Hyeon, T.; Lee, S. S.; Park, J.; Chung, Y.; Na, H. B. Journal of the American Chemical Society 2001, 123, 12798.

(12) Wagner, C. D.; Davis, L. E.; Zeller, M. V.; Taylor, J. A.; Raymond, R. H.; Gale, L. H. Surface and Interface Analysis 1981, 3, 211.

Supporting Information

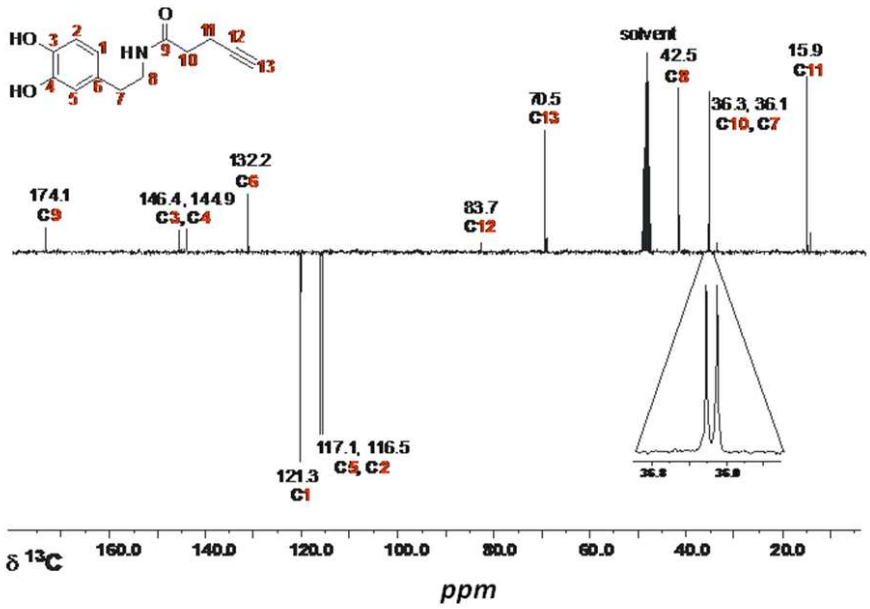

Figure S1. ^{13}C-APT NMR spectrum of Alkyne-Dopamine

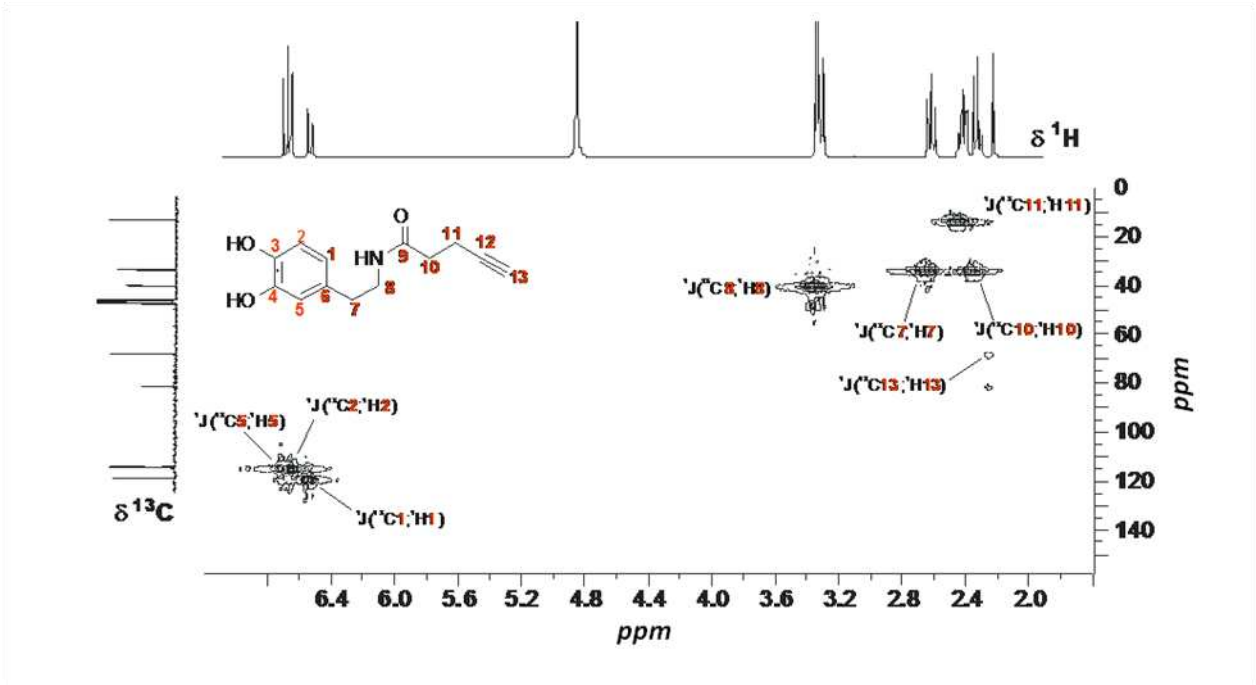

F*igure S2. gs-HSQC-^{1}H/^{13}C-NMR spectrum of Alkyne-Dopamine*

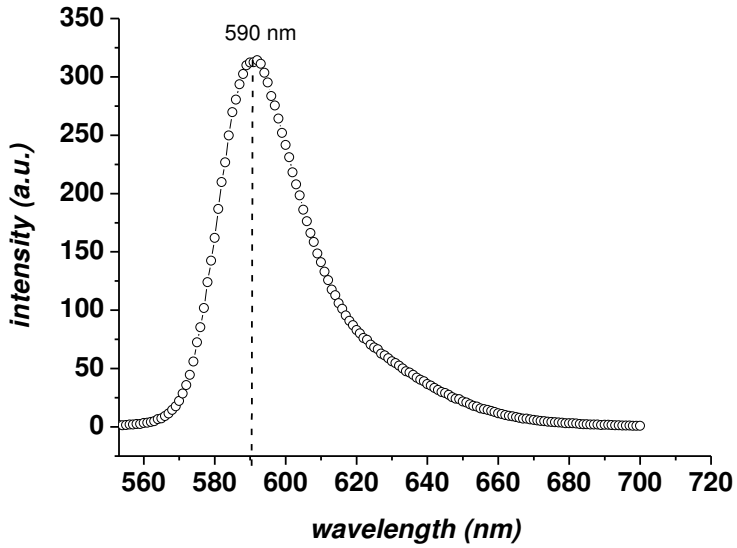

Figure S3. Fluorescence emission spectrum of N_3-Rhodamine dissolved in THF (excitation wavelength 543 nm)

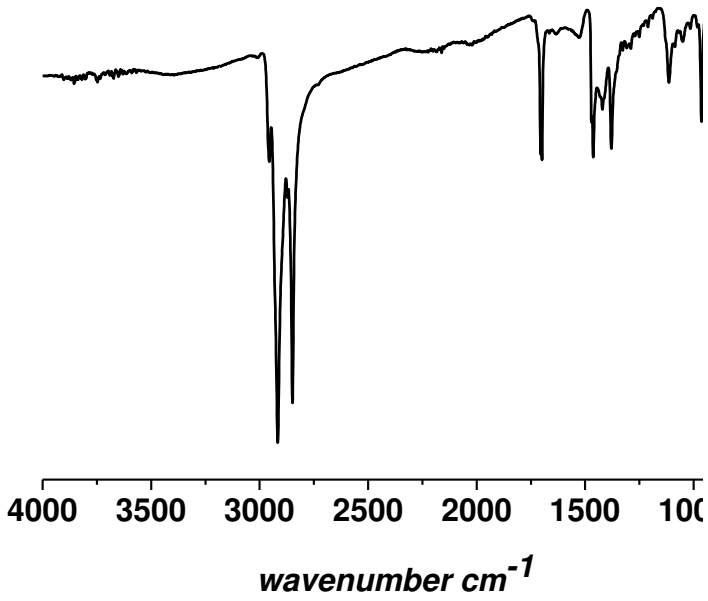

Figure S4. FT-IR spectrum of oleic acid stabilized Fe_3O_4 nanoparticles

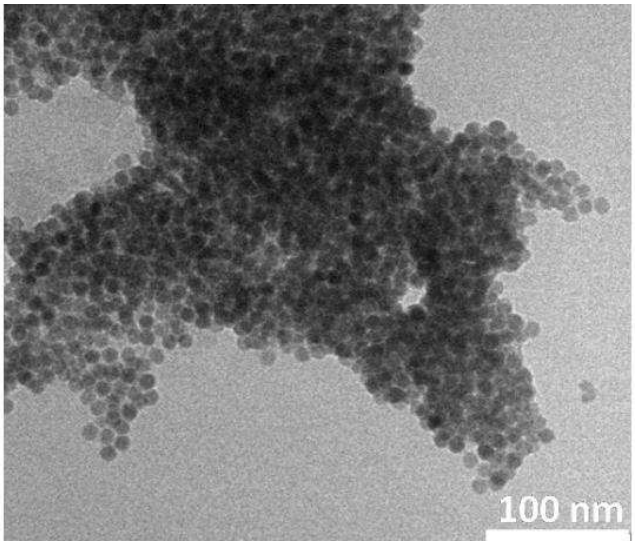

Figure S5. Reference reaction of non-click-functionalized Fe_3O_4 nanoparticles with N_3-PEG showing no PEG shell (in DMSO).

7.1. Synthesis of Cylindrical Polymer Brushes *via* Thiol-Ene Reaction from Poly(p-tert-butoxystyrene)-block-Polybutadiene Diblock Polymer

When a linear polymer is grafted with a large number of relatively short side-chains, cylindrical polymer brushes are formed.[1-3] Due to their anisotropic nature in topology, they have attracted more and more research interest in their synthesis, bulk, or solution properties, as well as in the applications of such polymers. They are also denoted as "bottle brushes" or "molecular brushes". Three main strategies have been successfully developed for the synthesis of CPBs: grafting through, grafting to, and grafting from. For instance, CPBs can be built by coupling reactions between the pre-formed endfunctional polymers and preformed multi-functionalized long backbones.[4-6] The advantage of this technique is that both backbone and side-chain can be well-defined since they are prepared separately. For example, Matyjaszewski et al. prepared both backbone and grafts by using atom transfer radical polymerizations (ATRP) and recently used click chemistry for the coupling reactions.[5] In this work, the diblock polymer poly(para-*tert*-butoxystyrene)-*block*-polybutadiene (ptSB), as backbone, is functionalized via thiol-ene reaction. The 1,2-polybutadiene units can directly be functionalized with low molecular weight thiol-compounds or thiol-endgroup functionalized polymers (e.g. SH-polyethylene glycol).

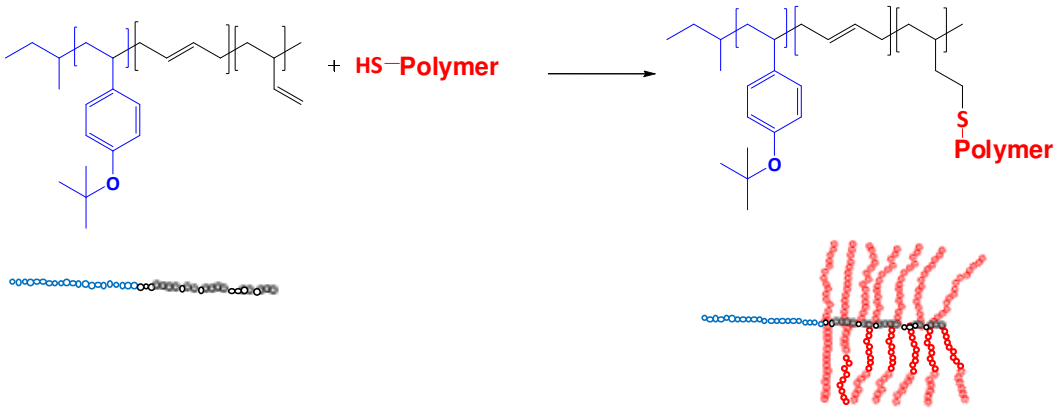

Scheme 7.1. Functionalization Strategy of poly(p-tert-butoxystyrene)-block-polybutadiene (ptSB) with Thiol-Ene Reaction

Methods

Size Exclusion Chromatography (SEC)

SEC measurements were performed at room temperature with PSS SDV Gel columns (30 × 8 mm, 5 µm particle diameter) with 10^2, 10^3, 10^4 and 10^5 Å pore diameter with a RI- and UV detector (λ = 254 nm). THF was used as elution solvent (flow rate 1.0 $mL \cdot min^{-1}$). All samples were filtered with a 0.2 µm PTFE Filter.

UV lamp

The UV lamp „HONLE UVAHAND 250“ (λ=250 nm) is used.

Transmission Electron Microscopy (TEM)

Transmission electron microscopy images were recorded in bright field mode with a Zeiss CEM 902 electron microscope operated at 80 kV and a LEO 922 OMEGA electron microscope operated at 200 kV. The polymer solutions were dip coated on a carbon-coated copper grid. Partially the grids were exposed to OsO_4 for preferential staining of the polybutadiene block (appears black). Data evaluation and processing was carried out with Soft Imaging Viewer, Digital Micrograph 365 Demo software and Image Tool.

Nuclear Magnetic Resonance (NMR)

^{1}H-NMR spectra were obtained with a Bruker „Bruker Ultrashield 300“ at an operating frequency of 300 MHz. Depending of the solubility of the sample deuterated chloroform ($CDCl_3$) or deuterated tetrahydrofuran (THF-d_8) was utilized.

FT-IR

IR spectra were recorded on a „Perkin Elmer Spectrum 100“ FT-IR spectrometer equipped with an ATR probe.

Dynamic Light Scattering (DLS)

For the determination of hydrodynamic radius DLS was performed on an ALV SLS/SLS-SP 5022F compact goniometer system with an ALV 5000/E correlator and a He-Ne laser (λ = 632.8 nm). Prior to the light scattering measurements (correlation times approximately 300 s

depending on signal strength) the sample solutions were filtered with filters with a pore size of 0.45 µm. The measured intensity correlation functions were subjected to CONTIN analysis.

Results and Discussions

Modification of polybutadiene and poly(p-tert-butoxystyrene)

The modification of the homopolymer polybutadiene was performed using the thiol-ene reaction. Therefore, thiol-endfunctionalized polyethylene glycol (SH-PEG) was used. Secondly, poly(para-*tert* butoxystyrene) was hydrolyzed with HCl. The hydrolyzed product was further click-functionalized by an esterification step.

Thiol-ene reaction of polybutadiene with SH-PEG (pB-g-PEG)

Figure 7.1 shows the thiol-ene reaction of polybutadiene with a 1,4-butadiene volume fraction of 77% and an 1,2 Polybutadiene fraction of 23% (M_w = 38.000 g mol^{-1}). SH-PEG was used to modify the polymer backbone. The synthesis of the cyclindrical polymer brush was carried out in THF and initiated with UV light.

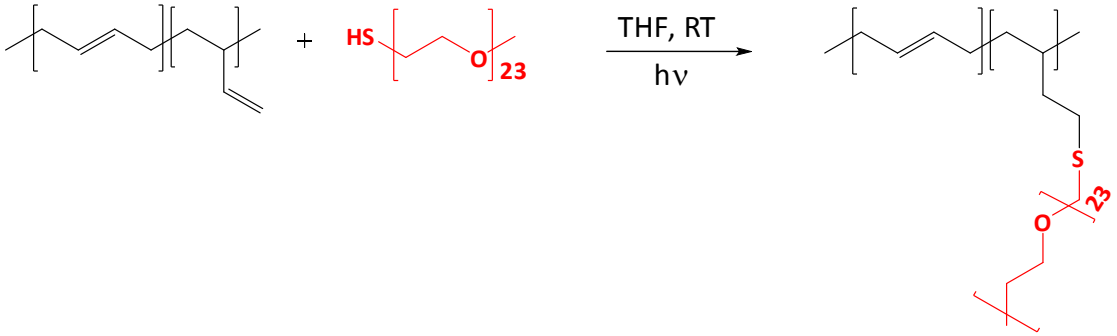

Figure 7.1. Scheme of UV initiated thiol-ene reaction of polybutadiene with SH-PEG.

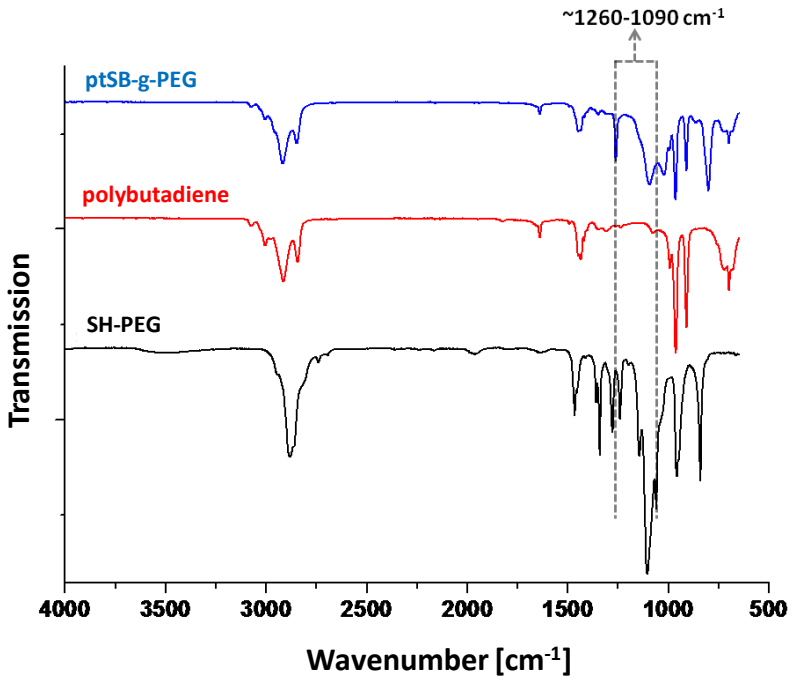

Figure 7.2. FT-IR-spectra of pB-g-PEG (blue), polybutadiene (red) and SH-PEG in THF: 1260-1050 cm^{-1} C-O-stretching vibration

The IR-spectrum of the thiol-ene product (pB-*g*-PEG) shows two additional characteristic peaks, 1260 cm^{-1} and 1090 cm^{-1}. These peaks present the C-O vibrations of the PEG unit which indicates the successful thiol-ene reaction. The observation was supported by the ^{1}H-NMR-Spectrum (Figure7.3.).

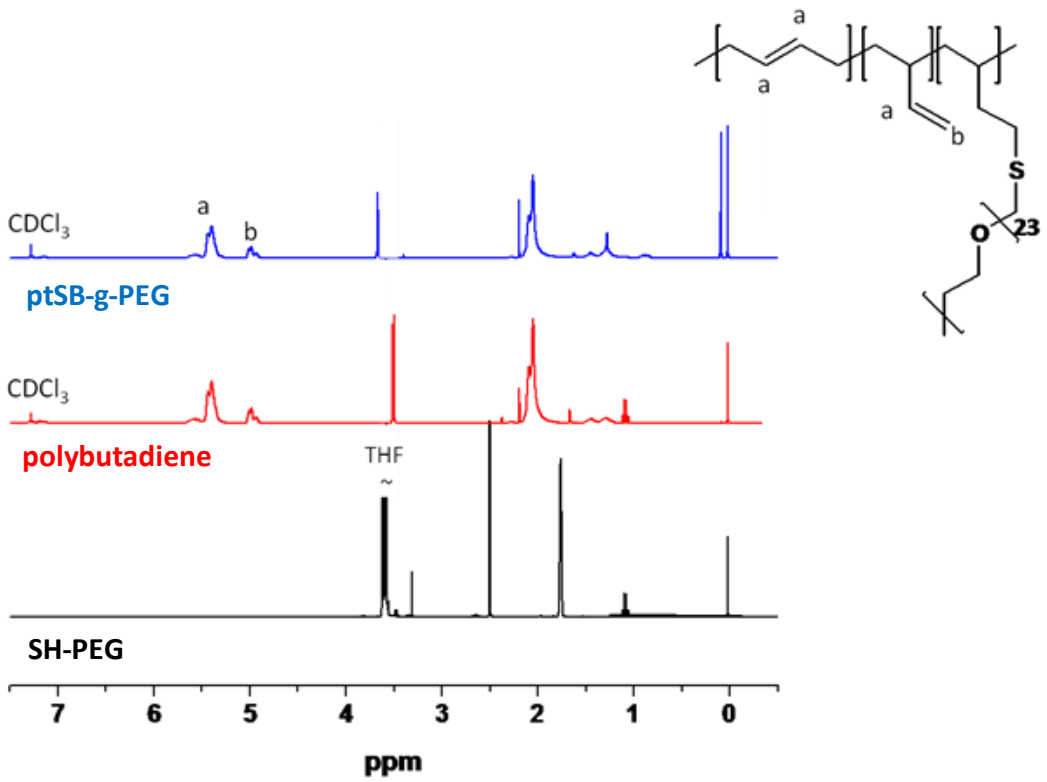

Figure 7.3. ^{1}H-NMR spectra of pB-g-PEG (blue) and polybutadiene (red) in $CDCl_3$. ^{1}H-NMR spectrum of SH-PEG (black) in THF-d_8: 5.3-5.7 ppm signal a, 5.0 ppm signal b.

The ^{1}H-NMR peaks can be assigned to the protons of the 1,4 polybutadiene in the range of 5.3-5.7 ppm, and the proton (signal a) of the 1,2 polybutadiene. Signal b corresponds to the two protons of 1,2 polybutadiene (5.0 ppm). The spectrum indicates that the protons of the 1,2 polybutadiene did not disappear completely which results in a partial functionalization. Integration of the areas of the characteristic polymer peaks gives information of the grafting density and therefore the approximate functionalization of the areas of signal a and b with 22%.

It has to be mentioned that the signal of 1,4 polybutadiene reduced as well which reveals that the thiol-ene reaction took place also at the 1,4 position of the polybutadiene.

Hydrolysis of Poly(p-tert-butoxystyrene)

Hydrolysis of poly(*p-tert*-butoxystyrene) (ptS) was carried out in 1.4-dioxane by addition of HCl at 120°C. ptS was synthesized via anionic polymerization at low temperatures with *tert*-butyllithium (Figure 7.4).

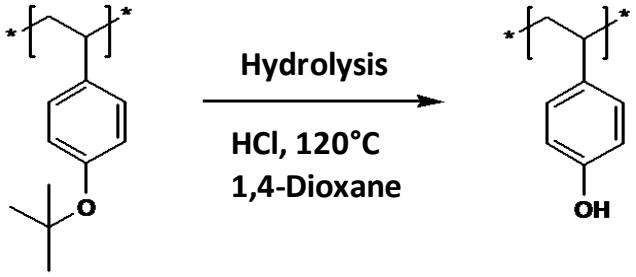

Figure 7.4. Reaction scheme for the hydrolysis of poly(p-tert-butoxystyrene)

The hydrolyzed ptS was characterized with FT-IR spectroscopy (Figure 7.5.). The vibration bond at 3335 cm^{-1} indicates the OH-stretch. The deformation peak of the C-O- group of the hydroxy group is found at 1160 cm^{-1}. These appearances and the diminuation of the signals of the *tert*-butoxy groups at 2980 cm^{-1}, 1450 cm^{-1} und 1367 cm^{-1} prove the successful hydrolysis.

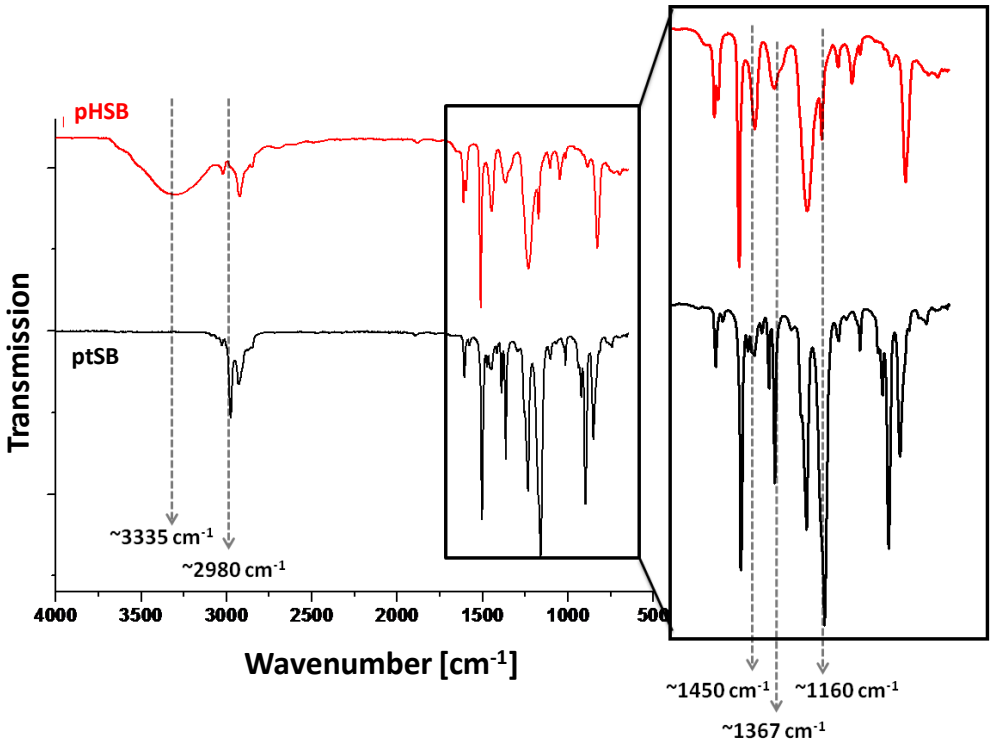

Figure 7.5. FT-IR-spectra (ATR) of the hydrolyzed polymer (pHS, red) and of poly(para-tert-butoxystyrene) (ptS, black) THF: 3335 cm^{-1} OH-stretching vibration, tert-butoxy groups: 2980 cm^{-1} CH_3-stretching vibration, 1450 cm^{-1} CH_3-stretching vibration, 1367 cm^{-1} CH_3-deformation vibration, 1160 cm^{-1} C-O-deformation vibration of the hydroxy groups.

With the integration of the areas of the OH-signal at 3335 cm^{-1} it is possible to determine the approximate yield of the reaction. This signal was chosen because it does not overlap with other vibration peaks. The calculation devotes a yield of 91%.

Poly(p-tert-butoxystyrene)-block-polybutadiene (ptSB)

In following section the thiol-ene reaction and the click chemistry (Huisgen [2+3] cycloaddition) were utilized for the functionalization of the diblockpolymer ptSB. For this reason cylindrical polymer brushes can be synthesized via modification of the polymer backbone ptSB. ptSB was synthesized via living anionic polymerization with sequential monomeraddition in THF. First of all, the molar and mass ratio of ptSB were calculated using ^{1}H NMR (Figure 7.6).

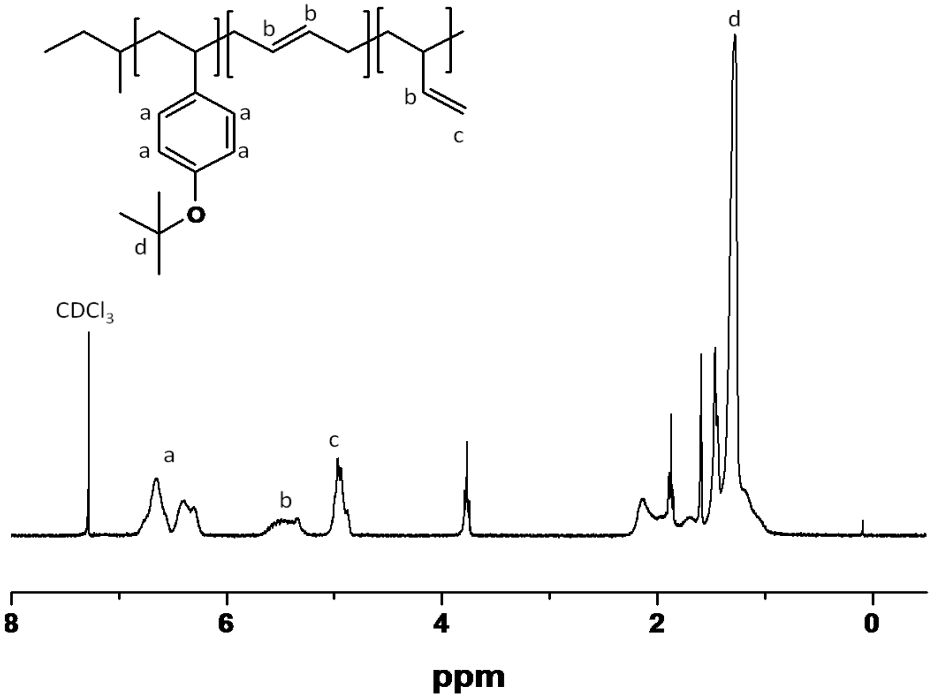

Figure 7.6. ^{1}H-NMR spectrum of ptSB in $CDCl_3$. Signal a shows the aromatic ring protons of the poly(tert-butoxystyrene) unit in the range of 6.3-6.8 ppm; signal b shows the protons of the 1,4-polybutadiene units and the protons of the 1,2-polybutadiene unit in the range of 5.3-5.7 ppm. Signal c correspond to the two protons of the 1,2-polybutadiene unit in the range of 4.8-5.1 ppm, Signal d: protons of the tert-butoxy unit at 1.2 ppm.

The molar and weight ratio of the polymer backbone ptSB were calculated:

Mol% of ptSB: $ptS_{47}B_{53}^{104}$ (104 is the molecular weight of ptSB (104.000 g·mol^{-1}) obtained from GPC measurements (Figure 7.7.) (wt% of ptSB: $ptS_{74}B_{26}$).

The SEC trace of ptSB is given in Figure 7.3. with a molar ratio of 104.000 g·mol^{-1} (PDI = 1.02).

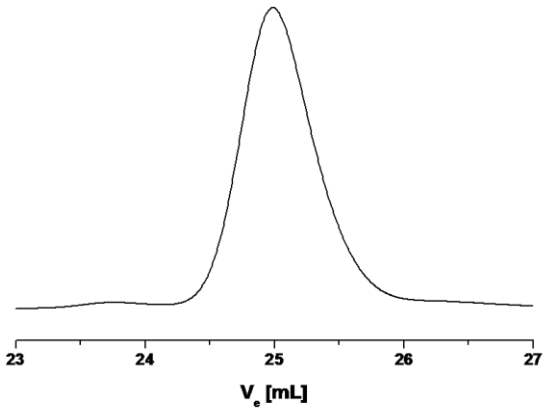

Figure 7.7. SEC trace of ptSB.

Thiol-ene reaction

Model reaction

First of all a modell reaction with a low molecular weight compound (1-dodecanethiol) was carried out (Figure 7.8.). The precursor ptSB was coupled with 1-dodecanethiol with AIBN as initiator and by UV irradiation.

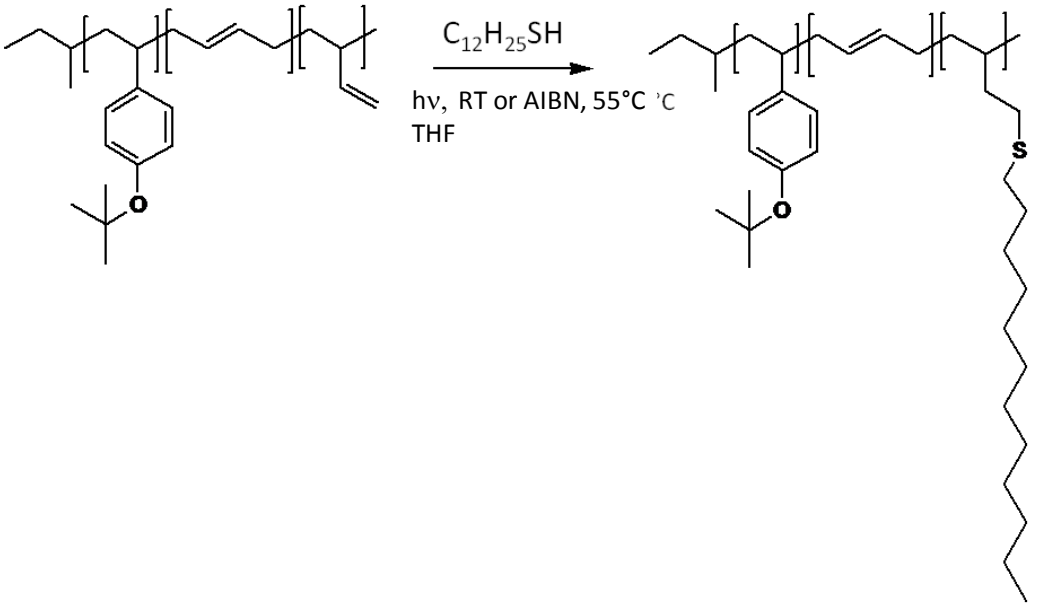

Figure 7.8. Thiol-ene reaction of ptSB with 1-dodecanethiol.

Figure 7.9. shows the IR spectra of the thiol-ene modified ptSB precursor initiated with UV light.

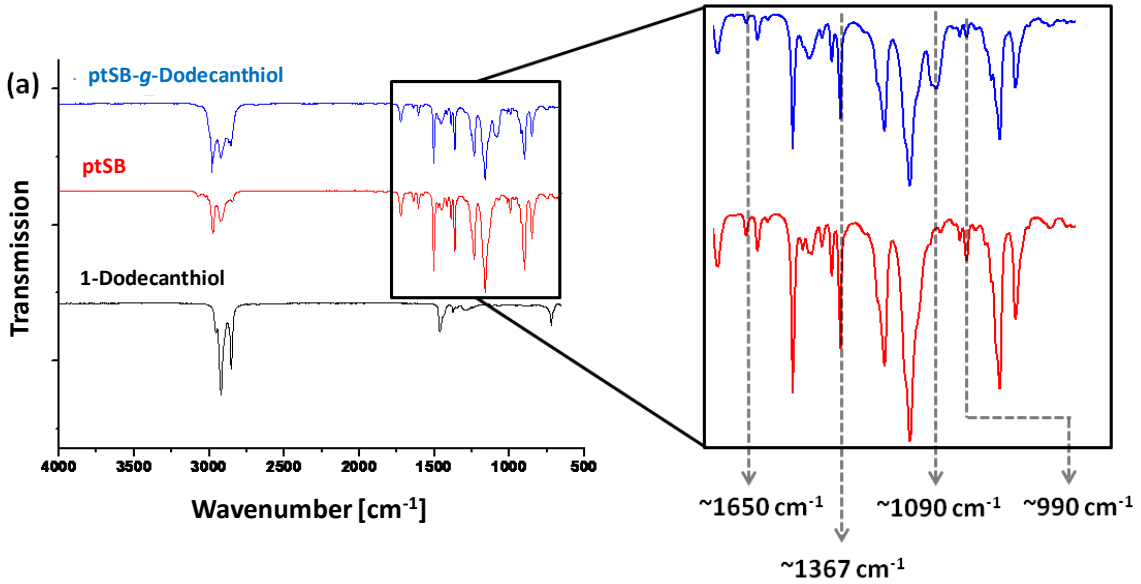

Figure 7.9. FT-IR spectra of UV initiated thiol-ene reaction with 1-dodecanethiol (THF) compared to ptSB and 1-dodecanethiol (THF): 1650 cm^{-1} C=C-stretching vibration, 1367 cm^{-1} tert-butoxystyrene, 1090 cm^{-1} C-C- vibration peak, 990 cm^{-1} C=C-deformation vibration.

The vibration peaks of the pB unit decrease (1650 cm^{-1} and 990 cm^{-1}). After reaction with UV light an additional peak appears which corresponds to the signals of the CH_2-groups of 1-dodecanethiol (1090 cm^{-1}). The signal at 1367 cm^{-1} can be assigned to the *tert*-butoxy unit of ptSB.

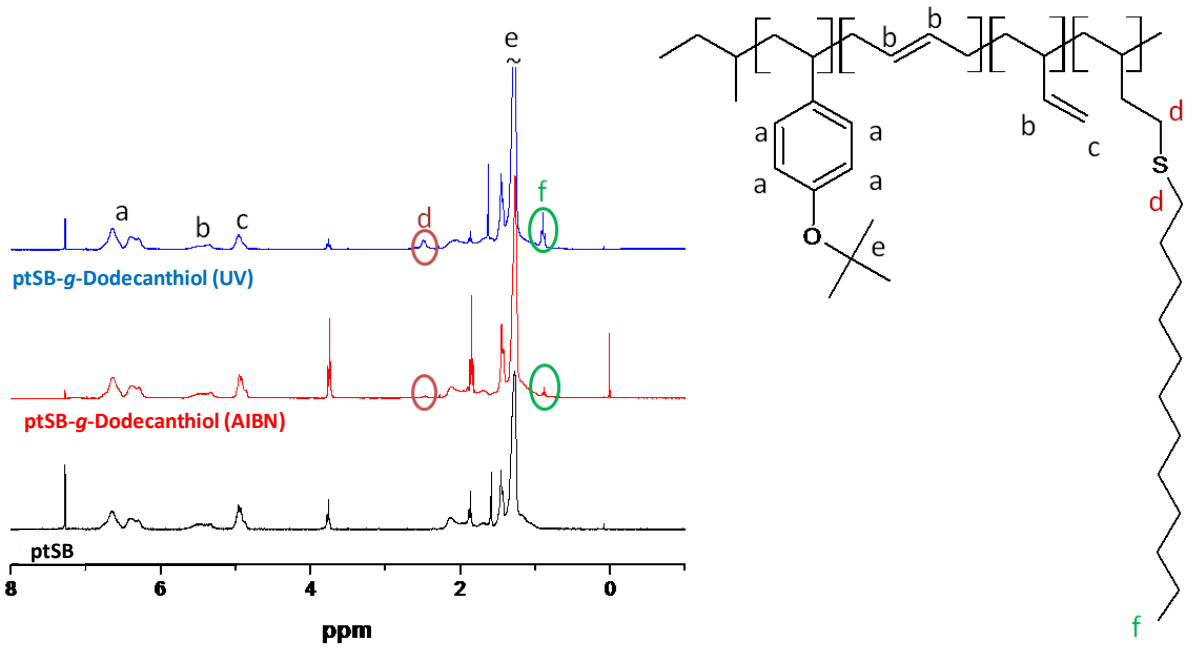

Figure 7.10. ^{1}H-NMR-spectrum of ptSB-g-Dodecanethiol, initiated with UV-lamp (blue), AIBN (red) and ptSB (black) in $CDCl_3$. 6.5 ppm signal a, 5.5 ppm signal b, 4.9 ppm signal c, 2.5 ppm signal d, 0.9 ppm signal e.

From the ^{1}H NMR spectrum can be seen that signals b and c of 1,2-polybutadiene did not diminish completely. Neither with AIBN nor UV lamp the reaction was complete. Nevertheless additional peaks appear after the thiol-ene reaction. Signal d (2.5 ppm) can be assigned to the protons next to the sulfur unit. The signal at 0.9 ppm corresponds to the protons of the methyl group of 1-dodecanethiol. It can be concluded that the UV initiated thiol-ene reaction is more efficient compared to the AIBN induced reaction. The integration of the signal peaks evokes following grafting densities: The grafting density for ptSB-*g*-dodecanethiol for the AIBN initiated reaction is 11%, for the UV initiated reaction 35%.

From the SEC traces can be seen that the molecular weights show for both reactions (UV induced and AIBN initiated reaction) a shift to higher molecular weight. Additionally, the shoulder at 23.5 mL increases. This peak results from the coupling product of the precursor which undergoes thiol-ene reaction as well.

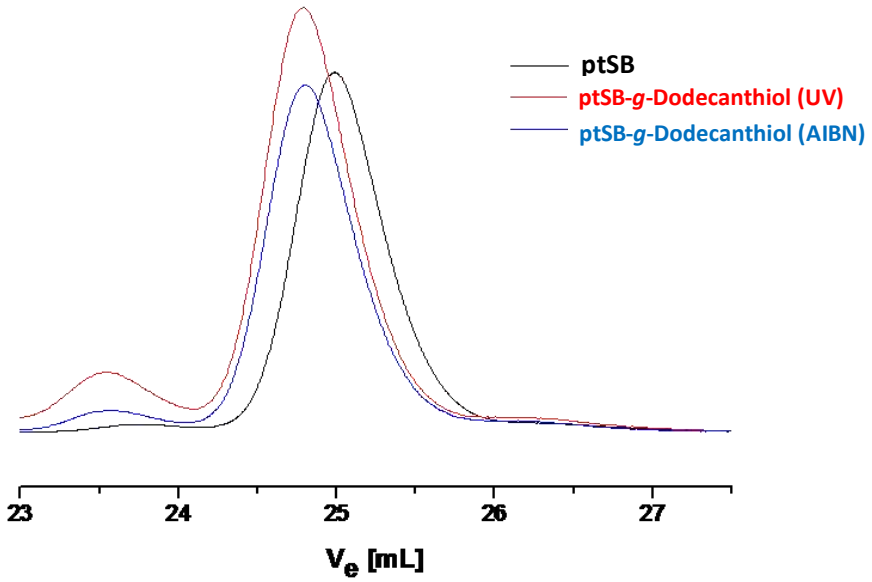

Figure 7.11. GPC traces of ptSB (black), UV initiated reaction (red) and AIBN-initiated reaction (blue)

As already evaluated from ^{1}H NMR spectra, the obtained conversion for UV induced reaction was 34%. From SEC measurements 13% of molecular weight increase was obtained. However, the change of solubility of the polymer plays a role for the elution in SEC measurements and therefore cannot be used as a satisfying method to determine the conversion. Nevertheless, IR spectra and ^{1}H NMR spectra can be drawn on the determination grafting densities or rather yields.

Thiol-ene Reaction of ptSB with SH-pNIPAAm$_{45}$ (ptSB-g-PNIPAAm$_{45}$)

Figure 7.12. displays the thiol-ene reaction with thiol-endfunctionalized poly-N-isopropylacrylamide (SH-pNIPAAm$_{45}$). The synthesis was conducted in 1,4-dioxane and initiated by UV light. After 24 hours the product was purified and analyzed with FT-IR spectroscopy and ^{1}H NMR.

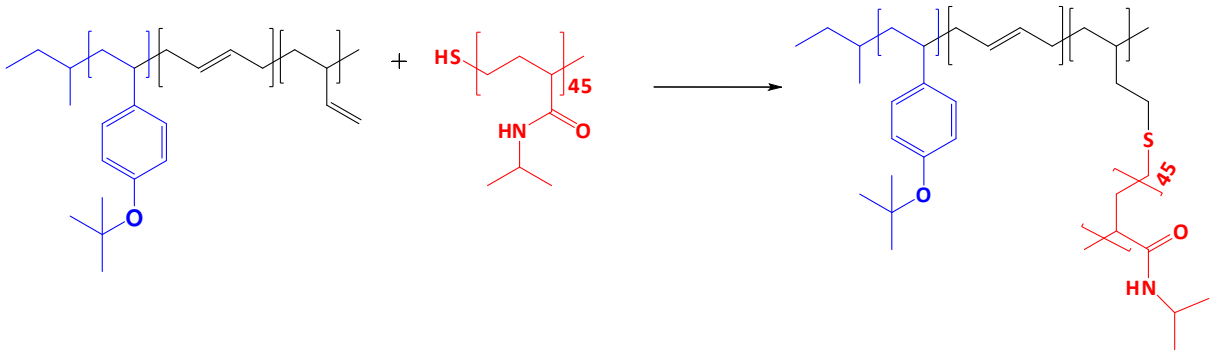

Figure 7.12. Scheme for thiol-ene coupling of ptSB with thiol-endfunctionalized pNIPAAm$_{45}$.

The IR spectrum of ptSB-*g*-PNIPAAm$_{45}$ (Figure 7.13.) shows clearly the N-H stretching vibration (3500-3300 cm^{-1}) of the pNIPAAm$_{45}$ side chains. The magnified region stresses the N-H deformation vibration at 1650-1540 cm^{-1} of the pNIPAAm$_{45}$ units. Furthermore the reduction of the deformation vibration of 1,2 polybutadiene units (990cm^{-1}) indicates the successful thiol-ene reaction.

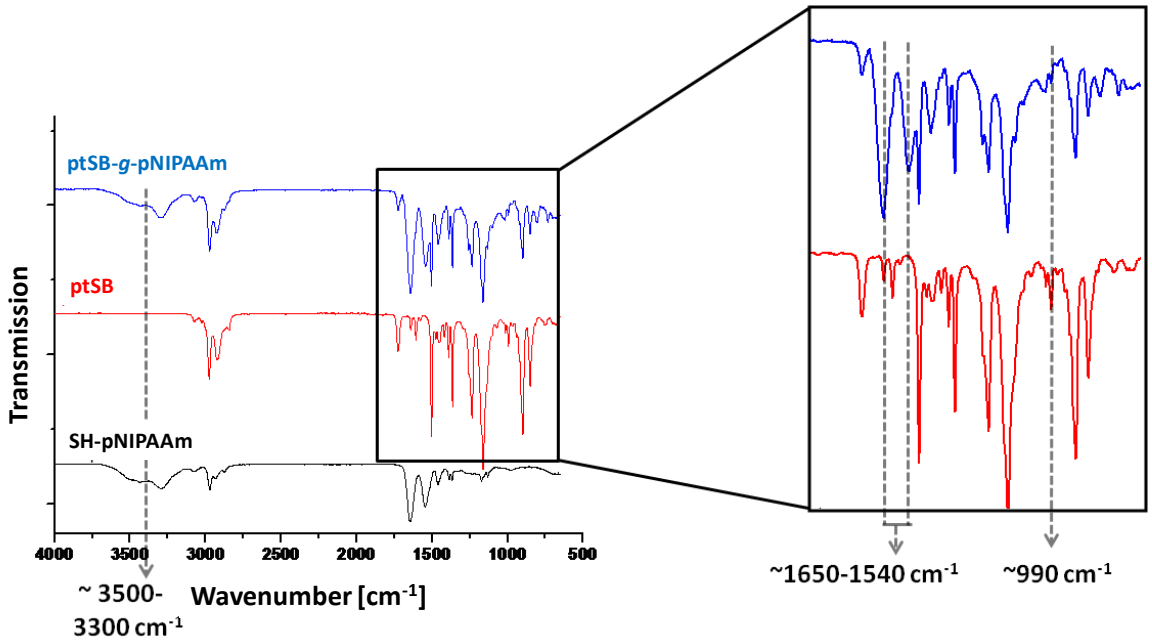

Figure 7.13. FT-IR-spectra of ptSB-*g*-PNIPAAm *(blue), ptSB (red) and SH-pNIPAAm (black) in THF. 3500-3300 cm^{-1} N-H-stretching vibration, 1650-1540 cm^{-1} N-H-deformation vibration, 990 cm^{-1}C=C-deformation vibration.*

The ^{1}H NMR gives information about the grafting density of the thiol-ene reaction with SH-pNIPAAm$_{45}$.

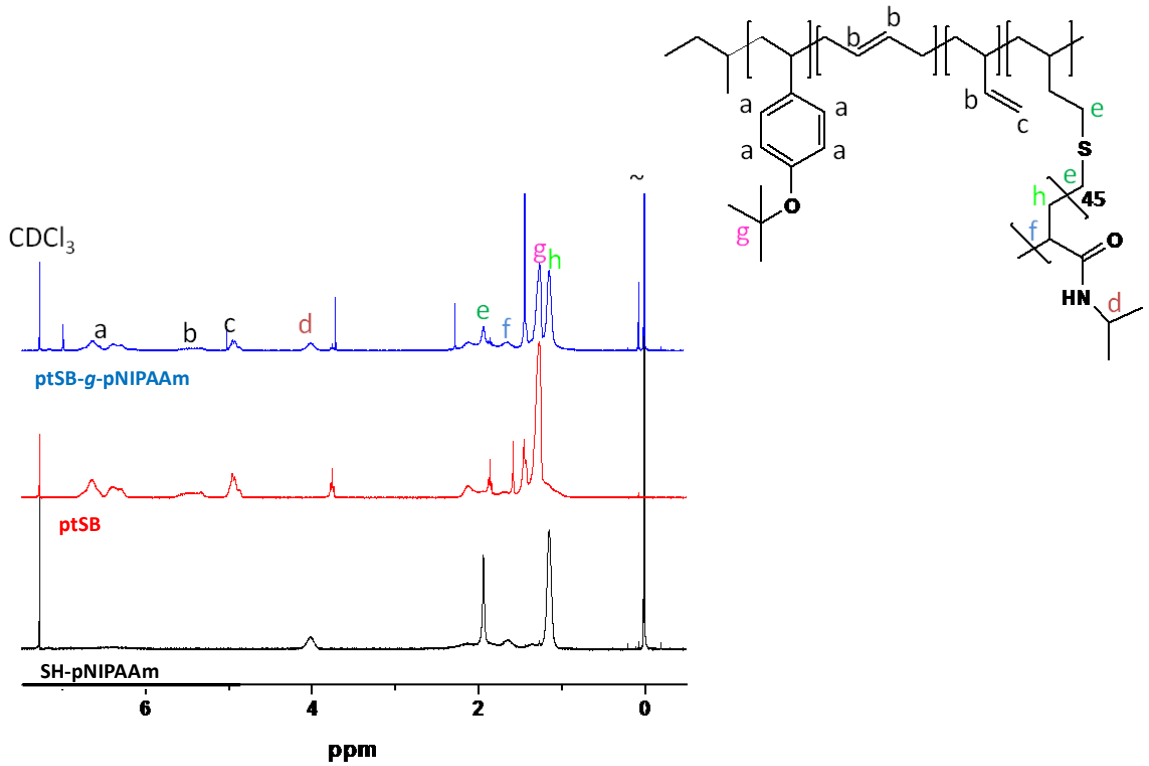

Figure 7.14. ^{1}H-NMR spectrum of ptSB-g-PNIPAAm (blue), ptSB (red) and SH-pNIPAAm (black) as reference (in $CDCl_3$). 6.5 ppm: a, 5.4 ppm: b, 4.9 ppm: c, 4.0 ppm: d, 1.9 ppm: e, 1.2 ppm: g, 1.1 ppm: h.

Signals b and c (5.4 ppm, 4.9 ppm) can be assigned to the protons of 1,2-polybutadiene. Signals at 4.0 ppm, 1.6 ppm and 1.1 ppm are signals of the $pNIPAAm_{45}$ block as marked in the ^{1}H NMR spectrum. Furthermore signal e derives from the protons adjacent to the sulfur group. The assignment of the signals allows the successful thiol-ene reaction of $pNIPAAm_{45}$ chains. Calculations of the peak areas of the ptSB-*g*-$pNIPAAm_{45}$ compared to the precursor ptSB gives an average grafting density of 57%.

TEM images of ptSB in THF show aggregates due to dewetting phenomenon after drying on a carbon-coated TEM grid. The light grey regions can be attributed to the poly(para-*tert*-butoxystyrene)-block whereaus the dark grey parts result from the polybutadiene block. ptSB-*g*-$pNIPAAm_{45}$ gives a different morphology (Figure 7.15).

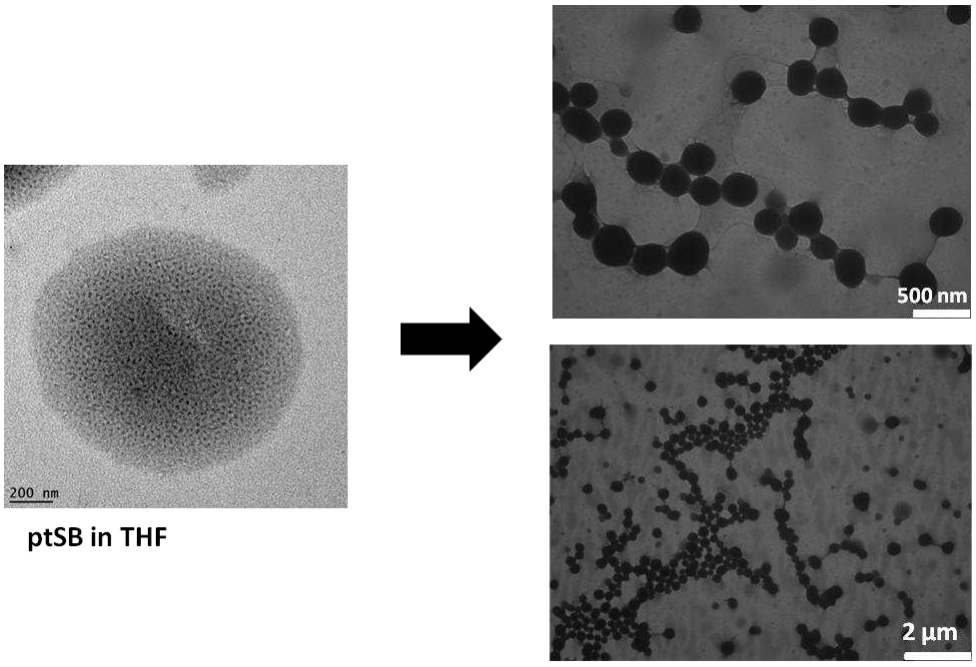

Figure 7.15. TEM images of ptSB in THF (left, stained with OsO_4) and ptSB-g-PNIPAAm$_{45}$ (right).

After thiol-ene reaction dark spherical aggregates are formed, possibly micelles, which are connected by bridges. The polymer was dissolved in DMSO which is a good solvent for both blocks and therefore it cannot be distinguished between the two blocks. DLS measurements (Figure 7.16.) show that these aggregates are present in solution (unweighted size distribution).

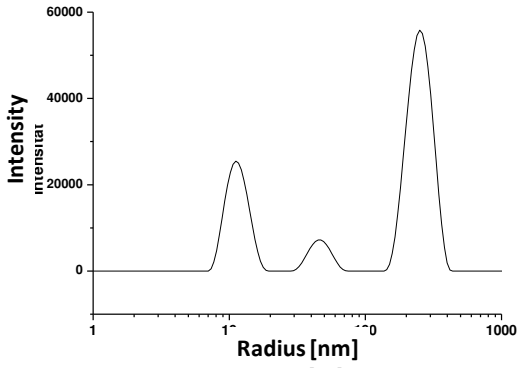

Figure 7.16. DLS measurement of ptSB-g-PNIPAAm$_{45}$

Thiol-Ene reaction with SH-PEG (ptSB-g-PEG)

In a second step, ptSB was modified with SH-endgroup modified poly(ethylene glycol). The reaction was started with UV light in 1,4-dioxane.

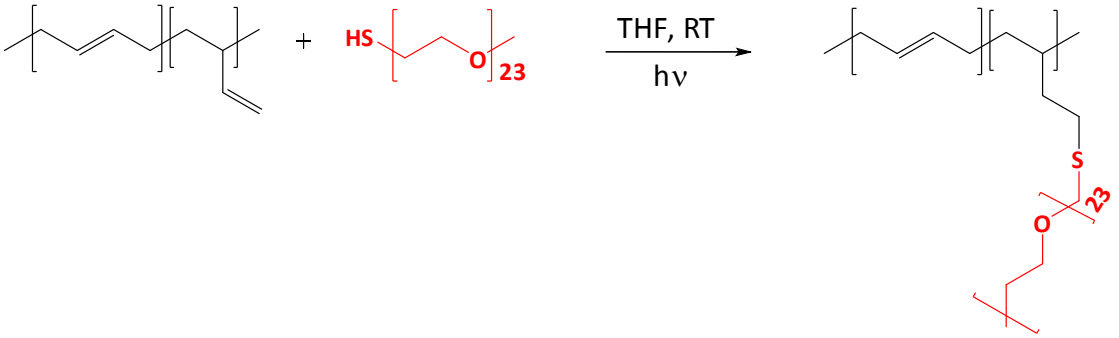

Figure 7.17. Thiol-ene functionaliziation of ptSB with SH-PEG (ptSB-g-PEG)

Here, FT-IR and ^{1}H NMR was carried out to demonstrate the sidechain functionalization.

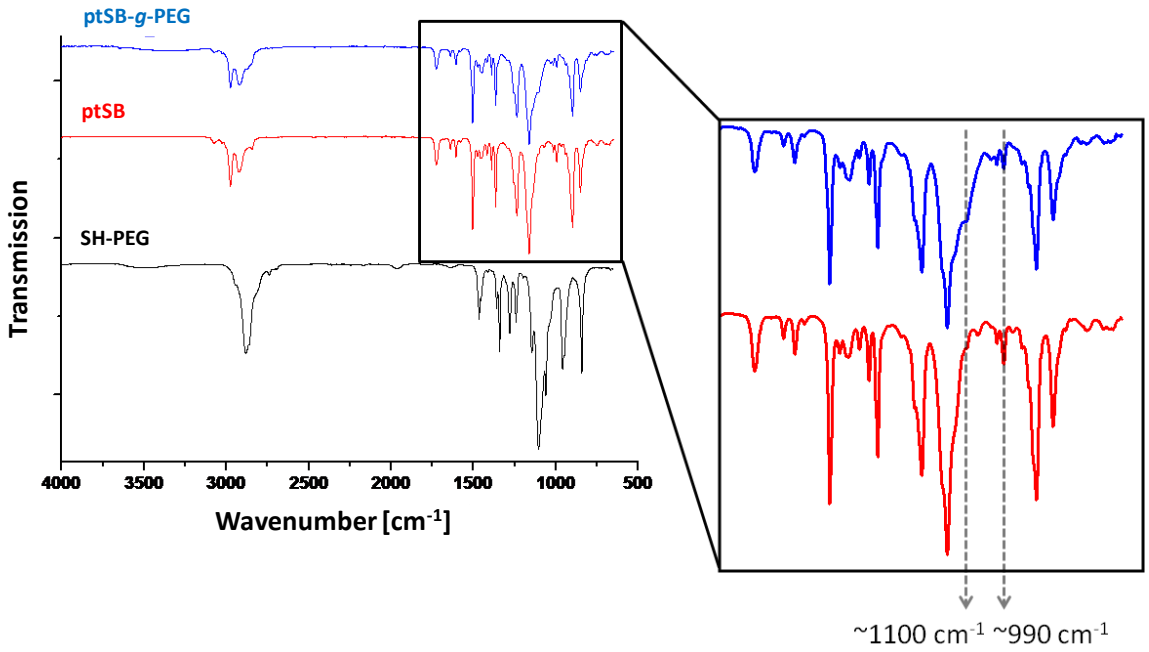

Figure 7.18. FT-IR-spectra of ptSB-g-PEG (blue), ptSB (red) and SH-PEG (black) in THF. 1100 cm^{-1} C-O-stretching vibration, 990 cm^{-1} C=C-deformation vibration.

The FT-IR spectrum of ptSB-*g*-PEG shows characteristic PEG bonds: 1100 cm^{-1} indicates the C-O-stretching vibration and the deformation vibration at 990 cm^{-1} of the double bonds which diminished nearly complete.

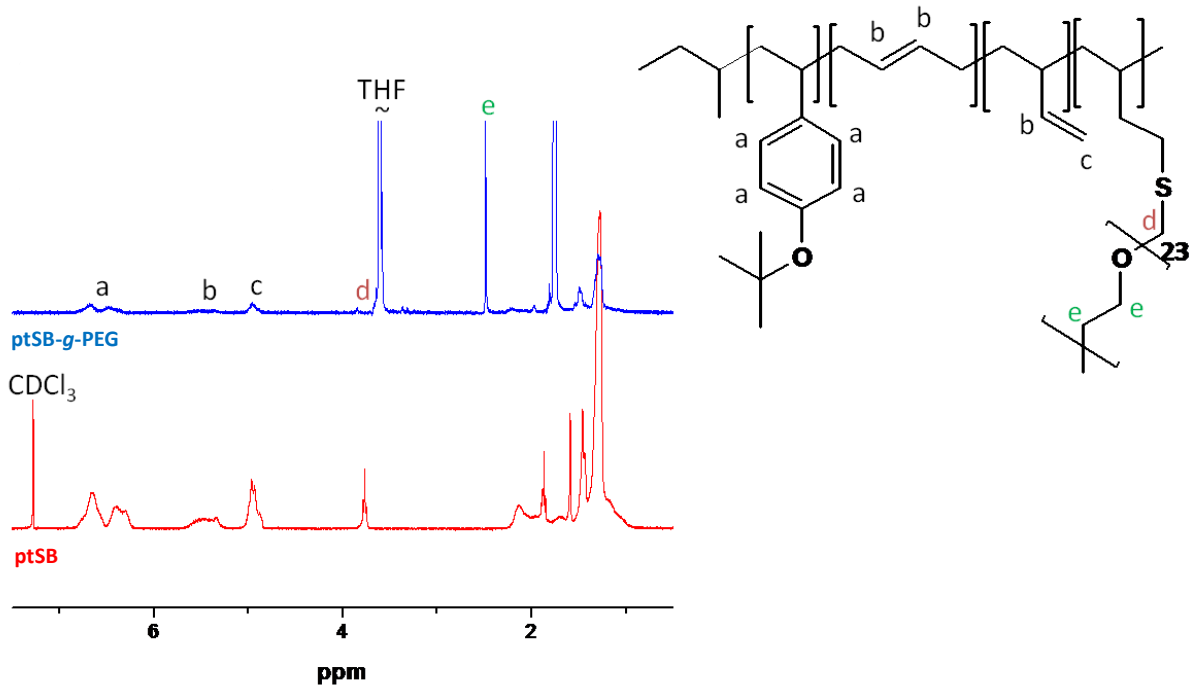

Figure 7.19. ^{1}H-NMR spectra of ptSB-g-PEG in THF-d_8 and ptSB (red) in $CDCl_3$. 6.5 ppm signal a, 5.4 ppm signal b, 4.9 ppm signal c, 3.64 ppm signal d, 2.48 ppm signal e.

It can be seen that signals b and c, which can be attributed to 1,2 polybutadiene unit are still present after reaction. Nevertheless signal e (2.48 ppm) can be assigned to the poly(ethylene glycol) unit (Signal d of the thioether bond (3.64 ppm) overlaps with the solvent peak). From the decrease of signals b and c a grafting density of 79% can be calculated.

Summary and Outlook

Cylindrical structures with a linear backbone and grafted side-chains were made via thiol-ene reaction. For this approach the backbone polymer poly(para-*tert*-butoxystyrene)-*block*-polybutadiene was used. The model reactions with low-molecular 1-dodecanethiol showed, that the thiol-ene reaction is most effective at room temperature and under UV irradiation. The synthesis of the brushes *via* thiol-ene reaction was performed with a polybutadiene-backbone and thiol-endfunctionalized pNIPAAm. A grafting density of 57 % was gained. Another modification was made with thiol-endfunctionalized poly(ethylene glycol) and a grafting density of 79 % was achieved. These experiments provide an evidence for the successful grafting of side-chains.

To obtain both side modified, Janus structured, cylindrical polymer brushes, the second block poly(*tert.*-butoxy styrene) can be hydrolyzed and further functionalized e.g. with a click-functionality.

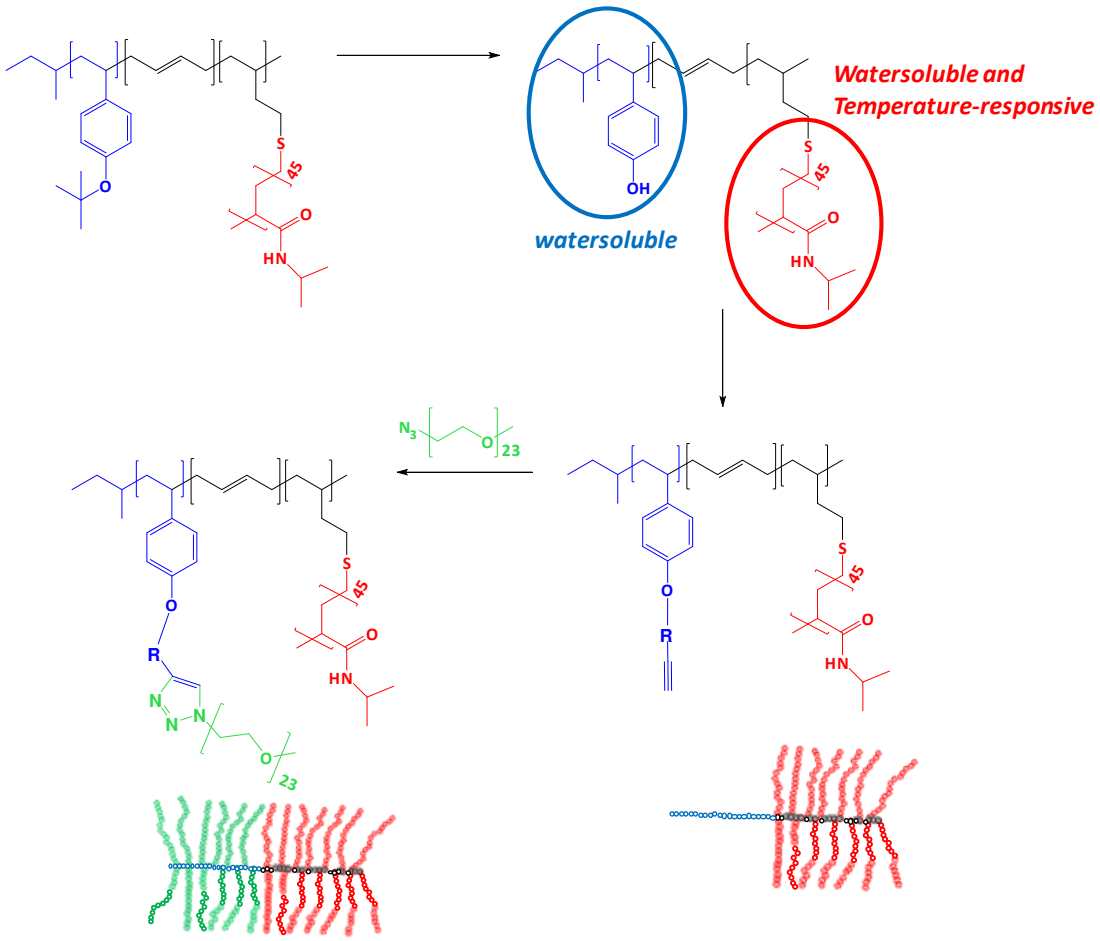

Figure 7.21. Schematic representation of the synthesis of cylindrical polymer brushes via thiol-ene reaction and Huisgen [2+3] cycloaddition

A second method is to hydrolyze the thiol-ene reaction product with pNIPAAm side-chains. Here, water-soluble cylindrical brushes could be achieved, because of the water-soluble polyhydroxystyrene-block and pNIPAAm sidechains. Furthermore, this polymer could also be functionalized to undergo the click reaction. This route also leads to cylindrical polymer brushes with AB-Janus structure (Figure 7.21.).

Advantage of the click chemistry and thiol-ene approach is the synthesis and characterization of well-defined side-chains and backbones before the coupling. On the contrary, the “grafting through” method often does not lead to a complete conversion of the macromonomer, consequently the side-chain length varies. In addition the results of the grafting density are comparable with “grafting from” methods. Therefore, the “grafting onto” method is an alternative technique to the “grafting from” method and can be assigned

to the synthesis of Janus cylindrical polymer brushes. The properties of these new structures will be analyzed in further reports.

Experimental Section

Materials

1-dodecanethiol (purum ≥ 97 %, Fluka), thiol-endfunctionalized poly-N-isopropylacrylamide (SH-PNIPAAm$_{45}$)[7], thiol-endfunctionalized polyethylenglycol (SH-PEG, creative PEGWorks, M_w = 1000 g·mol^{-1}), azide-endfunctionalized polyethylenglycol (creative PEGWorks, M_w = 1000 g·mol^{-1}), 2,6-Di-*tert*-butyl-*p*-kresol (purum > 99 %, Fulka), 4-dimethylaminopyridin (99 %, Aldrich), N-3-Dimethylaminopropyl-N'-ethylcarbodiimidhydrochloride (SigmaUltra), copper(I)bromide (Aldrich), Bis(2-dimethylaminoethyl)methylamine (Aldrich), 4-pentynoic acid (Aldrich), acetone (p.a., VWR), tetrahydrofurane (p.a., Sigma-Aldrich), 1,4-dioxane (p.a., Fisher Scientific), hydrochloric acid (32 %, Riedel de Haën), AIBN was recrystallized from methanol, dialysis tubes (SpectrumLabs, regenerated cellulose) MWCO: 1000 Da, 3500 Da and 8000 Da (depending on the sample).

Synthesis

Thiol-ene reaction of SH-PEG and polybutadiene

100 mg of polybutadiene (M_n = 38.000 g·mol^{-1}) was dissolved in 40 mL THF. The solution was purged with nitrogen for 30 min and 1.32·10^{-5} mol of SH-PEG (M_w = 1000 g·mol^{-1}) were added under nitrogen. The reaction was started with an UV lamp and reacted for 24 h. The solution was dialysed for 5 d against THF (MWCO 3500) and afterwards dried under vacuum.

Hydrolysis of poly(p-tert-butoxystyrene)

500 mg of poly(*p-tert*-butoxystyrene) was dissolved in 100 mL of 1,4-dioxane. 1 mL of HCl was added dropwise under stirring and stirred for 24 h at 120°C under reflux. The solution was concentrated and precipitated in water. The polymer was dried under vacuum.

Thiol-en reaction of poly(p-tert-butoxystyrene)-*block*-polybutadiene

Model reaction

1 g of the diblock polymer poly(*p-tert*-butoxystyrene)-*block*-polybutadiene was dissolved in 25 mL THF. Afterwards 1-dodecanethiol was added in a five-fold molar excess. The solution was degassed with argon for 20 min at room temperature or started with a three-fold molar excess of AIBN. For kinetic studies samples have been taken at certain time intervals. After 24 h the reaction was stopped by switching off the UV lamp or cooling down to room temperature. The solution was dialysed for three days against THF (MWCO 1000).

Thiol-en reaction of poly(p-tert-butoxystyrene)-*block*-polybutadiene with SH-PNIPAAm$_{45}$

14 mg of ptSB (M_n = 104.000 g·mol^{-1}) was dissolved in 5 mL of 1,4-dioxane. The solution was degassed for 20 min with argon and SH-pNIPAAm$_{45}$ (M_w = 5092 g·mol^{-1}) (five-fold excess with respect to ptSB) was added under argon. The reaction was started with an UV-lamp and stirred for 24h at room temperature. The reaction was stopped and dialysed against THF (MWCO 8000) for four days.

Thiol-en reaction of SH-PEG with ptSB

54 mg of ptSB (M_n = 104.000 g·mol^{-1}) was dissolved in 20 mL of 1,4-dioxane. The solution was degassed for 20 min with argon and SH-PEG (M_w = 1000 g·mol^{-1}) (5-fold excess with

respect to ptSB) was added under argon. The reaction was started with an UV-lamp and stirred for 24 h at room temperature. The reaction was stopped and dialysed against THF (MWCO 3500) for four days.

7.2. Appendix to Chapter VI

Alternative synthesis of Fe_3O_4 magnetic nanoparticles

Fe_3O_4 magnetic nanoparticles were prepared according to the publication described by Wan et al.[8] $Fe(acac)_3$ (1 mmol) and triethylene glycol (TREG, 30 mL, 99%) were mixed and slowly heated to reflux(～278 °C) and kept at reflux for 30 min under argon protection giving a black homogeneous colloidal suspension. After cooling down to room temperature, 20 mL of ethyl acetate was added to the reaction solution resulted in a black precipitation of magnetite nanoparticles which was then separated from the solution by a magnetic field. After washing with ethyl acetate, the particle solution was dialysed against water for 3-5 days. The Fe_3O_4 particles were obtained by freeze drying.

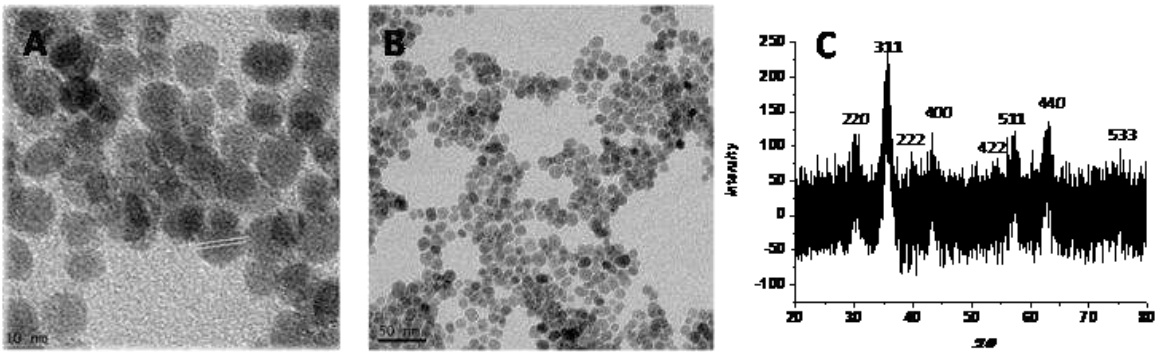

Figure 7.22. A and B: Monodisperse magnetite Fe_3O_4 nanoparticles via polyol approach. C: X Ray Diffraction of Fe_3O_4 nanoparticles synthesized via the polyol process.

Figure 7.22. shows a representative TEM image of the magnetite Fe_3O_4 nanoparticles. The synthesized nanoparticles, stabilized with tetramethylammonium hydroxide solution, are uniform in size and non-aggregated, which are in the range of 8-10 nm, which is in the superparamagnetic size range. X-ray diffraction (XRD) analysis supports that the nanoparticles are highly crystalline magnetite NPs.

Synthesis of Hydrophilic Fe_3O_4 Nanoparticles

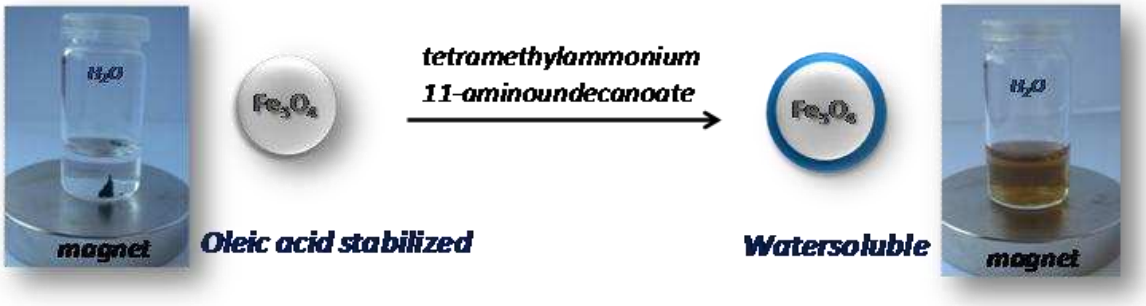

Water-soluble Fe_3O_4 nanoparticles were prepared according to the publication of Li et al.[9] Under ambient conditions, tetramethylammonium 11-aminoundecanoate (about 60 mg) was added to a hexane dispersion of oleic acid stabilized Fe_3O_4 nanoparticles (about 40 mg in 0.4 mL) in hexane. The mixture was shaken over night, during which time the particles precipitated and separated using a magnet. The precipitate was washed with dichloromethane and separated again using a magnet to remove excess surfactants before drying under N_2. The product was then dispersed in deionized water at neutral pH.

Synthesis of Silica-Coated Fe_3O_4 Nanoparticles

Hexane dispersed particles were dialysed against cyclohexane. 8.75 g of Igepal CO-520 (Polyoxyethylene (5) nonylphenylether, branched) was added to 120 mL of cyclohexane and subjected to ultrasonic treatment for 15 min. Then, 1 mL of Fe3O4 solution in cyclohexane (5 mg/mL) was added to the Igepal solution. After the mixture had been stirred for 3 h, 0.88 mL of ammonia solution (25%) was added. Finally, 0.6 mL of TEOS was added, and the mixture was allowed to age for 72 h for hydrolysis and condensation of the silica precursor. When methanol was added into the reaction solution, Fe_3O_4@SiO_2 nanoparticles were precipitated. They were collected by both magnetic separation and centrifugation, washed with methanol, and re-dispersed in ethanol.

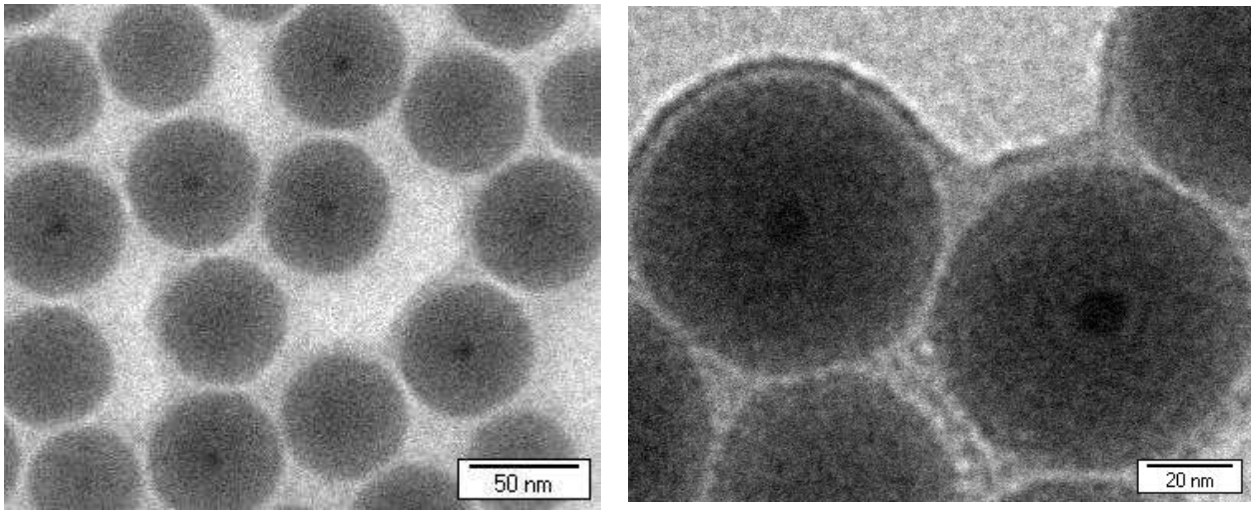

Figure 7.23. TEM images of Silica-coated iron oxide nanoparticles

Synthesis of N_3-coumarin

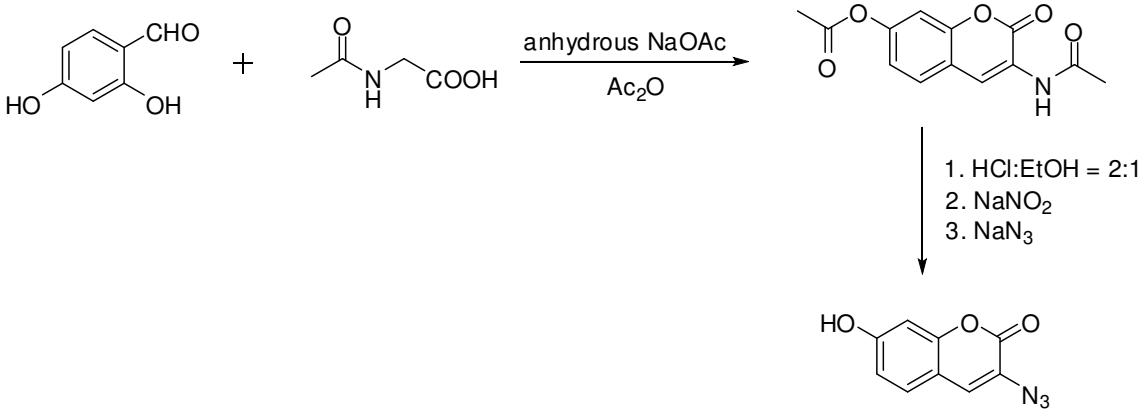

N_3-coumarin was synthesized according to the procedure described by Sivakumar et al.[8] A mixture of 2,4-dihydroxy benzaldehyde (5.52 g, 0.04 mol), *N*-acetylglycine (4.68 g, 0.04 mol), anhydrous sodium acetate (9.96 g, 0.12 mol) in acetic anhydride (200 mL) was refluxed under stirring for 7h. The reaction mixture was poured onto ice to give a yellow precipitate. After filtration, the yellow solid was washed with ice water before it was refluxed in a solution of concentrated HCl and ethanol (2:1, 60 ml) for 1.5 h, then ice water (80 mL) was added to dilute the solution. The solution was then cooled in an ice bath and $NaNO_2$ (5.52 g, 0.08 mol) was added. The mixture was stirred for 15 minutes and NaN_3 (7.8 g, 0.12 mol) was added in portions. After stirring for another 30 minutes, the resulting precipitate was filtered off, washed with water, and dried under reduced pressure to afford a brown solid (0.37 g, 4.5% overall yield).

^{1}H-NMR (DMSO-d_6, 300 MHz) δ 6.75 (d, J = 2.1 Hz, 1H), 6.80 (dd, J = 8.5, 2.1 Hz, 1H), 7.47 (d, J = 8.5 Hz, 1H), 7.58 (s, 1H), 10.51 (s, 1H). ^{13}C NMR (DMSO-d_6, 300 MHz) δ 102.2, 111.3, 113.8, 121.1, 127.8, 129.1, 152.8, 157.3, 160.3. Mass spectrometric analysis m/e calculated for M^+ $C_9H_5N_3O_3$ 203.03; found 203.

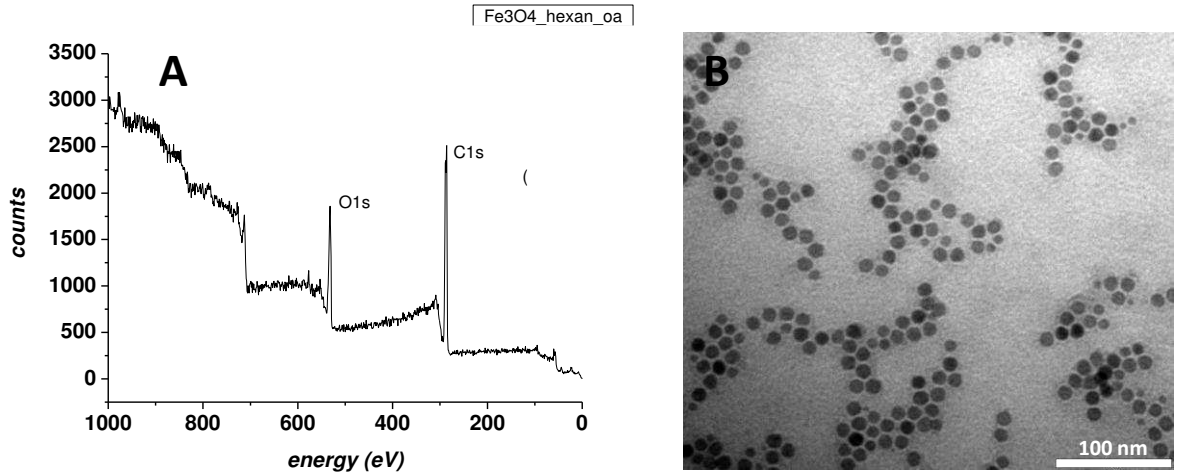

Figure 7.24. A) XPS measurement from blank oleic acid stabilized Fe_3O_4 nanoparticles; B) TEM image of alkyne-modified Fe_3O_4 nanoparticles

Synthesis of azido-fluorogenic compound 4-Azido-N-ethyl-1,8-naphthalimide

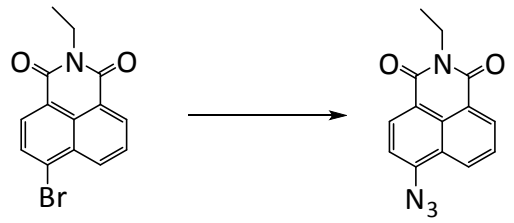

The synthesis was adopted to the publication described by Sawa et al.[10]

A mixture of 4-bromo-N-ethyl-1,8-naphthalimide (912 mg, 3.0 mmol) and sodium azide (975 mg, 15 mmol) in 12 ml of N-methylpyrrolidinone was stirred at 110° C for 1 h. The reaction mixture was diluted with water and extracted with ethyl acetate. The organic layer was washed with brine, dried over Na_2SO_4, and evaporated. The residue was purified by flash column chromatography on silica gel (ethyl acetate/hexane 1:5 → 1:3) to afford 4-Azido-N-ethyl-1,8-naphthalimide as a yellow solid (540 mg, 68%);

^{1}H-NMR (500 MHz, $CDCl_3$) δ 1.33 (t, 3H, J = 6.9 Hz), 4.24 (q, 2H, J = 6.9 Hz), 7.47 (d, 1H, J = 8.3 Hz), 7.75 (m, 1H), 8.44 (d, 1H, J = 8.3 Hz), 8.59 (d, 1H, J = 7.8 Hz), 8.65 (d, 1H, J = 7.3 Hz); Mass analysis: $M_{theor.}$ = 266.08 g mol^{-1}, $M_{exp.=}$ 266 m/z

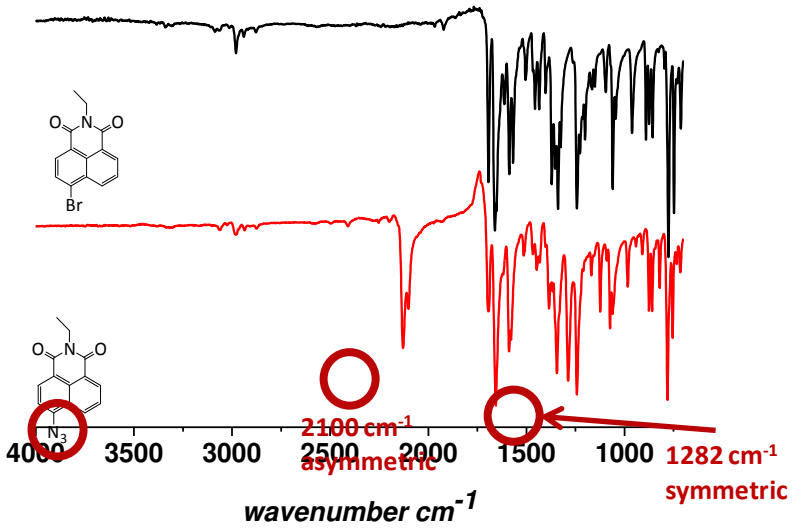

Figure 7.25. FT-IR spectra of of 4-bromo-N-ethyl-1,8-naphthalimide and 4-azido-N-ethyl-1,8-naphthalimide (2100 cm^{-1} asymmetric azide bond, 1282 cm^{-1} symmetric azide bond)

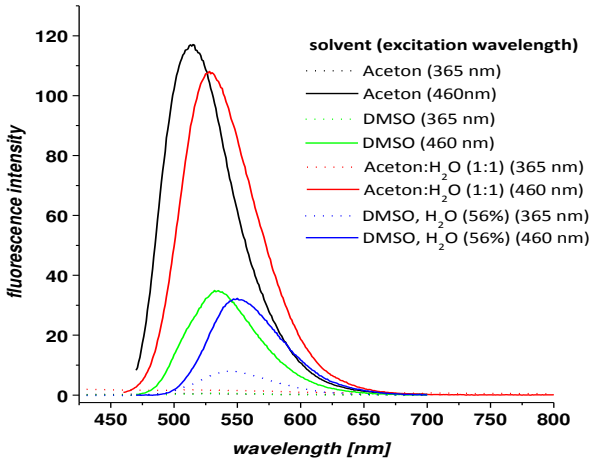

Figure 7.26. Fluorescence analysis of the N_3-fluorogenic compound (4-Azido-N-ethyl-1,8 naphthalimid) in different solvents indicates that a excitation wavelength of 460 nm leads to an emission peak at ~530 nm. The excitation wavelength of 365 nm entails no or very little emission in the same region.

Synthesis of fluorescent magnetic iron oxide nanoparticles with fluorogenic compound 4-Azido-N-ethyl-1,8-naphthalimide

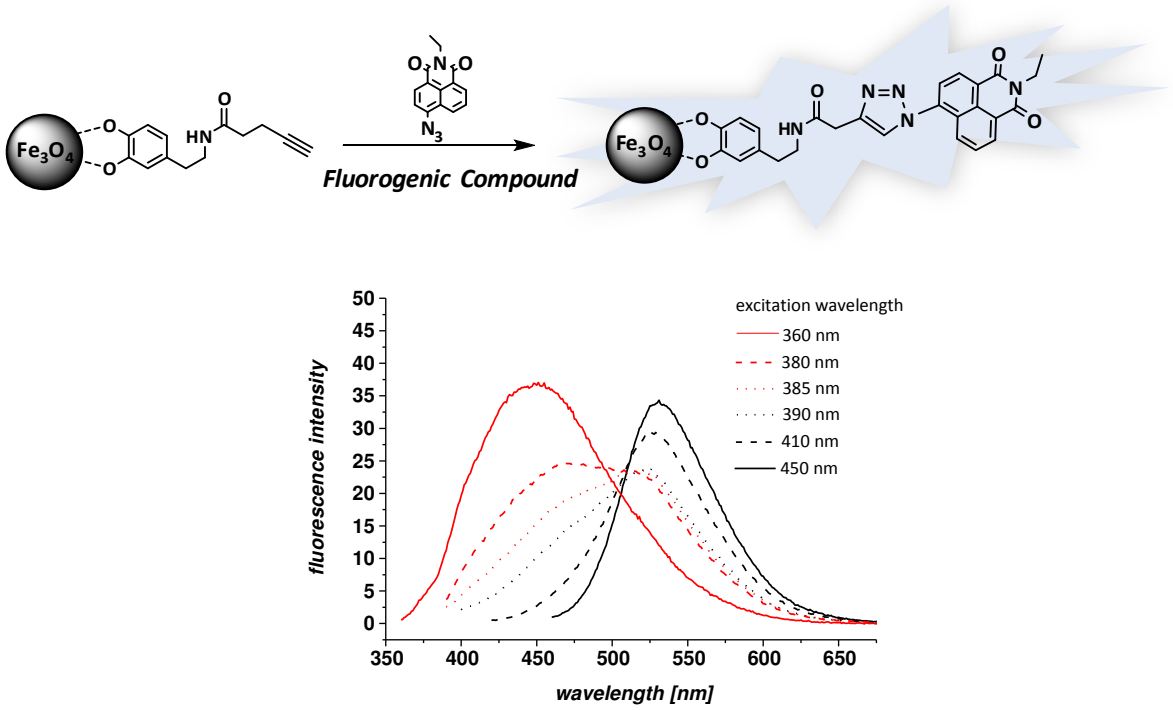

Figure 7.27. Fluorescence analysis of click-functionalized particles at different excitation wavelengths (450 nm - 360 nm) shows that the reaction was effective: The Fe_3O_4 particles emit at ~430 nm when excited with a 360 nm laser.

(1) Advincula, R. C.; Brittain, W. J.; Caster, K. C.; Rühe, J. *Polymer Brushes*; Wiley VCH: Weinheim, 2004.

(2) Sheiko, S. S.; Sumerlin, B. S.; Matyjaszewski, K. *Prog. Polym. Sci.* **2008**, *33*, 759.

(3) Zhang, M.; Müller, A. H. E. *J. Polym. Sci. Polym. Chem.* **2005**, *43*, 3461.

(4) Deffieux, A.; Schappacher, M. *Macromolecules* **1999**, *32*, 1792.

(5) Gao, H.; Matyjaszewski, K. *JACS* **2007**, *129*, 6633.

(6) Ryu, S. W.; Hirao, A. *Macromolecules* **2000**, *33*, 4765.

(7) Goldmann, A. S.; Walther, A.; Nebhani, L.; Joso, R.; Ernst, D.; Loos, K.; Barner-Kowollik, C. Barner, L.; Müller, A. H. E. *Macromolecules* **2009**, *42*, 3707.

(8) Sivakumar, K.; Xie, F.; Cash, B. M.; Long, S.; Barnhill, H. N.; Wang, Q. *Organic Letters* **2004**, *6*, 4603.

(9) Sun, S.; Zeng, H.; Robinson, D. B.; Raoux, S.; Rice, P. M.; Wang, S. X.; Li, G. *JACS* **2004**, *126*, 273.

(10) Sawa, M.; Hsu, T.-L.; Itoh, T.; Sugiyama, M.; Hanson, S. R.; Vogt, P. K.; Wong, C.-H. *Proceedings of the National Academy of Sciences* **2006**, *103*, 12371.

7.3. List of Publications

During the course of this thesis the following papers have been published (or submitted):

7. ***Goldmann, A. S.****; Schödel, C.; Walther A.; Yuan, J; Loos, K.; Müller, A. H. E.* Biomimetic Mussel Adhesive Inspired Clickable Anchors Applied to the Functionalization of Fe_3O_4 Nanoparticles, *Macromolecular Rapid Communication* (**2010**), submitted

6. **Goldmann, A. S.**; Walther, A.; Nebhani, L.; Joso, R.; Ernst, D.; Loos, K.; Barner-Kowollik, C.; Barner, L.; Müller, A.H.E. Surface Modification of Poly(divinylbenzene) Microspheres via Thiol-Ene-Chemistry and Alkyne-Azide Click Reactions, *Macromolecules*, **42**, 3707 *(***2009**)

5. Díez, I.; Pusa, M.; Kulmala, S.; Jiang, H.; Walther, A.; **Goldmann, A. S.**; Müller, A.H.E.; Ikkala, O. Color Tunability and Electrochemiluminescence of Silver Nanoclusters, *Angew. Chem. Int. Ed.* **48**, 2122 (**2009**)

4. Walther, A.; Millard, P.; **Goldmann, A. S.**; Lovestead, T.; Schacher, F.; Barner-Kowollik, C.; Müller, A.H.E.: Bis Hydrophilic Block Terpolymers via RAFT Polymerization: Toward Dynamic Micelles with Tunable Corona Properties, *Macromolecules* **41**(22), 8608 (**2008**)

3. **Goldmann, A. S.**; Millard, P.; Quémener, D.; Davis, T. P.; Stenzel, M. H.; Barner-Kowollik, C.; Müller, A.H.E.: Access to cyclic polystyrene via a combination of reversible addition fragmentation chain transfer (RAFT) polymerization and click chemistry, *Polym. Prepr. (Am. Chem. Soc., Div. Polym. Chem.)* **49**(2), 1 (**2008**)

2. Walther, A.; **Goldmann, A. S.**; Yelamanchili, R.S.; Drechsler, M.; Schmalz, H.; Eisenberg, A.; Müller, A.H.E.: Multiple Morphologies, Phase Transitions and Cross-Linking of Crew-Cut Aggregates of Polybutadiene-*block*-Poly(2-vinylpyridine) Diblock Copolymers, *Macromolecules* **41**, 3254 (**2008**)

1. **Goldmann, A. S.**; Quémener, D.; Millard, P.; Davis, T. P.; Stenzel, M. H.; Barner-Kowollik, C.; Müller, A.H.E.: Access to Cyclic Polystyrenes via a Combination of Reversible Addition Fragmentation Chain Transfer (RAFT) Polymerization and Click Chemistry, *Polymer* **49**, 2274 (**2008**)

7.4. Presentations at National and International Conferences

9. June 2009 • *Frontiers in Polymer Science, Mainz, Germany*

"Surface Modification of Divinylbenzene Microspheres *via* Thiol-Ene-Reaction and Click Chemistry" *(Poster Presentation)*

8. June 2009 • *Europolymer Conference (EUPOC), "Click"-Methods in Polymer and Material Science, Gargnano, Italy*

"Fluorescent Click-Functionalized Fe_3O_4 Magnetic Nanoparticles" *(Poster Presentation)*

7. April 2009 • *Zernike Institute, University of Groningen, The Netherlands*

"Azide-Alkyne and Thiol-Ene Reactions as Versatile Tools in the Synthesis of Cyclic Polymers and Surface-Functionalization of Microspheres" *(Invited Oral Presentation)*

6. August 2008 •*236th ACS National Meeting & Exposition, Philadelphia, PA, USA*

"Access to Cyclic Polystyrene via a Combination of Reversible Addition Fragmentation Chain Transfer (RAFT) Polymerization and Click Chemistry" *(Poster Presentation)*

5. February 2008 • *Macromolecular Colloquium, Freiburg i. Br., Germany*

"Cyclic Polymers: RAFT Polymer Chain Ends "Clicked Together" *(Poster Presentation)*

4. October 2007 • *Controlled / Living Polymerization Meeting (CLP´07), Antalya, Turkey*

"Cyclic Polymers: RAFT Polymer Chain Ends "Clicked" Together" *(Poster Presentation)*

3. October 2007 • *3rd STIPOMAT meeting, Les Diablerets, Switzerland*

"Ring-Shaped Polymers by Combination of RAFT and Click Chemistry" *(Poster Presentation, Poster Prize Winner)*

2. September 2007 • *IUPAC International Symposium on Ionic Polymerization, Kloster Banz, Germany*

"Ring-Shaped Polymers by Combination of RAFT and Click-Chemistry" *(Poster Presentation)*

1. February 2007 • *Australian Polymer Symposium, Hobart, Tasmania*

"Towards Ring-Shaped Polymers: Combining RAFT and Click-Chemistry" *(Oral Presentation)*

Glossary

a	Mark-Houwink exponent
ACVA	azobis(4-cyano valeric acid)
AFM	Atomic Force Microscopy
AIBN	2,2´-azobisisobutyronitrile
APT-NMR	Attached Proton Test Nuclear Magnetic Resonance Spectroscopy
ATR	Attenuated Total Reflection
ATRP	Atom Transfer Radical Polymerization
Bipy	2,2´-bipyridyl
BPATT	3-benzylsulfanylthiocarbonylsulfanyl propionic acid
BSA	bovine serum albumin
c	concentration
CDB	cumyl dithiobenzoate
$CDCl_3$	deuterated Chloroform
CH_2Cl_2	dichloromethane
Conv.	conversion
CPB	cylindrical polymer brushes
CRP	Living"/controlled radical polymerization
CTA	chain transfer agent
CuAAC	copper(I)-catalyzed azide–alkyne cycloaddition
CuBr	copper bromide
d	day, doublet
DCC	*N*,*N*'-dicyclohexylcarbodiimide
DLS	Dynamic Light Scattering
Θ	Theta
DMF	dimethylformamide
4-DMAP	4-dimethylaminopyridin
DMSO	dimethylsulfoxide
DNA	deoxyribonucleic acid
EDC	N-3-dimethylaminopropyl-N'-ethylcarbodiimidhydrochloride
ELSD	Evaporative Light Scattering detector
ESI-MS	Electrospray Ionization Mass Spectrometry
Fe	iron

Glossary

Fe_3O_4	magnetic iron oxid (nanoparticles)
FT-IR	Fourier transform infrared spectroscopy
g´	contraction factor
GPC	Gel Permeation Chromatography
h	hour
[η]	intrinsic viscosity
HEMA	(hydroxyethyl methacrylic)acid
HDA	Hetero Diels-Alder
HMBC	Heteronuclear Multiple Bond Correlation (2D NMR)
HMQC	Heteronuclear Multiple Quantum Coherence (2D NMR)
HPLC	High Pressure Liquid Chromatography
Ini	initiator
LACCC	Liquid Adsorption Chromatography at critical conditions
LCST	Lower critical solution temperature
LP	low pass
MALDI-ToF	Matrix Assisted Laser Desorption Ionisation –Time-of-Flight
MeOH	methanol
$MgSO_4$	magnesium sulfate
m	mass, multiplet
min	minute
MNP	magnetic nanoparticle
Mon	monomer
MWCO	molecular weight cutoff
M_n	molecular weight (number average)
M_w	molecular weight (weight average)
NIPAAm	N-Isopropylacrylamide
NMP	Nitroxide Mediated Radical Polymerization
NMR	Nuclear Magnetic Resonance Spectroscopy
2D NMR	Two-dimensional Nuclear Magnetic Resonance Spectroscopy
N_3-PEG	azido-endfunctionalized polyethylene glycole
N_3-PNIPAAm	azido-endfunctionalized poly(N-Isopropylacrylamide)
NP	nanoparticle

p.a.	per analysis
PCL	poly(ε-caprolacton)
PDI	polydispersity index
pDVB	poly(divinylbenzene) microspheres
PEG	polyethylene glycole
pHEMA	poly(hydroxyethyl methacrylic)acid
PM	*N*-(1-pyrenyl)maleimide
pNIPAAm	poly(N-isopropylacrylamide)
pS	polystyrene
PI	polyisoprene
ptS	poly(*p*-*tert*-butoxystyrene)
ptSB	poly(*p*-*tert*-butoxystyrene)-*block*-polybutadiene
RAFT	Reversible Addition Fragmentation Chain Transfer
RI	refractive index
RP	reverse phase
s	singlet
sec	second
SEC	Size exclusion chromatography
SEM	Scanning Electron Microscopy
SFRP	Stable free radical polymerization
SH-PEG	thiol-endfunctionalized polyethylene glycole
SH-pNIPAAm	thiol-endfunctionalized poly(N-Isopropylacrylamide)
t	time
TCEP	tris(2-carboxyethyl phosphine)
TEM	Transmission Electron Microscopy
THF	tetrahydrofuran
TMS	tetramethylsilane
UV	ultraviolet
UV-VIS	Ultraviolet-Visible Spectroscopy
V	volume
VISCO-SEC	Size-exclusion chromatographic system equipped with a differential viscometer

Glossary

λ	wavelength
XPS	X-Ray Photoemission Spectroscopy

Acknowledgements

I would like to make use of this occasion to thank the many people who provided me with support during the last three and a half years of scientific research. The journey of a PhD thesis is accompanied and supported by many people:

Firstly I would like to thank my supervisor and "Doktorvater" Prof. Axel H. E. Müller for providing me with the opportunity to study and to do research in MC II. I am always impressed by his ambitious and passionate personality (especially regarding research in polymer science) and I appreciate his constructive suggestions and kindness. His patience is exceptional and strongly contributes to the pleasant working atmosphere. I also thank him for proof-reading manuscripts, and for generously funding travel to several national and international conferences to present my work and for the unforgettable opportunity to spend eight months as an exchange student at the Centre of Applied Macromolecular Design (CAMD) at the University of New South Wales in Sydney. My time in Bayreuth was in every sense a great experience, particularly notable was the chance to collaborate with intelligent and pleasant people in an excellent polymer department.

I am also indebted to Prof. Christopher Barner-Kowollik for giving me the opportunity to work in his group at the CAMD in Sydney. His kind and helpful character made it easy to feel well received from the beginning. I thank him for his enormous enthusiasm which I find incredibly motivating, and for helping me making the "first steps" in RAFT polymerization in his department, which laid solid foundations for subsequent work upon my return to Bayreuth.

Of course I would like to make use of the occasion to thank many people from the CAMD who made the stay in Sydney unforgettable; particularly Dr. Martina Stenzel for great supervision and Dr. Leonie Barner for our fruitful collaboration.

Thanks to all of my other "CAMD colleagues" and friends who provided a very nice atmosphere: special thanks to Maribel Hernandez-Guerrero, Murat Barsbay, Francesca Bennet, Andrew Ah Toy, Maria Junkers and Thomas Junkers for great evenings, weekends and holidays. Thanks to Dr. Chakravarthy Gudipati, Dr. Damien Quémener, Leena Nebhani and Raymond Joso for your collaboration, help and support.

Acknowledgements

I would also like to express my gratitude to all colleagues in MCII for their help, not only chemistry but also for many other things. The atmosphere and team spirit at MC II was outstanding:

Dr. Holger Schmalz, Markus Müllner, Eva Betthausen, Annette Krökel, Dr. Marina Krekhova, Christopher Synatschke, Weian Zhang, Andreas Hanisch, Alexander Majewski, Alexander Schmalz, Stephan Weiß, Thomas Ruhland, Stefan Reinicke, Andrea Wolf, Joachim Schmelz, Susanne Edinger, André Pfaff, Sandrine Tea, Dr. Michael Witt and Kerstin Küspert.

Thank you Sabine for all the GPC, Visco-GPC, LACCC measurements and encouraging words.

Andreas (Dr. Walther), thanks for being a great colleague, all your support, motivation, TEM measurements and manuscript corrections. Your many scientific ideas helped me an incredible amount.

Thanks to Andrea Wolf, Melanie Förtsch, Annika Ochs, Dr. Andreas Walther, Benjamin Gossler and Dr. Markus Drechsler for TEM- and Cryo-TEM measurements, as well as Dr. Jiayin Yuan also for his never ending good mood, support and proof-reading.

Thanks to Andreas Hanisch, André Gröschel and Marietta Böhm for GPC measurements.

A special thanks to Prof. Dr. Katja Loos for all the XPS measurements and giving me the chance to work with the XPS instrument by myself.

I do not want to forget my colleagues who already left MC II: Harald Becker, Dr. Felix Schacher, Dr. Felix Plamper, Dr. Youyong Xu, Pierre Millard, Dr. Markus Burkhard, Dr. Jiayin Yuan, Dr. Manuela Schumacher, Astrid Göldel, Dr. Xavier André, Sergey Nosov, Dr. Markus Retsch, Jeannine Rockser, Denise Danz, Hans-Joachim Voigtländer and all other members and visitors who I met during my stay at MC II.

Lots of thanks to Gaby Oliver for her great help in bureaucratic things.

I had the pleasure to supervise and work with the students, Steffi Hiltl, Michaela Kersch and Daniela Pirner who made the advanced lab course, master thesis or bachelor thesis in our group. Furthermore thanks to the student assistants Susanne Mohr, Daniela Pirner and special thanks to Christine Schödel for her appreciated help in organic synthesis, especially column chromatography.

I benefit a lot from other close collaborations in Bayreuth and the access to many instruments, e.g. the Bayreuther Zentrum für Kolloide und Grenzflächen. Special thanks to Ingrid Otto and Melanie Pretzl for the Confocal Microscope images, Birgit Brunner, Dr. Ilgen and Mrs. Ott (Bayceer) for elemental analysis measurements.

Acknowledgements

I want to use the opportunity to thank the CSG e.V. (Chemiker Spass Gesellschaft), especially Eva Max who is heavily involved with the chemistry alumni association of Bayreuth. It is a great institution for keeping in touch after leaving Bayreuth and to extend ones scientific network.

At the same time I thank all of my friends for their support. They were always there, both when times were hard and when I wanted to relax after a long day in the lab.

Finally, I wish to thank my family for their continuous support during all these years, I truly appreciate everything you have done for me.

Erklärung

Die vorliegende Arbeit wurde von mir selbstständig verfasst und ich habe dabei keine anderen als die angegebenen Hilfsmittel und Quellen benutzt.

Ferner habe ich nicht versucht, anderweitig mit oder ohne Erfolg eine Dissertation einzureichen oder mich der Doktorprüfung zu unterziehen.

Bayreuth, den 18.12.2009

Anja Goldmann